

RESPONSE ANALYSIS OF PILES UNDER LATERAL LOADS

A

Dissertation

Submitted in Partial Fulfillment of the Requirements
for Award of the Degree of

**MASTER OF ENGINEERING
IN
STRUCTURAL ENGINEERING**

By

PUTHAPATT CHAKRADHAR BABU

University Roll No. 8810

College Roll No. 07/STR/04

Under the Guidance of

Prof. A.Trivedi

&

Dr. A.K. Sahu, Asst. Professor



Department of Civil and Environmental Engineering
Delhi College of Engineering
Delhi University, Delhi-110042

JUNE 2006

CERTIFICATE

This is to certify that the thesis entitled “**Response Analysis of Piles under Lateral Loads**” is being submitted by Puthapatt Chakradhar Babu, is a bonafide record of student’s own work carried by him under our guidance in partial fulfillment of requirement for the award of the Degree of **Master of Engineering (Structural Engineering), Dept. of Civil and Environmental Engineering, Delhi College of Engineering, Delhi.**

The matter embodied in this dissertation has not been submitted for the award of any other degree.

Dr. A. Trivedi
Professor
Civil Engineering Department
Delhi College of Engineering,
Delhi-110042

Dr. A.K. Sahu
Asst. Professor
Civil Engineering Department
Delhi College of Engineering,
Delhi-110042

ACKNOWLEDGEMENT

I express my sincere gratitude to Dr.A.Trivedi, Professor, Civil Engineering Department, Delhi College of Engineering, Delhi and Dr.A.K.Sahu, Assistant Professor, Civil Engineering Department, Delhi College of Engineering, Delhi under whose able guidance I have carried out the present work. It would not have been possible for me to complete this thesis, without their critical suggestions, constant inspiration and timely help.

I pay my sincere thanks to Prof. P.B.Sharma, Principal, D.C.E and Prof.P.R.Bose, Head of the Department, Department Civil Engineering, D.C.E, Delhi, for providing me the necessary facilities and required co-operation.

I also express my grateful thanks to all the Faculty Members for their valuable suggestions and help, wherever needed.

Co-operation extended by my friends and my family during the project is also duly acknowledged.

Place: New Delhi

Puthapatt Chakradhar Babu

Date:

Roll No.:8810

(Class Roll No: 07/str/04)

TABLE OF CONTENTS

Acknowledgement	
List of figures	
List of tables	
Nomenclature	
Abstract	1
1. Introduction	2
Organization of the Thesis	3
2. Soil – Pile Interaction	4
2.1 Classification of piles	4
2.2 Piling Materials	4
2.3 Piling Sections	5
2.4 Soil Parameters	6
2.4.1 Soil Modulus	6
2.4.2 Modulus of Subgrade Reaction	10
2.4.3 Shear Modulus of soil	12
2.5 Soil – Pile Behavior	13
2.5.1 Load Displacement Behavior	13
2.6 Forces Acting on Piles	14
2.6.1 Axially Loaded Piles	14
2.6.2 Laterally Loaded Piles	16
2.7 Criterion for Safe and Economic Design	16
2.8 Summary	17
3. Methods of Analysis	18
3.1 Introduction	18
3.2 Experimental Methods	19
3.2.1 Full Scale Pile Test Programs	19
3.2.2 Model Scale Pile Test Programs	20
3.3 Numerical Methods	21
3.3.1 Finite Element Method	21
3.3.2 Boundary Element Method	21

3.3.3 Discrete Element Method	22
3.3.4 Explicit Finite Difference Method	23
3.4 Analytical Methods	24
3.4.1 Beam on Winkler Foundation Model	24
3.4.2 p –y Curve Analysis	25
3.4.2.1 Piles in Soft Clay	26
3.4.2.2 Piles in Stiff Clay	28
3.4.2.3 Piles in Sand	30
3.4.3 Elastic Continuum Approach	33
3.4.4 Finite Element Analysis	34
3.5 Summary	35
4. Winkler’s Analysis of Laterally Loaded Piles	36
4.1 Background	36
4.2 Discussion on the results of Winkler’s model	39
4.3 Summary	46
5. Numerical Analysis of Laterally Loaded Piles	47
5.1 Introduction	47
5.2 Description of Model	49
5.2.1 Displacement and Stress Field	49
5.2.2 Solutions for Laterally Loaded Piles	53
5.2.3 Boundary Conditions	55
5.3 Critical Pile Length	56
5.4 Load Transfer Factor	57
5.4.1 Computational Procedure for γ Determination	58
5.5 Modulus of Subgrade Reaction and Fictitious Tension	61
5.6 Analysis of Pile Response	66
5.6.1 Effect of Various Head and Base Conditions	66
5.6.2 Effect of Fines Content	74
6. Conclusions	76
REFERENCES	
APPENDIX A	

LIST OF FIGURES

Fig 2.1	Different types of pile cross sections	5
Fig.2.2.	Calculating a Modulus	7
Fig.2.3.	Definition of soil modulus	8
Fig.2.4.	Variation of soil modulus with depth	11
Fig.2.5.	Lateral deflections in axially loaded pile	15
Fig.3.1.	Schematic view of laterally loaded pile	18
Fig.3.2.	Nonlinear p-y curves for laterally loaded piles at various depths x.	26
Fig 3.3	Characteristic shapes of the p-y curves for soft clay	27
Fig 3.4	Characteristic shape of p-y curves for static and cyclic loading in stiff clay in the presence of free water (Reese et al., 1975)	29
Fig 3.5	Characteristic shape of p-y curves for static and cyclic loading in stiff clay with no free water (Reese and Welch, 1975)	30
Fig 3.6	Characteristic shape of p-y curves for static loading in sand (Cox et al., 1974)	31
Fig 3.7	API Coefficients for sand	32
Fig 3.8	API initial modulus of subgrade reaction	32
Fig.4.1	Single pile model	36
Fig.4.2.	Comparison of pile behavior in clay and sand soil With respect to (a) moment (b) deflection	40
Fig.4.3.	Moment variation for different types of soils in clay and sand	41
Fig.4.4.	Deflection variations for different types of soils in clay and sand	42
Fig.4.5.	Effect of pile cross sectional shape on (a) moment (b) deflection	43
Fig.4.6.	Effect of pile cross sections size on (a) Moment (b) Deflection in clay	44
Fig.4.7.	Effect of the modulus of sub-grade reaction on (a) Moment (b) Deflection	45
Fig.4.8.	Load – deflection curve	46
Fig 5.1	Schematic of pile-soil system: (a) single pile; (b) Pile element analysis.	52

Fig 5.2	Stress and displacement field adopted in the load transfer analysis	52
Fig 5.3	Pile- head and -base conditions.	57
Fig 5.4	Determination of load transfer factor (clamped head and free head).(a) Effect of slenderness ratio (b) Effect of Poisson's ratio	60
Fig 5.5	Determination of load transfer factor for various pile head and base conditions.	61
Fig 5.6	Variation of (a) the modulus of sub-grade reaction and (b) Normalized Fictitious Tension for various head and base conditions	63
Fig 5.7	Variation of (a) the modulus of sub-grade reaction and (b)Normalized Fictitious Tension w.r.t. Slenderness ratio (FeHCP(P))	64
Fig 5.8	Variation of (a) the modulus of sub-grade reaction and (b)Normalized Fictitious Tension w.r.t. Poisson's ratio (FeHCP(P))	65
Fig 5.9	Single pile (FeHCP(P)) response due to variation in slenderness ratio (a) Pile head deformation (b) Pile head rotation (c) Maximum bending moment	68
Fig 5.10	Single pile (free head - P) response due to variation pile – soil relative stiffness (a) Pile head deformation (b) Pile head rotation (c) Maximum bending moment	70
Fig 5.11	Single pile (free head clamped pile) response due to variation in soil pile relative stiffness w.r.t Poisson's ratio	71
Fig 5.12	Single pile (fixed head) response due to variation in pile – soil relative stiffness (a) pile head deformation (b) Normalized maximum bending moment	72
Fig 5.13	Single pile (free head) response due to variation in pile – soil relative stiffness acted upon by a moment Mo (a) Pile head deformation (b) pile head rotation	73

Fig 5.14	Effect of variation in percentage fine content on pile head rotation	74
Fig 5.15	Effect of variation in percentage fine content on pile head deformation	75
Fig 5.16	Effect of variation in percentage fine content on normalized bending moment	75

LIST OF TABLES

Table 2.1	Regression parameters for calculation of G_s (Salgado <i>et al</i> , 2000)	13
Table.4.1	Value range for the static stress-strain modulus (E_s) for selected soils (Bowles, 1996)	38
Table.4.2	Values of modulus of sub-grade reaction (Terzaghi, 1955)	38
Table 5.1	Parameters for estimating the load transfer factor (Guo, 2001)	58

NOMENCLATURE

a, b	parameters for estimating pile response
A	factor to account for cyclic or static loading
B(z), and C(z)	reflect pile-base conditions
c	Shear strength at depth z
C ₁ , C ₂ , C ₃	Coefficients as a function of ϕ'
C _g , e _g , and n _g	Regression constants that depend solely on the soil
D, d	The diameter or width of the pile.
D _p	The change in pressure of the cavity
D _r	Relative density
e	Void ratio.
E _d	Dilatometer modulus
E ₅₀	Secant modulus at half ultimate stress in an un-drained test
E _p I _p	The pile flexural stiffness
E _s	Soil secant (Elastic Modulus of Elasticity of soil)
E _{sp}	The pressure meter modulus
E _p /G*	The pile-soil relative stiffness
(E _p /G*) _c	The critical pile-soil stiffness
FeHCP	Free-head, clamped pile
FeHFP	Free-head, floating pile
FxHCP	Fixed-head, clamped pile
FxHFP	Fixed-head, floating pile
G _s	The shear modulus
G*	The modified soil shear modulus
H(z), and I(z)	reflect pile-head boundary conditions,
J	Constant taken as 0.5 for soft clay and 0.25 for medium clay
K _o (γ)	Modified Bessel functions of the second kind of order zero
k	The modulus of subgrade reaction for the Winkler's springs
k _h	The modulus of horizontal subgrade reaction in N/m ³
L	Length of the pile
L _c	Critical pile length,
M _o	Moment
n _h	The constant of horizontal sub grade reaction expressed in
N	The fictitious tension
P _A	Reference stress in the same units as σ'_m i.e. kPa
P _u	Ultimate resistance (force/unit length) (s=shallow, d=deep)
P	Lateral load
p	Soil reaction at a point along the pile in N/m
q _c	Cone penetration resistance kPa
r _o	Radius of the pile
U _k	The energy for unit pile movement ($y = 1$) per unit pile length;
U _N	The energy for unit pile rotation ($dy/dz = 1$) per unit pile length;
U _m	The energy for unit radial rotation ($d\phi/dr = 1$) per unit radial length

U_n	The energy for unit radial variation ($\phi = 1$) per unit radial length
V_o'	The volume of the measuring cell at average pressure
$y(z)$	The pile displacement
Z	Depth
λ_s	Lami's constant
ν_s	Poisson's ratio
σ'_m	Mean effective stress;
$\sigma_r, \sigma_\theta, \sigma_z$	Radial, circumferential and vertical stresses within the surrounding soil
$\varepsilon_r, \varepsilon_\theta, \varepsilon_z$	Radial, circumferential and vertical strains within the surrounding soil
$\gamma_{r\theta}, \gamma_{\theta z}, \gamma_{rz}$	Shear strains within the $r - \theta, \theta - z$ & $r - z$ planes
σ_{ij} & ε_{ij}	The stress and strain components in the surrounding soil of the pile
δU	The variation of potential energy of the pile-soil system
δW	The virtual work
$\phi(r)$	The radial attenuation function
γ	Load transfer factor
γ'	Average effective unit weight from ground surface to p-y curve
ϕ'	Angle of internal friction in sand
ε_{50}	Strain at 50 percent of the ultimate strength from a laboratory stress-strain curve.
θ	Angle between the line joining the center of the pile cross-section to the point of interest and the direction of the n^{th} loading component.

ABSTRACT

As a foundation problem, the analysis of a pile under lateral loading is complicated by the fact that the soil reaction is dependent on the pile movement, and the pile movement, on the other hand, is dependent on the soil response. Thus, the problem is one of soil-structure interactions. Many methods such as the subgrade reaction method, the elastic continuum approaches that have been developed for the analysis of laterally loaded soil-pile system modeled piles as a flexible beam. But the available experiments demonstrate that the displacement field around a laterally loaded pile is significantly different from that around a beam overlying on an elastic medium. Thus, different modulus for beams and lateral piles should be adopted.

It is with this background in this thesis an attempt has been made to implement a load transfer approach to simulate the response of laterally loaded single piles embedded in a homogeneous medium, by introducing a rational stress field. In the present work, generalized solutions for a single pile and the surrounding soil under various pile-head and base conditions were established. With the solutions, a load transfer factor, correlating the displacements of the pile and the soil has been adopted. Expressions are also developed for fictitious tension and the modulus of subgrade reaction in terms of the load transfer factor. The model parameters such as load transfer factor, Poisson's ratio, slenderness ratio, the soil-pile relative stiffness are investigated in order to have a better understanding of the relationship between these parameters. The effects of the results of this load transfer approach are compared with Winkler's model. The results for the pile rotation, pile deflection and maximum bending moment are evaluated for sandy soils of varying fine contents.

CHAPTER 1

INTRODUCTION

It was once said that it is wise to build your house on a rock. However, what if the closest rock that is big enough is 10 meters under the soil? What happens when a structure much larger than a house needs to be built? It was these questions that guided engineers towards the concept of pile design. Piles are long, firm, column-like members that are embedded in the soil to provide axial as well as lateral support of structures such as buildings, piers and bridges. Often, piles are installed near each other to create groups to optimize the support of the structure. Both a single pile and groups of piles rely significantly upon the conditions of the surrounding soil. Piles are often the first members of a structure to be installed. They are also some of the most expensive members. Therefore, it is very important to analyze piles under various loadings i.e. under axial and lateral loadings.

Most of the methods that are developed to analyze the piles, assume piles as flexible beams. In the uncoupled (Winkler) model, the elastic springs are generally represented by modulus of subgrade reaction. This modulus was obtained through fitting with relevant rigorous numerical solutions (e.g., Vesic, Terzaghi etc). The problem is that the fitting to different reactions (e.g. deflection or moment of a beam or a pile) generally leads to different values of modulus. This difference in modulus implies that (1) the uncoupled model is not sufficiently accurate for simulating the pile-soil interaction; and (2) the use of the available modulus developed for beams to pile analysis is only an interim measure. The available experiments demonstrate that the displacement field around a laterally loaded pile is significantly different from that around a beam sitting on an elastic medium. Thus, different modulus for beams and lateral piles should be adopted.

As in the analysis of vertically loaded piles, the subgrade modulus is affected by the soil response in radial direction. To accommodate this effect, a two parameter model has been developed with suitable uncoupled expressions relating the pile displacement to a radial attenuation function for soil displacement are generally assumed for displacements in the radial and circumferential directions, which are then implicitly

linked (coupled) through a fitting factor. This two parameter model that has been developed is not providing reliable results at high Poisson's ratios. It is with this background in this thesis an attempt has been made to develop a load transfer approach to simulate the response of laterally loaded single piles embedded in a homogeneous medium, by introducing a rational stress field.

In the present work, generalized solutions for a single pile and the surrounding soil under various pile-head and base conditions were established. With the solutions, a load transfer factor, correlating the displacements of the pile and the soil, was estimated and expressed as a simple equation. Expressions were developed for the modulus of subgrade reaction for a Winkler model as a unique function of the load transfer factor. Expressions are also developed for fictitious tension in terms of the load transfer factor. The model parameters such as load transfer factor, Poisson's ratio, slenderness ratio and the soil-pile relative stiffness are investigated in order to have a better understanding of the relationship between these parameters. The entire analysis has been done using Mathematica 5.1 and MATLAB 7.0

ORGANISATION OF THE THESIS

Chapter 2 includes about the classification of piles, soil parameters and the importance of their relationship. An introduction about the laterally loaded piles is also presented.

Chapter 3 presents various methods of analysis of laterally loaded piles and their significance.

Chapter 4 gives preliminary investigation of the laterally loaded pile behavior using Winkler's model. Analysis of piles for various piles cross sectional types, sizes, soil types etc has been done.

Chapter 5 deals with the load transfer approach analysis of laterally loaded piles. In this chapter, various relations for different pile base and head conditions have been given. The inter relationship between various model parameters like load transfer factor, pile-soil stiffness, slenderness ratio, Poisson's ratio etc are investigated.

Chapter 6 presents conclusions of the present work and future scope of the study.

Appendix A deals with the computational procedure for determination of the shear modulus of elasticity.

CHAPTER 2

SOIL-PILE INTERACTION

Piles are driven in weak soils to support heavy structures and transfer their loads to the surrounding soils. They are usually subjected to lateral forces and moments as well as axial forces. Unlike axial forces, which normally produce deformations in the direction of the pile axis, lateral forces may produce deformations in any direction of the pile. The design of pile foundations under lateral loads normally is governed by the maximum deflection of the pile.

2.1 CLASSIFICATION OF PILES

Piles can be classified in many ways, for example, by the material it's made of, by method of load transfer, by amount of ground disturbance, by fabrication method, and by method of installation.

- Pile material: Piles can be made of different materials such as, concrete, steel, timber and composite. Traditional composite piles are made of steel and concrete or timber and concrete.

- Method of load transfer: Piles can be classified according to the method of load transfer into; end-bearing piles, friction piles, combined end-bearing and friction piles, and laterally loaded piles.

- Amount of ground disturbance during installation: Large-displacement piles, small-displacement piles, and non-displacement piles.

- Pile fabrication method: prefabricated or cast in place.

- Method of installation, driven piles, bored piles and a combination of driven and bored piles.

2.2 PILING MATERIALS

The commonly used materials for piling are steel, concrete and timber. Because of their high performance as construction materials, they have been recommended over other materials.

Steel piles

Steel piles are normally used in the form of H or pipe piles. Steel has very high compressive and tensile strengths in addition to its high modulus of elasticity. It has a

high capability of carrying heavy loads down to deep bearing strata. Steel piles have the advantages of high load capacity and ease of splicing so that they can be shipped in any required length. They also have the ability of being driven through different soil layers even soft rocks and hard material layers.

Concrete piles

Concrete is the most common traditional construction material used today. It has the ability to carry large axial forces and bending forces when reinforced with steel bars. Concrete members can be designed for the desired shape and strength. They are easy to drive and have the ability to withstand hard driving. Concrete piles are available in the following main categories:

1. Pre-cast concrete piles
2. Cast-in place concrete piles
3. Composite concrete piles.

Timber piles

Timber piles are usually made of straight tree trunks after removing their branches. They are easy to cut, easy to handle and can last for long periods of time under normal environmental conditions. Timber piles can be found as round untrimmed logs or sawed square sections. They are usually used as friction piles in granular soils, sands, silts and clays.

2.3 PILE SECTIONS

Piles can be found in different types of cross sections as shown below. The most common shapes are the H-section for steel piles, circular sections for concrete piles and polygonal sections for pre-stressed piles.

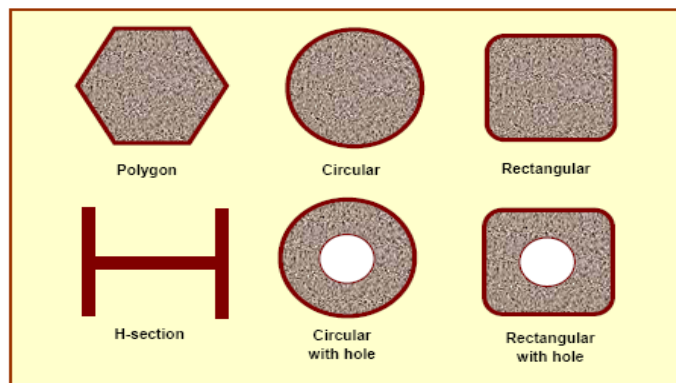


Fig 2.1: Different types of pile cross sections

2.4 SOIL PARAMETERS

Before going further, it is important to discuss the importance of the soil parameters like modulus of elasticity of soil, modulus of subgrade reaction, shear modulus of the soil etc.

2.4.1 Soil Modulus

The modulus of a soil is the most difficult parameter estimate because it depends on so many factors such as the state of soil, loading conditions, etc. The following section will discuss some of the aspects involved in the soil moduli. In the first part, the modulus is defined then the factors effecting like the state of soil and then its applications, and its relation to the soil coefficient of sub grade reaction and shear modulus of soil.

2.4.1.1 Definition

Let us consider the stress-strain curve obtained from a tri-axial test. The sample is a cylinder wrapped in an impermeable membrane and confined by all round (hydrostatic) pressure. Then the vertical stress is increased gradually and the nonlinear, stress-strain shown in Fig.2.2 is obtained. Elasticity assumes that the strains experienced by the soil are linearly related to the stresses applied. In reality, this is not true for the soils and there lies one complexity. The equations of elasticity for this axisymmetric loading relate the stresses and the strains in the three directions as shown in Fig (2.2). Because of the axisymmetry, equations (2.1) and (2.2) in Fig (2.2) are identical. In equations (2.1) and (2.3) there are two unknowns: the soil modulus, E and the Poisson's ratio, ν . In the tri-axial test, it is necessary to measure the stress applied in both directions as well as the strains induced in both directions in order to calculate the modulus of the soil. Indeed, one needs two simultaneous equations to solve for E and ν . Note that the modulus is not the slope of the stress-strain curve. An exception to this statement is the case where the confining stress is zero as it is for a typical concrete cylinder test or an unconfined compression test on clay. In order to calculate the Poisson's ratio, it is also necessary to measure the stresses applied in both directions as well as the strains induced in both directions. Note that the Poisson's ratio is not the ratio of the strains in both directions [equation (2.5) on Fig (2.2)]. An exception to this statement is again the case where the confining pressure is zero. Because soils do not exhibit a linear stress-strain curve, many moduli can be defined from the tri-axial test results for example.

In the previous paragraph, it was pointed out that the slope of the stress-strain curve is not the modulus of the soil, however the slope of the curve is related to the modulus and it is convenient to associate the slope of the stress-strain to a modulus. Indeed this gives a simple image tied to the modulus value; note however that in the figure 2.3 the slope is never labeled as modulus E but rather as slope S.

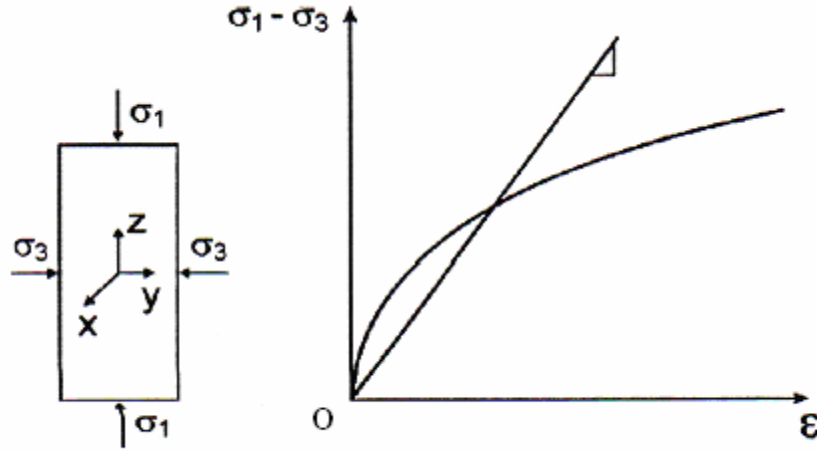


Fig 2.2 Calculating a Modulus

$$\varepsilon_{xx} = \frac{1}{E}(\sigma_{xx} - \nu(\sigma_{yy} + \sigma_{zz})) = \frac{1}{E}(\sigma_3 - \nu(\sigma_1 + \sigma_3)) \quad (2.1)$$

$$\varepsilon_{yy} = \frac{1}{E}(\sigma_{yy} - \nu(\sigma_{xx} + \sigma_{zz})) = \frac{1}{E}(\sigma_3 - \nu(\sigma_1 + \sigma_3)) \quad (2.2)$$

$$\varepsilon_{zz} = \frac{1}{E}(\sigma_{zz} - \nu(\sigma_{xx} + \sigma_{yy})) = \frac{1}{E}(\sigma_1 - \nu(\sigma_3 + \sigma_3)) \quad (2.3)$$

$$E = \frac{\sigma_1 - 2\nu(\sigma_3)}{\varepsilon_{zz}} \quad (2.4)$$

$$\frac{\varepsilon_{xx}}{\varepsilon_{zz}} = \frac{\sigma_3 - \nu(\sigma_1 + \sigma_3)}{\sigma_1 - 2\nu\sigma_3} \quad (2.5)$$

Referring to Fig.2.3, if the slope is drawn from the origin to a point on the curve (O to A) in Fig.2.3, the secant slope S_s is obtained and the secant modulus E_s is calculated from it. One would use such a modulus for predicting the movement due to then first application of a load as in the case of a spread footing. If the slope is drawn as the tangent to the point considered on the stress-strain curve then the tangent slope S_t is obtained and the tangent modulus E_t is calculated from it. One would use such a modulus

to calculate the incremental movement due to an incremental load as in the case of the movement due to one more storey in a high-rise building. If the slope is drawn as the line which joins points A and B on Fig.2.3, then the unloading S_u is obtained and the unloading modulus E_u is calculated from it. One would use such a modulus when calculating the heave at the bottom of an excavation or the rebound of a pavement after the loading by a truck tire (resilient modulus). If the slope is drawn from point B to point D in Fig.2.3, then the reloading slope S_r is obtained and the reload modulus E_r is calculated from it. One would use this modulus to calculate the movement at the bottom of an excavation if the excavated soil or a building of equal weight was placed back in the excavation or to calculate the movement of the pavement under reloading by the same truck tire. If the slope is drawn from point B to point C on Fig 2.3, then the cyclic slope S_c is obtained and the cyclic modulus E_c is calculated from it. One would use such a modulus and its evolution as a function of the number of cycles for the movement of a pile foundation subjected to repeated wave loading.

Whichever of these moduli are defined and considered, the state in which the soil is at a given time like intensity of packing, structure of the soil i.e., intensity of disturbance, water content present in the soil, pre-stressing condition of the soil i.e., over consolidated, under consolidated or normally consolidated and also type of load acting on the soil also affect the modulus.

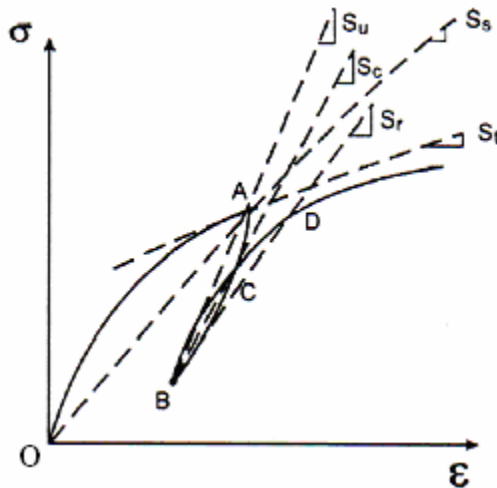


Fig 2.3 Definition of soil modulus

2.4.1.2 Expressions for stress-strain modulus E_s by several test methods:

Cone Penetration Test (CPT):

Vesic (1970)

$$\text{Sand: } E_s = (1 + D_r^2) * q_c \quad (2.6)$$

D_r = relative density

Briaud (1992)

$$\text{Clay: } E_s = 2.5 * q_c \quad (2.7)$$

$$\text{Sand: } E_s = 1.15 * q_c \quad (2.8)$$

where q_c = cone penetration resistance kPa

Standard Penetration Test (SPT):

$$E_s = 250 (N + 15) \text{ in kPa} \quad (2.9)$$

N = penetration number for a required number of blows

Pressure Meter Test (PMT):

Pressure meter operates on the principle of expanding a rigid cylinder into the soil and being resisted by an infinitely thick cylinder (the soil).

$$G_s = V_o' * (D_p / D_v)$$

(2.10)

Where G_s = the shear modulus

V_o' = the volume of the measuring cell at average pressure $D_p = V_o + V_c$

D_p = the change in pressure of the cavity

Then the pressure meter modulus is calculated from the expression as given below

$$E_{sp} = E_s = G_s * [2 * (1 + \nu)] \quad (2.11)$$

Dilatometer test (DMT):

According to Marchetti (1980) dilatometer modulus (E_d) is related to modulus E_s as given below

$$E_s = E_d * (1 - \nu^2) \quad (2.12)$$

Another term that is sometimes used in place of E_s is the coefficient (or modulus) of horizontal subgrade reaction, k_h , expressed in units of force per unit volume (Terzaghi 1955). The relationship between E_s and k_h can be expressed as:

$$E_s = k_h D \quad (2.13)$$

where D is the diameter or width of the pile.

E_s is a more fundamental soil property as it does not depend on the pile size.

2.4.2 Modulus of Sub-grade Reaction

In analysis of piles under lateral loads using sub grade reaction approach, two stiffness parameters are needed: (1) The flexural stiffness of the pile (EI) and (2) The horizontal stiffness of the soil, E_s , G_s , or k_h . In theory of elasticity, the soil stiffness is expressed by Young's modulus E_s or shear modulus G_s . However, soil stiffness may also be defined by the modulus of horizontal subgrade reaction (FL^{-2}) as:

$$K_h = -p/y \quad (2.14)$$

where p = Soil reaction at a point on the pile per unit of length along the pile (FL^{-1})
 y = Deflection at that point (L).

Thus actual soil reaction becomes independent of the soil continuity and is assumed to be replaced by closely spaced independent elastic springs. Figure 2.4 shows the typical soil reaction versus deflection curve (p - y curve) for soil surrounding a laterally loaded pile.

For soil reactions less than one-third to one-half of the ultimate soil reaction, the p - y relationship can be expressed adequately by a tangent modulus. The slope of the modulus variation with respect to depth is called as coefficient of horizontal subgrade reaction, k_h . For soil reaction exceeding approximately one-third to one-half of the ultimate soil reaction, the secant modulus shown by the dashed line should be considered, thus making modulus a function of the deflection. The actual variation of sub grade modulus with depth is also shown in Fig.2.4.

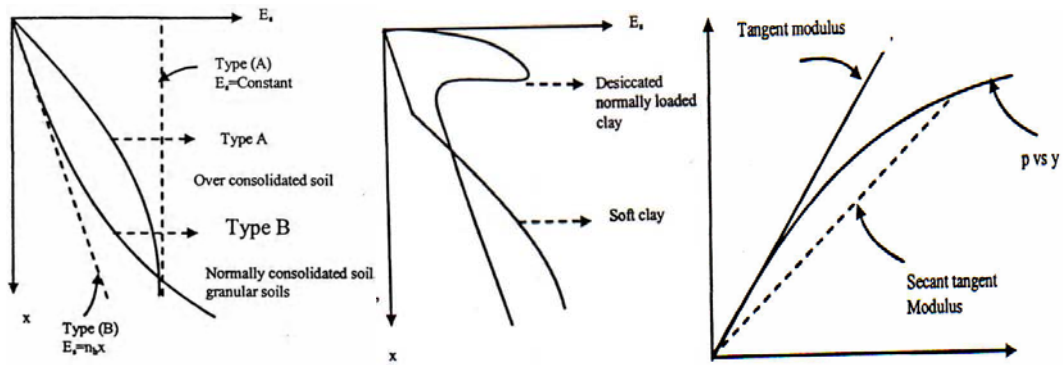


Fig.2.4 Variation of soil modulus with depth

It has been explained that both stiffness and the ultimate soil resistance are lower near the soil boundary (Davisson, 1963). As discussed earlier, as per the theory of subgrade modulus, the soil stiffness is represented by a series of independent elastic springs, while in reality they are interrelated in a complex fashion. Researchers have proved and validated this theory and have shown that for a long relatively flexible member such as a pile, the error in the computed bending moments based on the subgrade modulus assumption is no more than a few percent when compared to the theory of elasticity solution. Therefore, the subgrade modulus concept has a reasonable theoretical foundation and can be used extensively for computing response of piles under lateral loads.

Terzaghi (1955) presented an extensive discussion regarding the effect of the size of the loaded area on the subgrade modulus. Davisson (1963) showed for elastic approach without plastic soil behaviour, after k_h has been determined for a given pile, modulus value is unchanged if the pile width D is changed, i.e. irrespective of the increase or decrease in the pile depth the deflection of the pile becomes fixed. It was also proved by Davisson (1963) that any variation in the inertia of the pile in the lateral direction is not going to have any change in the load deflection behaviour for the above case, however affecting the ultimate soil reaction.

Cohesive soils:

Brooms (1964a) has given for elastic cohesive soils

$$k_h = \frac{1.67E_{50}}{d} \quad (2.15)$$

where E_{50} = secant modulus at half ultimate stress in an un-drained test.

Cohesion-less soils:

For granular soils, **Terzaghi** (1955) recommends that k_h can be considered directly proportional to the depth z . The expression for k_h is given as

$$k_h = n_h * z \quad (2.16)$$

where n_h is the constant of horizontal sub grade reaction expressed in FL^{-3} and the values as suggested by Terzaghi are given in table 4.2. It can be shown that k_h is proportional to depth for normally consolidated clays and this assumption is also valid for normally consolidated silts.

Vesic (1961), based on the analysis of an infinite beam on elastic foundation, suggested the following expression.

$$k_h = \left(\frac{0.65}{d} \right) \left(\frac{E_s}{1 - \nu_s^2} \right)^{1/2} \sqrt{\frac{E_s d^4}{E_p I_p}} \quad (2.17)$$

The term $E_p I_p$ = the pile flexural stiffness;

d = width of the pile;

E_s = soil secant (elastic); and

ν_s = Poisson's ratio.

2.4.3 Shear Modulus of Soil

The shear modulus G_s is defined as the ratio of shear stress to the shear strain and is given by

$$G_s = E_s / (2 * (1 + \nu_s)) \quad (2.18)$$

where ν_s = Poisson's ratio.

Empirical equation that has been provided for the calculation of shear modulus of soil as provided by Hardin and Richart (1963) is given as

$$G_s = C_g P_A^{1-n_g} \frac{(e_g - e)^2}{1 + e} \sigma_m'^{n_g} \quad (2.19)$$

where C_g , e_g , and n_g = regression constants that depend solely on the soil (and are therefore intrinsic soil variables) as given in the table 2.1 below;

σ'_m = mean effective stress;

P_A = reference stress in the same units as σ'_m usually taken as 100kPa; and e = void ratio.

Table 2.1 Regression parameters for calculation of G_s (Salgado *et al*, 2000)

Silt (%)	C_g	e_g	n_g	e
0	612	2.17	0.439	0.633
5	454	2.17	0.459	0.609
10	357	2.17	0.592	0.583
15	238	2.17	0.745	0.500
20	270	2.17	0.686	0.423

The computational procedure for calculating the shear modulus of elasticity has been provided in the Appendix A.

2.5 SOIL-PILE BEHAVIOR

Analysis and design of piles under the different types of loading usually start with the understanding of the soil-pile interaction process. Soils, in general, are non-homogenous materials that are found in layers along the pile length and each layer may have different properties from the next layer. The soil-pile interaction will not have the same behavior along the pile shaft; therefore, variation in soil properties has to be taken into consideration. Piles embedded in soil can be represented by beam-column elements with geometric and material nonlinear behavior. Soil-pile behavior can be classified into two categories; the first category is axial load-friction behavior, in which a unique relationship is assumed between the skin friction, shear stress, and the relative deflection between soil and the pile at each depth. The second category is lateral load-displacement behavior, in which the pile will be subjected to a lateral soil pressure if it is battered or has a lateral loading in form of shear or moment applied at the top.

2.5.1 LOAD – DISPLACEMENT BEHAVIOR

Soil behavior can be represented by a set of load-displacement curves to describe its response under different types of loadings. Three major categories of curves are usually used in this regard; each of them describes a single characteristic of the soil: lateral load-displacement (p-y) curves, load-slip (f-z) curves, and load-settlement (q-z) curves. The soil response in all three categories is assumed to be nonlinear. The modulus of sub-grade reaction, which was originated by Winkler, is one of the most commonly used methods in pile analysis. In this method the surrounding soil to the embedded pile can be replaced by a series of vertical and lateral springs to represent both the

longitudinal and lateral soil resistance. The spring properties are usually obtained from the load–displacements curves that represent the resistance force as a function of the displacement in the force direction. The derivation of load displacement curves has been performed through means of correlations with results from real field experiments on instrumented loaded piles. The accuracy of such curves to represent a particular pile behavior depends on the similarity between the pile in the study and the pile test model in terms of soil properties and loading conditions.

2.6 FORCES ACTING ON PILES

Pile foundations are structural members that give support and transfer loads from one structure to another. A pile can be considered as a special type of column that carries axial and flexural loads but with different cases of boundary conditions. Generally, the column is a cast-in-place structure whereas the pile is a pre-cast or prefabricated element which requires handling, transporting, and driving. Due to the different circumstances that involve the whole process of pile construction, the design should include all factors affecting its durability and performance.

Piles may be subjected to different kinds of forces during handling and while they are in service. Piles must be designed to handle loads without damage.

- (a) Crushing under the permanent design load,
- (b) Crushing caused by impact force during driving,
- (c) Bending stresses due to horizontal forces,
- (d) Bending stresses due to curvature in the pile.

Also piles must have adequate surface area, in the case of friction piles, so that they will provide the highest contact area to transfer the loads from the pile to the surrounding soil.

2.6.1 AXIALLY LOADED PILES

Piles are usually designed for full capacity which is the maximum load the pile can support without failure. The maximum allowable stress on a pile section should not exceed the allowable limits. A pile under axial compression may reach one of the following four limit states.

1. Structural failure of the pile body such as crushing or yielding.
2. Stability failure due to buckling.
3. Bearing capacity failure of the soil under the pile

4. Excessive pile settlement

No pile is likely to be entirely straight. Any curvature causes bending stresses. It is important to give consideration to lateral as well as eccentric forces on piles, since stresses may increase rapidly from these causes when combined with stresses from direct axial loads. An axially loaded pile may be subjected to buckling. The pile will buckle during service when the loading reaches or exceeds its critical buckling load. This case is rare but it may occur for end-bearing piles in soft soils or partially embedded piles. Also a pile may buckle during driving which may cause some deviation from the desired position.

The critical buckling load for an ideal pin ended column is given by the Euler equation:

$$P_{cr} = \frac{\pi^2 EI}{L^2} \quad (2.20)$$

where EI = flexural stiffness of the pile
 L = Length of the pile

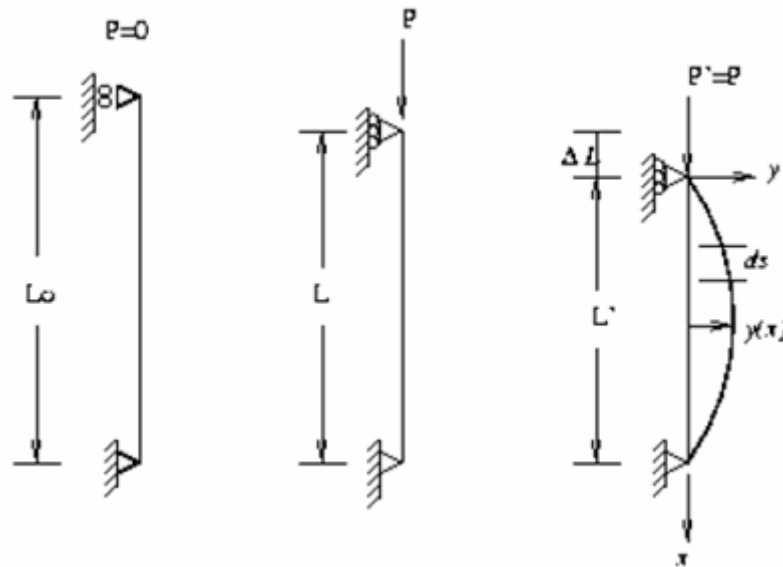


Fig 2.5: Lateral deflections in axially loaded pile

2.6.2 LATERALLY LOADED PILES

Lateral loads on piles usually come from different sources like wind pressure, horizontal live loads, earth and water pressure, induced lateral soil movements such as construction, excavation, tunneling activities and blasts etc to the near by site of the piles, and earthquake effects. Piles under lateral loads must be designed to withstand these loads or any combinations of loads without failing. Piles in groups are normally subjected to a combination of both axial and lateral loads. In the past, designers used to consider piles as axially loaded members only, and the lateral loads were assumed to be carried by batter piles. Current pile designers consider the full range of vertical (or battered) laterally loaded structural members, fully or partially embedded in the ground, as laterally loaded piles (Bowles 1996).

It has been found that the lateral support provided by any soil except the softest or most fluid is generally sufficient to prevent pile failure from buckling for the embedded portions. For portions in water or above the ground, unsupported, the pile should be designed as a column under direct loads unless lateral forces are present, in which case the design should include the lateral forces. The design of laterally loaded vertical piles is normally governed by the maximum allowed deflection or the structural capacity of the pile. It has been found that reaching the ultimate capacity of the soil is something unattainable or unacceptable because it requires considerable displacement. Thus, in designing a single pile or a group of vertical piles, the lateral deflection and the structural capacity of the pile not the soil should be the determining factors.

2.7 CRITERION FOR SAFE AND ECONOMIC DESIGN

Like any other structure, piles should be designed to satisfy certain requirements. From engineering point of view, the design of piles should be effective, such that, the chosen piles have to be practical, economical and have an adequate margin of safety. Pile foundations are different from other structures above the ground. Many factors are leading to the difficulties in pile design like the uncertainties in loads and in soil properties. The variability of soil in combination with unanticipated loads or subsequent soil movements can result in settlement problems over which the designer may have little control. Environmental effect is another important factor in the selection and design of

pile foundations. The loss of pile section due to such problems will result in reduction of load capacity. The continuous decrease in cross section with time will lead to a major failure of the structure.

The main factors that determine the selection of the type of piles are the type of the structure and soil condition. The likely foundations are deep, large size footings using cofferdam construction, caissons, groups of large-diameter drilled shafts, or groups of a large number of steel piles. Surface and subsurface geologic and geotechnical conditions are also the other main factors in determining the type of foundations. Subsurface conditions, especially the depths to the load bearing soil layer or bedrock, are the most crucial factors. Diameters of the piles and inclined piles are two important factors to consider in terms of deformation compatibility.

Piles should be designed for both axial and lateral loading conditions. The two principal design considerations for piles under axial loads are ultimate load capacity and settlement. The ultimate load capacity of a pile may be governed either by the structural capacity of the pile or the bearing capacity of the soil. Piles that are subjected to lateral loads must also be safe against ultimate failure of the soil or the pile, and excessive lateral deflections. Axially loaded piles may fail in compression or by buckling. Buckling may occur in long and slender piles that extend for the portion of their lengths through water or air. A scour of the soil around the piles could expose portion of their lengths and increase the likelihood of buckling. Laterally loaded piles will fail in flexure if the induced bending moment exceeds the moment capacity of the pile. The structural capacity of the pile is dependent on both the moment and axial load.

2.8 SUMMARY

In this chapter, an overview of the classification of the piles, its cross sectional types has been given. A brief discussion about the axially loaded and laterally loaded piles has been made. Important soil parameters like soil modulus, the modulus of subgrade reaction and shear modulus of the soil details and their interrelationships are provided. Soil pile interaction behavior and its significance, important design criterion that are needed to be followed are provided at the end of the section. It is with this background in next chapter an attempt was made to discuss the various methods that are available for analysis of laterally loaded piles.

CHAPTER 3

METHODS OF ANALYSIS

3.1 INTRODUCTION

Piles are primarily designed to carry axial loading, but in several situations they are subjected to lateral displacements as well as shear and moment applied at the pile head. Therefore, the pile foundation has to be designed to sustain static and cyclic lateral loads. The problem of piles under lateral loading is much more complex than that of axially loaded piles. Axially loaded piles may be designed using simple static methods, while laterally loaded piles require, sometimes, the solution of the fourth-order differential equation because of their non-linear behavior. The problem also can be solved as a beam on elastic foundation with nonlinear soil-pile interaction behavior. Numerous studies have been conducted trying to investigate the behavior of laterally loaded piles. Figure 3.1 shows a laterally loaded pile subjected to head shear and moment. Each point on the pile will undergo a translation y in the y -direction and a rotation dy/dx about the x -axis. The soil around the pile will also develop pressure p that resists the lateral displacement of the pile.

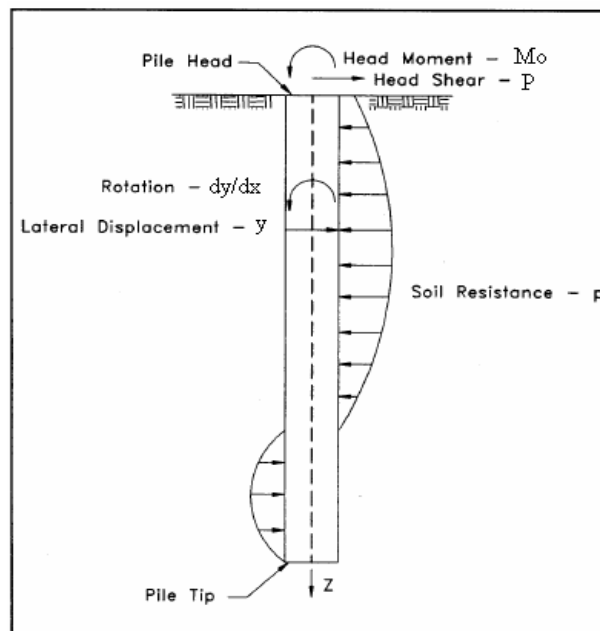


Fig 3.1: Schematic view of laterally loaded pile

The methods used to analyze the response of single piles and pile groups can be categorized into two main approaches; empirical (full-scale and model testing) and theoretical (analytical and numerical). Empirical methods rely on actual in-situ testing or physical laboratory experiments to back figure the characteristics of the pile-soil system such as p-y curves. Theoretical approaches use analytical methods to characterize the pile-soil system and are based on derived solutions including the finite element and boundary element solutions. The following section provides a brief description of the various approaches available.

3.2 EXPERIMENTAL METHODS

A wide range of field and laboratory experiments has been performed by researchers attempting to provide parameters for and to validate soil-pile-structure interaction (SPSI) analytical methods. These experimental methods have been concerned with the load-deformation behavior of soil-pile systems both singly and in groups, at small to large strains, loaded statically, cyclically, dynamically, or seismically, by exciting the pile head or the soil mass, and covering a variety of pile types and soil conditions. In-situ tests have the advantage of providing “correct” soil and pile stress conditions, whereas laboratory tests offer the flexibility and economy of making parametric studies in a controlled environment. Taken together, field and laboratory tests of soil-pile interaction complement each other and provide a valuable body of data where recorded SPSI response is lacking. The following sections provide a comprehensive survey of soil-pile experimental research published in the literature; the purpose of such a review is to understand the adequacy of previous work and the dimensions of further research needs.

3.2.1 Full Scale Pile Test Programs

Pile load test programs conducted in the field offer the distinct advantages of utilizing real soil, real piles, and realistic soil-pile stress conditions. They are limited in the sense that loading is applied in a “top down” fashion, concentrating the effects of inertial interaction and ignoring the effects of kinematics’ interaction.

Reese and co-workers (Reese and Welch, 1975; Reese et al., 1974; Reese et al., 1975) developed a number of criteria for developing single pile p-y curves in clay and sand based on experimental studies. The criteria were based on field tests performed on

0.3- 1.5 m diameter piles which were fitted with strain gauges to obtain moment data over the length of the piles. The experiments were focused primarily on flexible piles and static loading. Matlock (1970) also performed experimental tests on soft clay to derive p-y curves for similar diameter single piles.

3.2.2 Model Scale Pile Test Programs

Model pile tests have offered a wealth of information for SPSI studies, but they must be carefully considered in the context of the particular scale model testing method and its inherent limitations. Scale model tests are economical, versatile, and conducive to parametric studies and repeatability tests. A technique known as “modeling of models” can improve the confidence of the modeling methodology. Both kinematics and inertial interaction effects may be studied, and pile groups with attached superstructures can be readily constructed and tested. Principal limitations of scale model testing include the difficulty in fully satisfying all relevant scale modeling criteria, adequately replicating realistic soil-pile stress fields, and the boundary effects of test containers.

The use of scale models in geotechnical engineering offers the advantage of simulating complex systems under controlled conditions, and the opportunity to gain insight into the fundamental mechanisms operating in these systems. In many circumstances (e.g., a static lateral pile load test), the scale model may afford a more economical option than the corresponding full-scale test. For other investigations (e.g., seismic soil-pile interaction), scale model tests allow the possibility of simulating phenomena that cannot be achieved “at-will” in the prototype. The practice of conducting parameter studies with scale models can be used to augment areas where case histories and/or prototype tests provide only sparse data. In addition to qualitative interpretation, scale model test results are often used as calibration benchmarks for analytical methods, or to make quantitative predictions of the prototype response. For such applications it is necessary to have a set of scaling relations that relate the observed model and predicted prototype behavior which is described by a theory of scale model similitude. They are dimensional analysis, similitude theory, and the method of governing equations.

A number of centrifuge tests (McVay et al. 1995, Barton 1984 etc.,) and 1-g model tests (Cox *et al.*) have been done to know the behavior of piles under various loading conditions.

3.3 NUMERICAL METHODS

The numerical methods may be classified as follows:

- The finite element method (FEM)
- The finite difference method (FDM),
- The boundary element method (BEM), and
- The discrete element method (DEM).

3.3.1 Finite Element Method

The finite element method is a numerical approach based on elastic continuum theory that can be used to model pile-soil-pile interaction by considering the soil as a three-dimensional, quasi-elastic continuum. Finite element techniques have been used to analyze complicated loading conditions on important projects and for research purposes. The salient features of this method have been discussed in the later sections.

3.3.2 Boundary Element Method

Significant advances have been made in the development of the boundary element method and as a consequence, this technique provides an alternative to the finite element method under certain circumstances, particularly for some problems in rock engineering (Beer and Watson, 1992). The main advantages and disadvantages can be summarized as follows.

Advantages

- Pre- and post-processing efforts are reduced by an order of magnitude (as a result of surface discretisation rather than volume discretisation).
- The surface discretisation leads to smaller equation systems and less disk storage requirements, thus computation time is generally decreased.
- Distinct structural features such as faults and interfaces located in arbitrary positions can be modeled very efficiently, and the nonlinear behavior of the fault can be readily included in the analysis (Beer, 1995).

Disadvantages

- Except for interfaces and discontinuities, only elastic material behavior can be considered with surface discretisation.

- In general, non-symmetric and often fully-populated equation systems are obtained.
- A detailed modeling of excavation sequences and support measures is practically impossible.
- The standard formulation is not suitable for highly jointed rocks when the joints are randomly distributed.
- The method has only been used for solving a limited class of problems, e.g., tunneling problems, and thus less experience is available than with finite element models.

3.3.3 Discrete Element Method

The methods described so far are based on continuum mechanics principles and are therefore restricted to problems where the mechanical behavior is not governed to a large extent by the effects of joints and cracks. If this is the case, discrete element methods are much better suited for numerical solution. These methods may be characterized as follows:

- Finite deformations and rotations of discrete blocks (deformable or rigid) are calculated.
- Blocks that are originally connected may separate during the analysis.
- New contacts which develop between blocks due to displacements and rotations are detected automatically.

Due to the different nature of a discrete analysis, as compared to continuum techniques, a direct comparison seems to be not appropriate. The major strength of the discrete element method is certainly the fact that a large number of irregular joints can be taken into account in a physically rational way. The drawbacks associated with the technique are that establishing the model, taking into account all relevant construction stages, is still very time consuming, at least for 3-D analyses. In addition, a lot of experience is necessary in determining the most appropriate values of input parameters such as joint stiffness. These values are not always available from experiments and specification of inappropriate values for these parameters may lead to computational problems. In addition, runtimes for 3-D analyses are usually quite high.

3.3.4 Explicit Finite Difference Method

The finite difference method does not have a long-standing tradition in geotechnical engineering, perhaps with the exception of analyzing flow problems including those involving consolidation and contaminant transport. However, with the development of the finite difference code FLAC (Cundall and Board, 1988), which is based on an explicit time marching scheme using the full dynamic equations of motion, even for static problems, an attractive alternative to the finite element method was introduced. Any disturbance of equilibrium is propagated at a material dependent rate. This scheme is conditionally stable and small time steps must be used to prevent propagation of information beyond neighboring calculation points within one time step. Artificial nodal damping is introduced for solving static problems in FLAC. The method is comparable to the finite element method (using constant strain triangles) and therefore some of the arguments listed above basically hold for the finite difference method as well. However, due to the explicit algorithm employed some additional advantages and disadvantages may be identified.

Advantages

- The explicit solution method avoids the solution of large sets of equations.
- Large strain plasticity, strain hardening and softening models and soil-structure interaction are generally easier to introduce than in finite elements.
- The model preparation for simple problems is very easy.

Disadvantages

- The method is less efficient for linear or moderately nonlinear problems.
- Until recently, model preparation for complex 3-D structures has not been particularly efficient because sophisticated pre-processing tools have not been as readily available, compared to finite element preprocessors.
- Because the method is based on Newton's law of motion no converged solution for static problems exists, as is the case in static finite element analysis.

3.4 ANALYTICAL METHODS

Three criterion must be satisfied in the design of pile foundations subjected to lateral forces and moments: 1) the soil should not be stressed beyond its ultimate capacity, 2) deflections should be within acceptable limits, and 3) the structural integrity of the foundation system must be assured.

The first criteria can be addressed during design using ultimate resistance theories such as those by Brooms (1964a, 1964b) or Brinch Hansen (1961). The second and third criteria apply to deflections and stresses that occur at working loads. The behavior of piles under working load conditions has been the focus of numerous studies over the past 40 to 50 years. Many of these techniques which are mainly used for single piles can be modified to predict the behavior of closely spaced piles, or pile groups. Modifications for group response are often in the form of empirically or theoretically derived factors that are applied, in various ways, to account for group interaction effects such as pile spacing, group arrangement, group size, pile-head fixity, soil type and density, pile displacement etc.

Analytical methods for predicting lateral deflections, rotations and stresses in single piles can be grouped under the following four headings:

- Winkler approach,
- p-y method,
- Elastic continuum approach, and
- Finite element methods.

3.4.1 Beam on Winkler Foundation Model

The Winkler approach, also called the subgrade reaction theory, is the oldest method for predicting pile deflections and bending moments. The pile is modeled as a beam while the surrounding soil is modeled using continuously distributed springs and dashpots (in presence of dynamic loads). Pile nonlinearity may be considered in the analysis using an appropriate nonlinear material model. The details of this approach will be discussed in the next chapter.

The subgrade reaction method is widely employed in practice because it has a long history of use, and because it is relatively straight forward to apply using available chart and tabulated solutions, particularly for a constant or linear variation of E_s with

depth. Despite its frequent use, the method is often criticized because of its theoretical shortcomings and limitations. The primary shortcomings of this approach are:

1. The modulus of subgrade reaction is not a unique property of the soil, but depends intrinsically on pile characteristics and the magnitude of deflection,
2. The method is semi-empirical in nature,
3. Axial load effects are ignored, and
4. The soil model used in the technique is discontinuous. That is, the linearly elastic Winkler springs behave independently and thus displacements at a point are not influenced by displacements or stresses at other points along the pile.

3.4.2 p –y Curve Analysis

The common approach in solving laterally loaded piles is through using p-y curves that represent the soil behavior under various loading. The p-y approach for analyzing the response of laterally loaded piles is essentially a modification of the basic Winkler model, where p is the soil pressure per unit length of a pile and y is the pile deflection. The soil is represented by a series of nonlinear p-y curves that vary with depth and soil type. The p-y curves for laterally loaded piles can be established based on calculations from test results of instrumented full-scale piles. Several factors may influence the accuracy of the p-y curves such as soil properties, number of tests, pile geometry, layers of soil, and nature of loading. Figure 3.2 shows a representation of a nonlinear p-y curves and their variation along the pile depth.

The American Petroleum Institute (API, 1994) recommended practice for offshore platforms gives guidance in determining p-y curves. The origin of the API equation for sand evolved from work by Reese, Cox, and Koop (1974) who established a set of equations based on the forces associated deformation of a soil wedge and the lateral deformation of a rigid cylinder into soil. They established the early shape of the soil load deflection p-y curve based on the soil sub-grade modulus. The procedure was modified by Bogard and Matlock (1980) principally as a simplification by consolidation of terms. The shape of the p-y curve was finally based on work by Parker and Reese (1970).

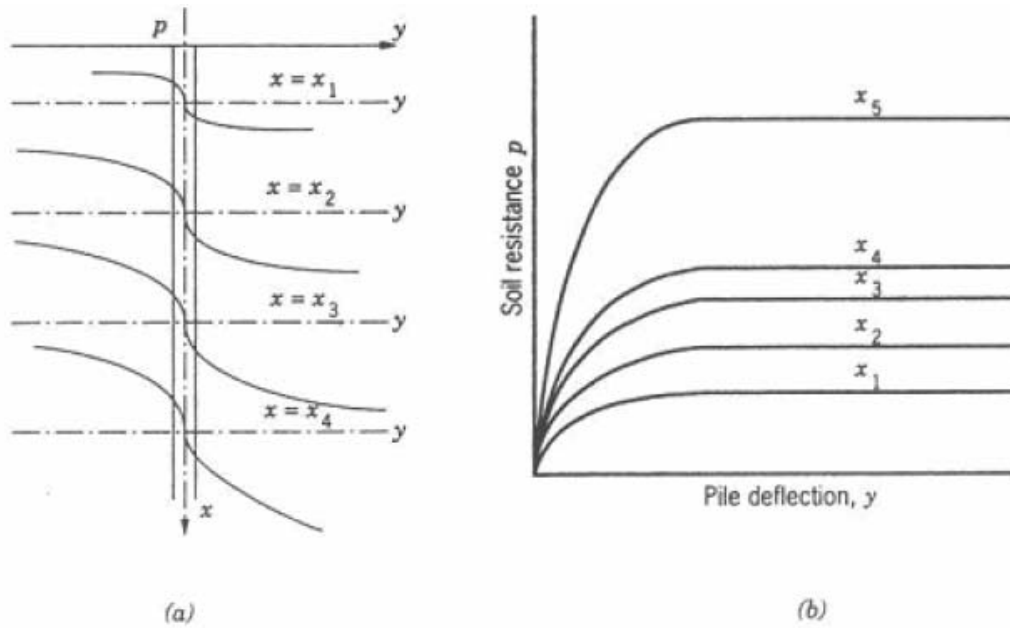


Fig 3.2: Nonlinear p-y curves for laterally loaded piles at various depths x .

3.4.2.1 Piles in Soft Clay

Matlock (1970) performed a series of lateral load tests on some instrumented 320 mm diameter and 12.8 meters long steel pipe piles driven in clays and subjected to static loads.

The lateral soil resistance was expressed in the following form

$$\frac{p}{p_u} = 0.5 \left(\frac{y}{y_{50}} \right)^{1/3} \quad (3.1)$$

where

p_u = ultimate lateral soil resistance per unit length of the pile

y_{50} = lateral movement of the soil corresponding to 50% of the ultimate lateral soil resistance.

y = lateral movement of the soil

The ultimate lateral resistance p_u can be calculated as the smaller of

$$p_u = \left(3 + \frac{\gamma'}{c} z + \frac{J}{d} z \right) c \cdot d \quad (3.2)$$

$$p_u = 9 \cdot c \cdot d \quad (3.3)$$

γ' = average effective unit weight from ground surface to p-y curve

c = shear strength at depth z

d = width of pile or diameter of the pile

J = constant taken as 0.5 for soft clay and 0.25 for medium clay

z = depth from ground surface to the p-y curve

Z_r = depth below soil surface to bottom of reduced resistance zone. Equations 3.2

and 3.3 can be solved simultaneously to get the value of Z_r , for a condition of constant strength with depth.

Figure 3.3 shows the shapes of the p-y curves for static and cyclic loading recommended by Matlock (1970) for soft clays above the water table.

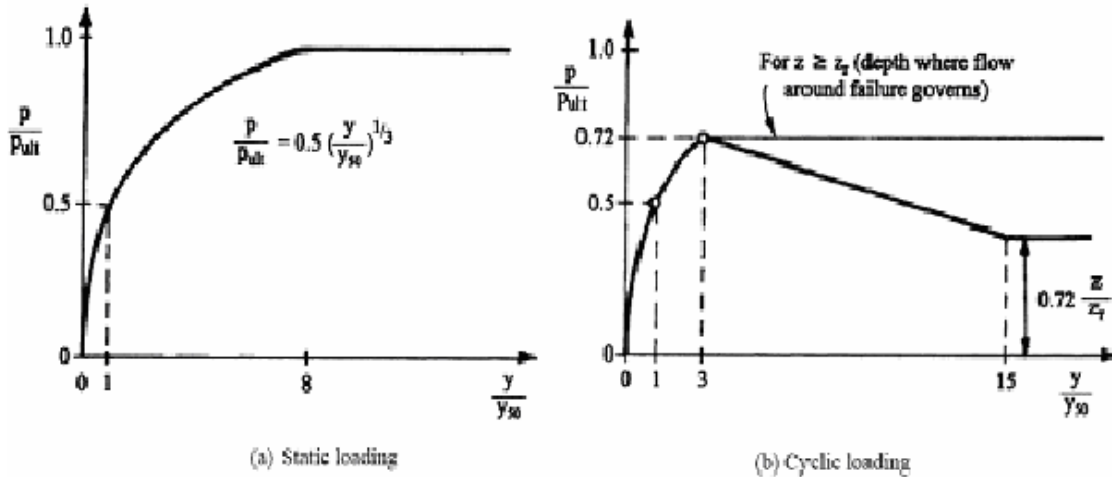


Fig 3.3: Characteristic shapes of the p-y curves for soft clay

The lateral displacement at 50% of the ultimate soil resistance can be calculated from the following equation

$$y_{50} = 2.5 \varepsilon_{50} d \quad (3.4)$$

where ε_{50} = Strain at 50 percent of the ultimate strength from a laboratory stress-strain curve. These values are found to vary in between 0.004 to 0.020 after filed tests were conducted.

3.4.2.2 Piles in Stiff Clay

Stiff clay with free water

Reese et al. (1975) describe lateral load tests employing two steel-pipe piles that were 15.2 m long, with a diameter of 610 mm. The piles were driven in a stiff clay site near Manor, Texas. The clay at the site was strongly over consolidated and fissured. The undrained shear strength of the clay was measured by unconsolidated undrained triaxial tests with confining pressure equal to the overburden pressure. The undrained shear strengths varied from around 70 kPa near the surface to 1100 kPa at the toe of the piles. The site was excavated to a depth of about 0.9 m and water was kept above the surface of the site for several weeks prior to obtaining data on the soil properties. The values of ϵ_{50} were found from experiment but scatter was great. On an average, the ϵ_{50} values ranged from 0.004 to 0.007.

Both of the piles were instrumented using electrical-resistance strain gauges for measurement of bending moment. The gauge readings were taken with a rapid electronic data-acquisition system. Curvature was calculated from these readings, which in turn was used to infer moment (assuming a linear moment-curvature relationship). The loads were applied 0.3 m above ground line. One pile was loaded under static loading with the load being increased until the bending moment was near yield moment. The second pile was tested under cyclic loading and the loads were cycled under each increment until deflections were stabilized. The number of cycles of loading was on the order of 100 and applied at a rate of two cycles per minute.

Experimental p-y curves were derived through a combination of methods. First, p was obtained by double-differentiating the bending moment diagram using the following procedure. The modulus of subgrade reaction for a particular moment curve was assumed to be described by a two-parameter function, i.e. $k = \alpha z^n$. Non-dimensional solutions for soil reaction profiles were developed that are a function only of α and n. Using these relations, numerical values of α and n were obtained by a fitting technique described in Reese and Cox (1968). This procedure was repeated for each load and corresponding moment curve. Values of y were obtained through double integration of curvature readings. The p and y values were coupled to generate p-y curves, and the characteristic shapes of these p-y curves for static and cyclic loading are shown in Figure 3.4.

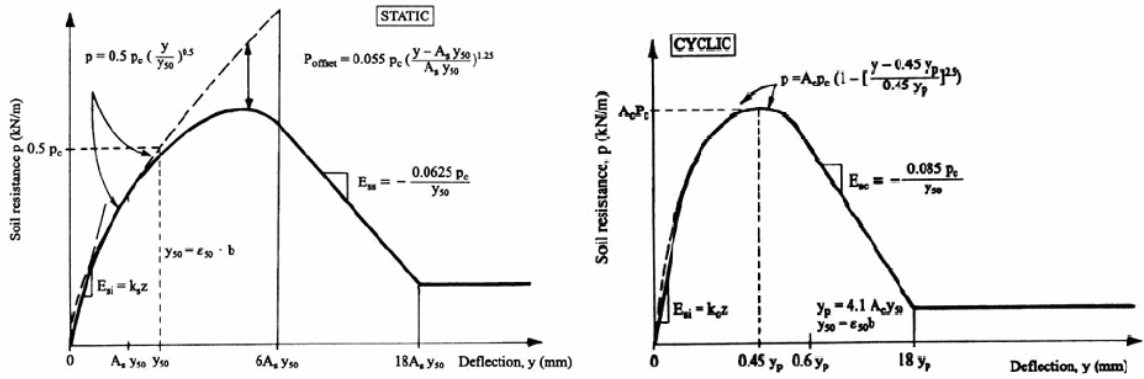


Fig 3.4: Characteristic shape of p-y curves for static and cyclic loading in stiff clay in the presence of free water (Reese et al., 1975)

Stiff clay without free water

Reese and Welch (1975) reported the results of a test of a drilled shaft with a diameter of 760 mm and penetration length of 12.8 m. An instrumented steel pipe, with a diameter of 260 mm formed the core of the shaft. Concrete was placed around the shaft along with a rebar cage, consisting of 44.5 mm diameter bars. The site, near Houston, Texas, consisted of overconsolidated, fissured clay, locally known as Beaumont clay. The water table was at a depth of 5.5m. The measured undrained shear strength, which averaged between 75kPa to 163kPa, was evaluated with unconsolidated-undrained triaxial compression tests with confining pressures equal to the overburden pressure. Values of ϵ_{50} averaged 0.005.

Both static and cyclic lateral loads were applied just above ground line. A polynomial describing a truncated power series was used to fit the measured moment data vs. depth. The deflection of the shaft was determined by double-integrating the polynomial fit curve. The second differentiation of this curve yields values of soil reaction. Boundary conditions used were the measured deflections at the top of the shaft and an assumed zero deflection at the bottom of the shaft. Field measurements of moments along the pile were compared to analytical predictions derived using the field

derived p-y curves. Figure 3.5 shows the resulting characteristic shape of p-y curves

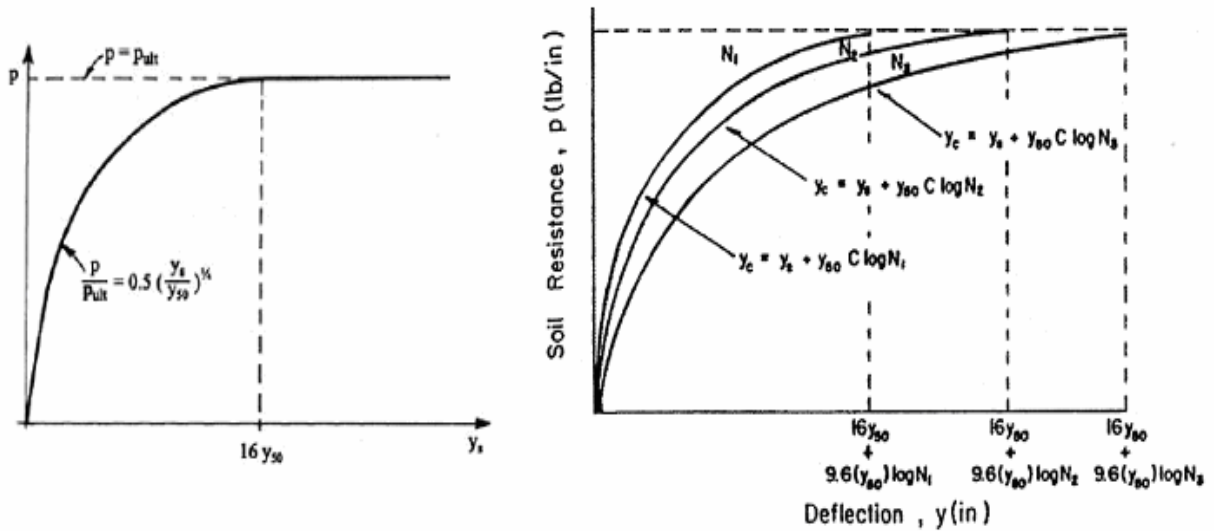


Fig 3.5: Characteristic shape of p-y curves for static and cyclic loading in stiff clay with no free water (Reese and Welch, 1975)

3.4.2.3 Piles in Sand

Cox *et al.* (1974) describe lateral load tests employing two steel-pipe piles that were nearly 21 m long and 610 mm in diameter. Both piles were driven into sand at a site on an island near Corpus Christi, Texas. The soil at the site was uniformly graded, fine sand with a friction angle of 39 degrees. The water level was kept just above the mud line throughout the test. One pile was subjected to static loading while the second underwent cycling loading. Both piles were instrumented with electrical-resistance strain gauges. The method for inferring p-y curves from the test results was similar to that employed by Reese *et al.* (1975) for the stiff clay with free water case. Figure 3.6 shows the characteristic shape of p-y curves for static loading in sand (Cox *et al.*, 1974).

Lateral bearing capacity for sand: The ultimate lateral bearing capacity for sand has been found to vary from a value at shallow depths determined by Equation 3.5 to a value at deep depths determined by Equation 3.6. At a given depth the equation giving the smallest value of P_u should be used as the ultimate bearing capacity.

$$P_{us} = (C_1 Z + C_2 D) \gamma' Z \quad (3.5)$$

$$P_{ud} = C_3 D \gamma' Z \quad (3.6)$$

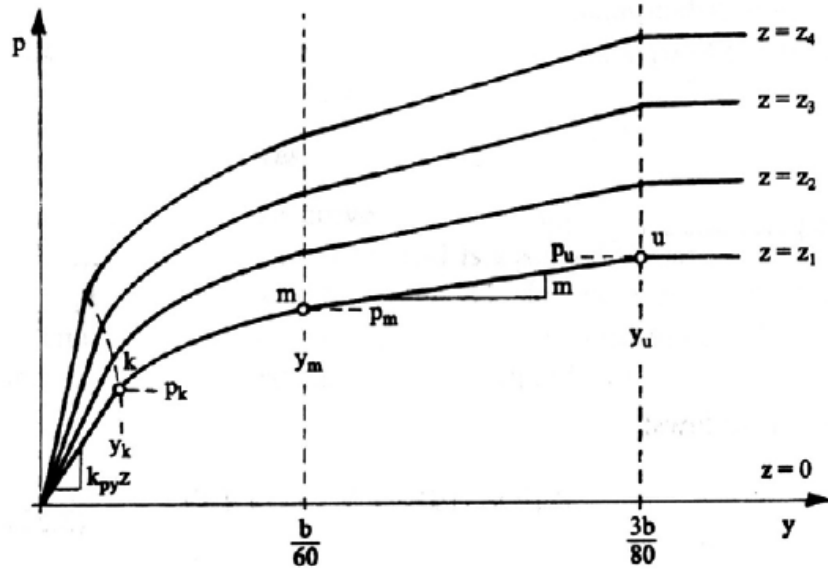


Fig 3.6: Characteristic shape of p-y curves for static loading in sand (Cox et al., 1974)

where

P_u = ultimate resistance (force/unit length) (s=shallow, d=deep)

γ' = average effective unit weight from ground surface to p-y curve

Z = depth

ϕ' = angle of internal friction in sand

C_1 = Coefficient determined from Figure 3.7 as a function of ϕ'

C_2 = Coefficient determined from Figure 3.7 as a function of ϕ'

C_3 = Coefficient determined from Figure 3.7 as a function of ϕ'

D = average pile diameter from surface to depth

The lateral soil resistance-deflection (p-y) relationship for sand is also nonlinear and in the absence of more definitive information may be approximated at any specific depth Z , by the following expression.

$$P = A p_u \tanh [(k Z y) / (A p_u)] \quad (3.7)$$

where

A factor to account for cyclic or static loading continued.

$A = 0.9$ for cyclic loading.

$A = (3.0 - 0.8 Z/D) \geq 0.9$ for static loading.

k = initial modulus of subgrade reaction in force per volume units and can be determined from Figure 3.8 as a function of angle of internal friction.

y = lateral deflection.

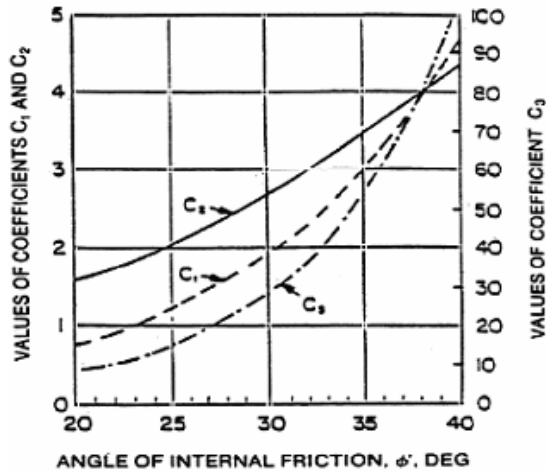


Fig 3.7: API Coefficients for sand.

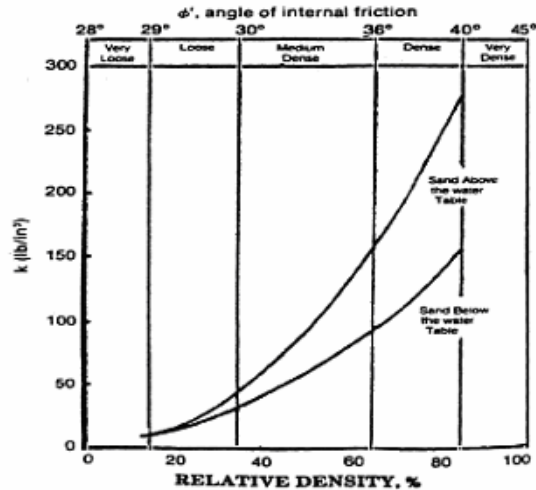


Fig 3.8: API initial modulus of subgrade reaction.

The p-y method is readily adapted to computer implementation and is available commercially in the computer programs LPILEPlus 5.0 (1985 - 2006) and COM624 (1993). The method is an improvement over the subgrade reaction approach because it accounts for the nonlinear behavior of most soils without the numerical limitations inherent in the subgrade reaction approach. However, the method has some limitations, as described below:

1. The p-y curves are independent of one another. Therefore, the continuous nature of soil along the length of the pile is not explicitly modeled.
2. Suitable p-y curves are required. Obtaining the appropriate p-y curve is analogous to obtaining the appropriate value of E_s ; one must either perform full scale instrumented lateral load tests or adapt the existing available standard curves (default curves) for use in untested conditions. These default curves are limited to the soil types in which they were developed; they are not universal.
3. A computer is required to perform the analysis.

3.4.3 Elastic Continuum Approach

Poulos (1971a, 1971b) presented the first systematic approach for analyzing the behavior of laterally loaded piles and pile groups using the theory of elasticity. Because the soil is represented as an elastic continuum, the approach is applicable for analyzing battered piles, pile groups of any shape and dimension, layered systems, and systems in which the soil modulus varies with depth. The method can be adapted to account for the nonlinear behavior of soil and provides a means of determining both immediate and final total movements of the pile. This approach is based on Mindlin's (1936) closed form solution for the application of point loads to a semi-infinite mass. The accuracy of these solutions is directly related to the evaluation of the Young's modulus and the other elastic parameters of the soil.

The pile is assumed to be a vertical strip of length L , width D (or diameter, D , for a circular pile), and flexural stiffness $E_p I_p$. It is divided into $n+1$ elements and each element is acted upon by a uniform horizontal stress p . The horizontal displacements of the pile are equal to the horizontal displacements of the soil. The soil displacements are expressed as:

$$\{y_s\} = \frac{d}{E_s} [I_s] \{p\} \quad (3.8)$$

where

$\{y_s\}$ = the column vector of soil displacements,

$\{p\}$ = the column vector of horizontal loading between soil and pile, and

$[I_s]$ = the $n+1$ by $n+1$ matrix of soil displacement influence factors determined by integrating Mindlin's equation, using boundary element analyses.

The finite difference form of the beam bending equation is used to determine the pile displacements. The form of the equation varies depending on the pile-head boundary conditions. Poulos and Davis (1980) present expressions for free-head and fixed-head piles for a number of different soil and loading conditions. One of the biggest limitations of the method (in addition to computational complexities) is the difficulty in determining an appropriate soil modulus, E_s .

3.4.4 Finite Element Analysis

The finite element method is a numerical approach based on elastic continuum theory that was initially developed for the analysis of problems in structural mechanics, but it was realized later that this method can be applied to solutions for many other kinds of problems. One such problem where this method can be used was pile-soil-pile interaction by considering the soil as a three-dimensional, quasi-elastic continuum. Finite element techniques have been used to analyze complicated loading conditions. Main features of this powerful method include the ability to simulate any combination of axial, torsion, and lateral loads; the capability of considering the nonlinear behavior of structure and soil; and the potential to model pile-soil-pile-structure interactions.

The method works on the principle of solving the problem by going from a small part to the whole. The whole medium of the problem is assumed to consist of a combination of small parts joined together to form the whole structure. Various types of elements are used to represent the different structural components. For instance, we can use three-dimensional two-node beam elements to model the piles, pier columns, and pier cap, and three-dimensional 9- node flat shell elements for the pile cap. Interface elements are often used to model the soil-pile interface. These elements provide for frictional behavior when there is contact between pile and soil, and do not allow transmittal of forces across the interface when the pile is separated from the soil. The small parts (elements) then are assembled to reach the final solution. Solutions resulting from finite element analysis are not exact solutions. Pile displacements and stresses are evaluated by solving the classic beam bending equation using one of the standard numerical methods. Numerous finite element codes are available with high capabilities in handling very complicated structures. ANSYS, ABAQUS, NASTRAN etc are such software's which are used nowadays widely for analysis purpose. Analysis of a structural problem using finite element method briefly consists of the following three stages:

1. Building the model (Preprocessing).
2. Applying loads and obtain solutions (Solution).
3. Reviewing the results (Post Processing)

Advantages

- a) Nonlinear material behavior can be considered for the entire domain analyzed.
- b) Structural features in the soil or rock mass, such as closely spaced parallel sets of joints or fissures, can be efficiently modeled.
- c) Time dependent results can be obtained and more intricate conditions such as battered piles, slopes, excavations, tie-backs, and construction sequencing can be modeled.
- d) Special formulations are now available for other types of geotechnical problem, e.g., seepage analysis, and the bound theorem solutions in plasticity theory.
- e) The method has been extensively applied to solve practical problems and thus a lot of experience can be gained.

Disadvantages

The following disadvantages are particularly pronounced for 3-D analyses and are less relevant for 2-D models.

- a) The entire volume of the domain analyzed has to be discretized, i.e., large pre- and post-processing efforts are required.
- b) Due to large equation systems, run times and disk storage requirements may be excessive (depending on the general structure and the implemented algorithms of the finite element code).
- c) The method is generally not suitable for highly jointed rocks or highly fissured soils when these defects are randomly distributed and dominate the mechanical behavior.
- d) Performing three- dimensional finite element analyses requires considerable engineering time for generating input and interpreting results. For this reason, the finite element method has been used mainly for analysis of piles rather than for design.

3.5 SUMMARY

In this chapter an understanding of the various methods of analyses has been made. With this background in the next chapter to have a preliminary understanding of behavior of piles Winkler's analyses was done.

CHAPTER 4

WINKLER'S ANALYSIS OF LATERALLY LOADED PILES

4.1 BACKGROUND

Though there are many methods with their advantages the Beam-on-Winkler-Foundation model, as it is a basic, versatile and efficient approach to pile foundation analysis, has been adopted for the preliminary investigation of single piles under lateral loading. The Winkler approach, also called the subgrade reaction theory, is the oldest method for predicting pile deflections and bending moments. The pile is modeled as a beam while the surrounding soil is modeled using continuously distributed springs and dashpots (if dynamic loads are under consideration) as shown in the Fig.4.1 below.

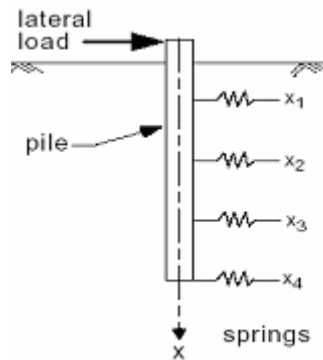


Fig.4.1: Single pile model

The behavior of a single pile can be analyzed using the equation of an elastic beam supported on an elastic foundation (Hetenyi 1946), which is represented by the 4th order differential beam bending equation:

$$E_p I_p \frac{d^4 y}{dz^4} + Q \frac{d^2 y}{dz^2} + E_s y = 0 \quad (4.1)$$

where

E_p = the modulus of elasticity of the pile,

I_p = the moment of inertia of the pile section,

Q = the axial load on the pile,

z = the vertical depth,

y = the lateral deflection of the pile at point z along the length of the pile
and E_s = the modulus of soil reaction (or soil modulus).

The approach uses Winkler's modulus of sub-grade reaction concept to model the soil as a series of unconnected linear springs with stiffness, E_s , expressed in units of force per length squared (FL^{-2}).

The governing equation for the deflection of a laterally loaded pile, obtained by ignoring the axial component, is:

$$\frac{d^4 y}{dz^4} + \frac{E_s}{E_p I_p} y = 0 \quad (4.2)$$

Solution to above equation has been obtained by making simplifying assumptions regarding the variation of E_s (or k_h) with depth. E_s is the modulus of soil reaction (or soil modulus) defined as:

$$k_h = -p/y \quad (4.3)$$

where

p = the lateral soil reaction per unit length of the pile, and

y = the lateral deflection of the pile (Matlock and Reese, 1960). The negative sign indicates the direction of soil reaction is opposite to the direction of the pile deflection.

The solution of the differential equation is obtained by employing appropriate boundary conditions, soil response and soil modulus values respectively. The boundary conditions at the top are shear force is equal to lateral load applied and bending moment applied is equal to applied moment (in the present case it is zero). At the bottom of the pile for a long length slope and deflections are zero. The numerical solution has been programmed using the programming language MATLAB 7.0.

The data that has been used in calculation are as given below. Unless otherwise mentioned these are the values that are taken throughout.

Concrete pile elastic modulus of elasticity (E_p) = 2.8×10^{10} N/m²

Pile diameter in meters (D) = 0.7

Pile length in meters (L) = 12

Lateral load in N (P) = 30000

Table 4.1: Value range for the static stress-strain modulus
Es for selected soils (Bowles, 1996)

Type of soil	Modulus of elasticity, MPa
Very soft clay	2-15
Soft clay	5-25
Medium clay	15-50
Hard clay	50 – 100
Sandy clay	25 - 250
Silt	2 – 20
Silty sand	5 – 20
Loose sand	10 – 25
Dense sand	50 – 81
Loose sandy gravel	50 – 150
Dense sandy gravel	100 – 200

Table 4.2: Values of modulus of sub-grade reaction (Terzaghi, 1955)

Type of soil	Modulus of sub grade reaction in kN/m ³
Loose sand	1100 – 3300
Medium sand	3300 – 11000
Dense sand	11000 – 23400

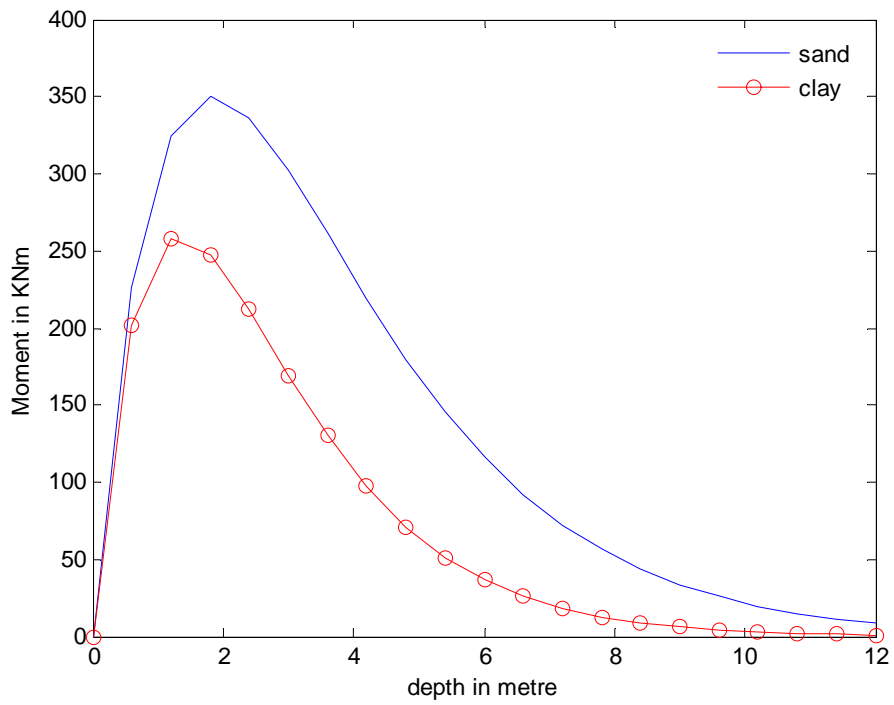
4.2 DISCUSSION ON THE RESULTS OF WINKLER'S MODEL

It was observed from the results that deflections and bending moments of piles in sand are almost twice to that of clay. This is due to the fact that the stiffness of soil is mainly a function of confining pressure and the soil has low confining pressure at the top. In the case of different kinds of same soil type i.e., sand or clay, deflections and bending moments are varying depending on the variations in the denseness of the soil depicting the effect of considering the variation of modulus.

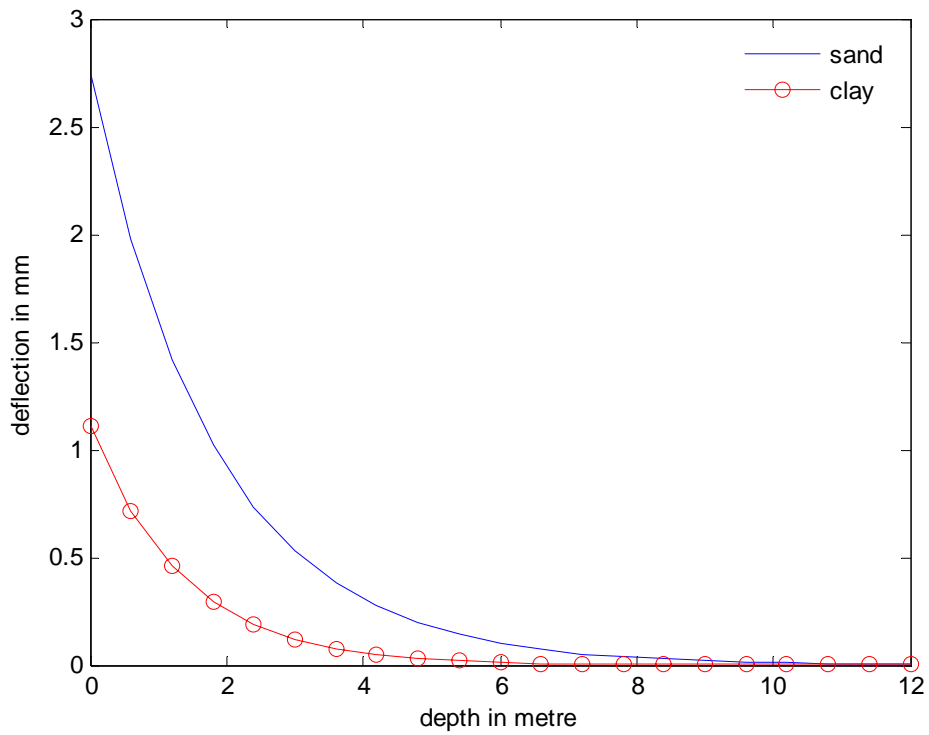
In case of piles with varying cross sectional shape (i.e., considering for two cases square and circular of side and diameter equal to 0.7m) in sandy soils it has been observed that moments generated in circular are less in comparison to square pile. Almost same is the case with reference to deflections. This trend of behavior may be attributed to the rigidity of the pile.

In case of varying pile sizes, it has been observed that piles with small diameter are showing larger deflection at shallow depths in comparison with large diameter piles. But this trend has been reversed at larger depths.

For varying modulus of sub-grade reaction in case of sands the deflections and bending moments decreased as the relative density of the soil increased again stressing the importance of soil properties. For varying lateral loads it is observed that as the lateral load increases pile deflections and moments also increased in proportion. For observed behavior of different lateral loads application maximum pile deflection values are taken to obtain the relationship between lateral load and pile head deflection.



(a) Moment variation with depth



(b) Deflection variation with depth

Fig 4.2: Comparison of pile behavior in clay and sand soil With respect to (a) moment (b) deflection.(Using Bowles,1996)

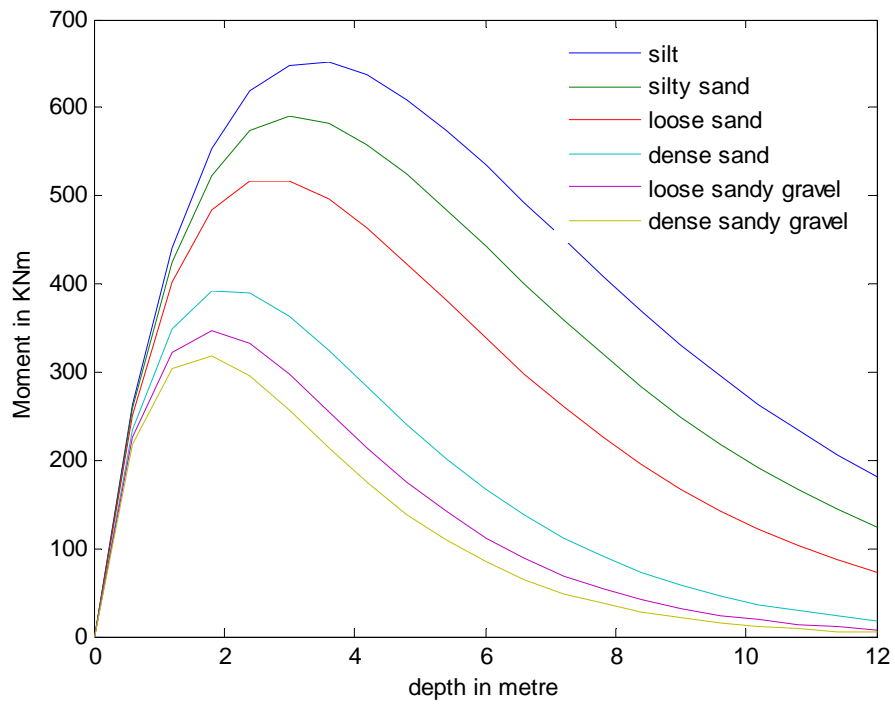
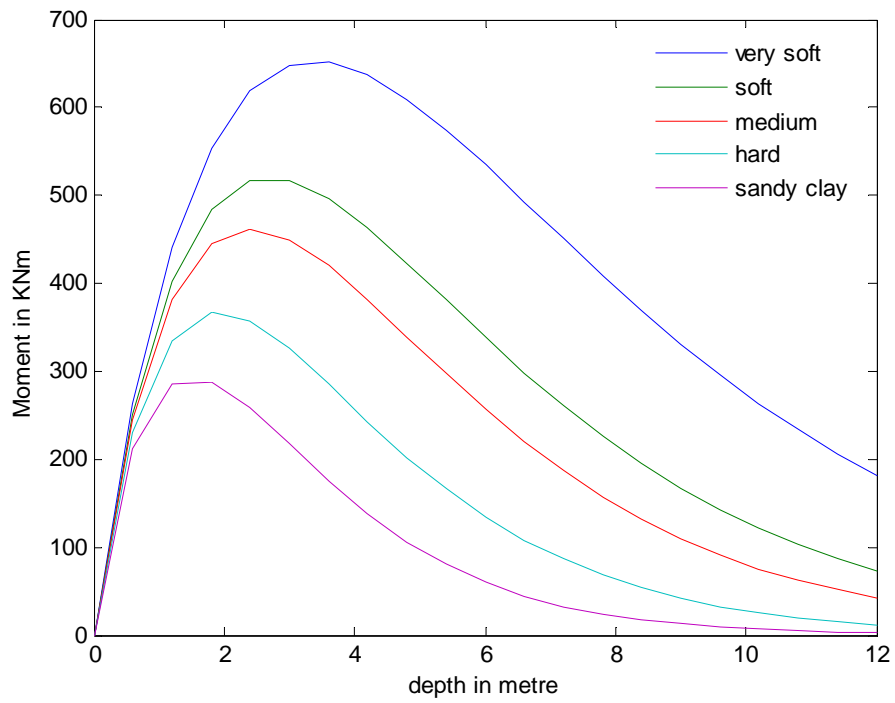


Fig 4.3: Moment variation for different types of soils in clay and sand (Using Bowles, 1996)

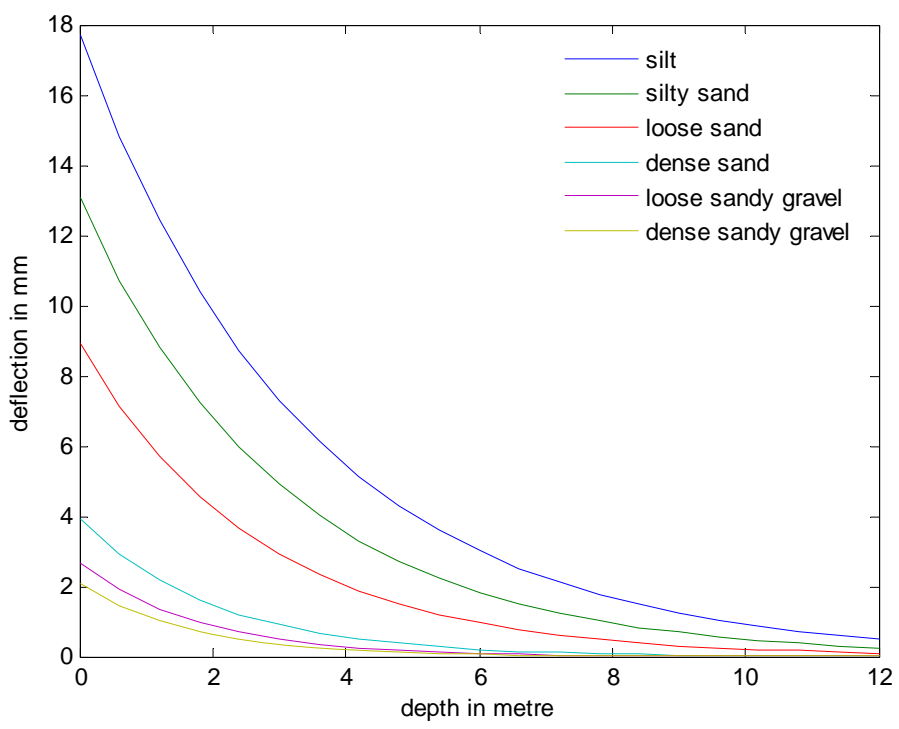
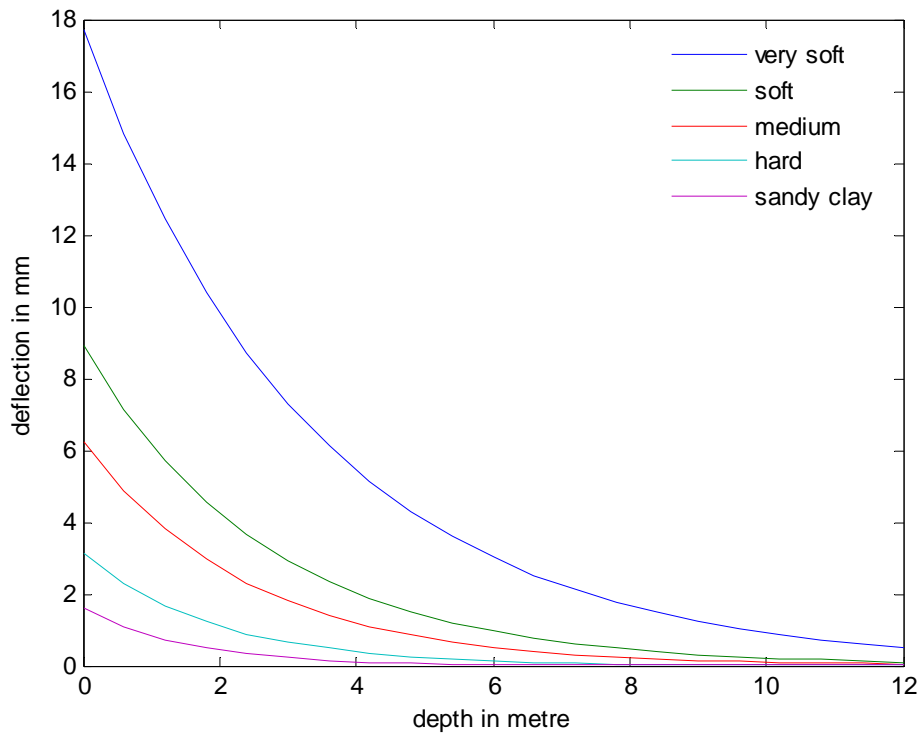
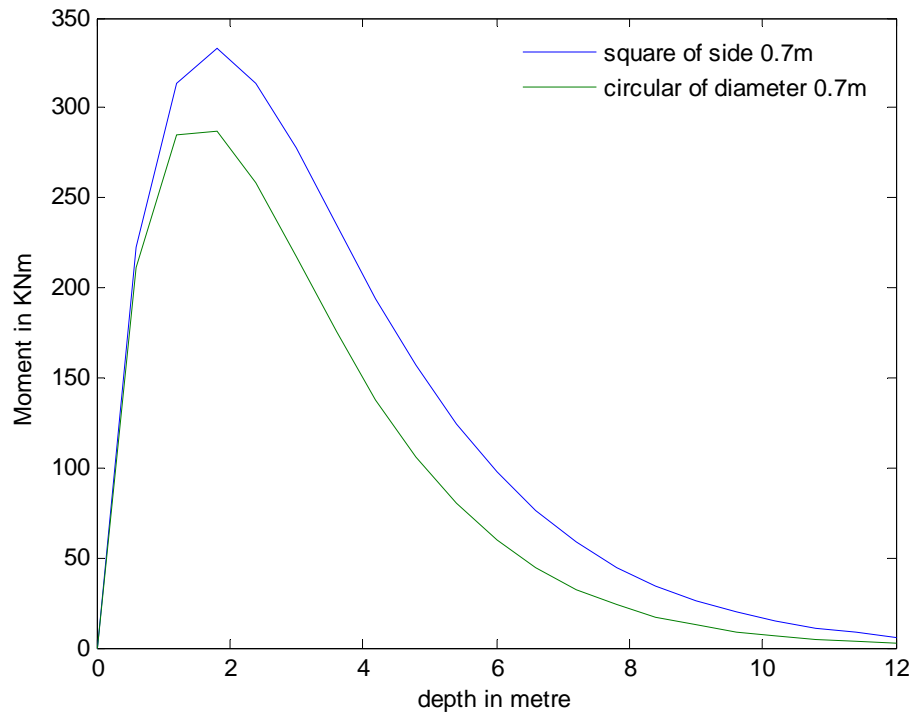
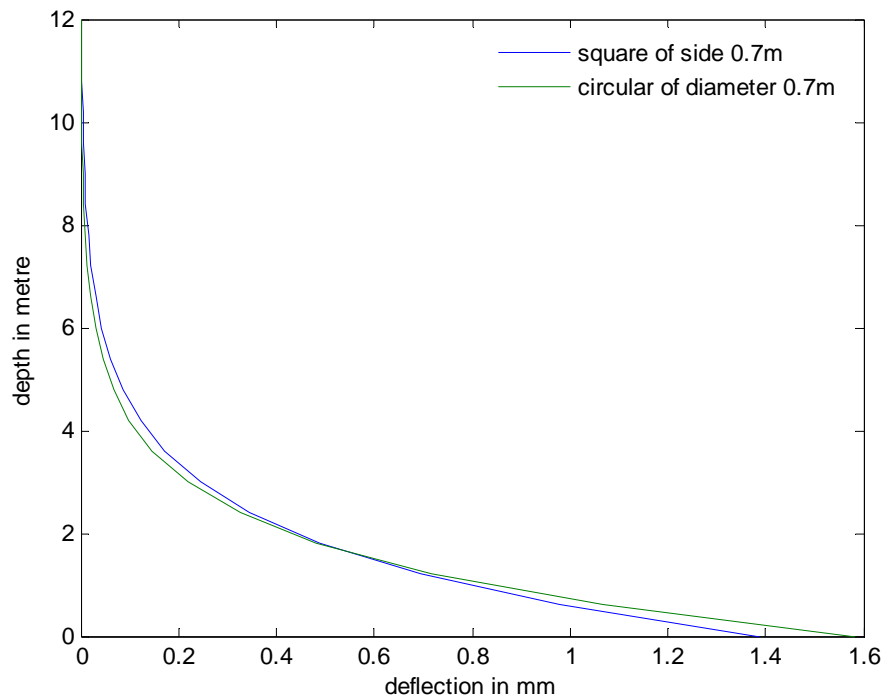


Fig 4.4: Deflection variations for different types of soils in clay and sand (Using Bowles, 1996)

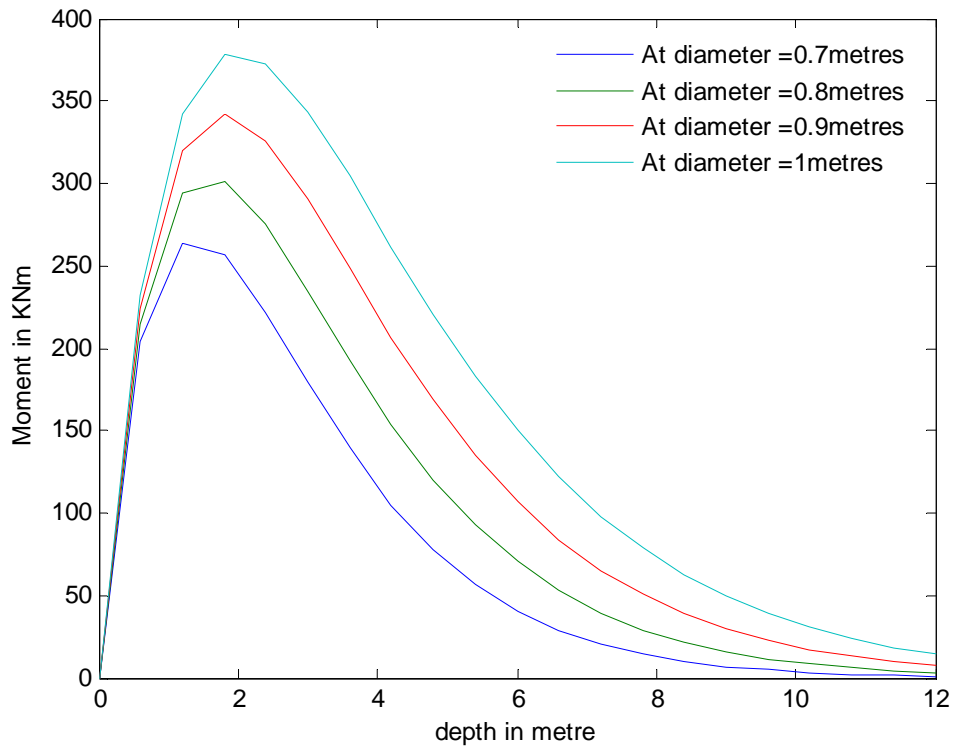


(a) Moment distribution with respected to depth

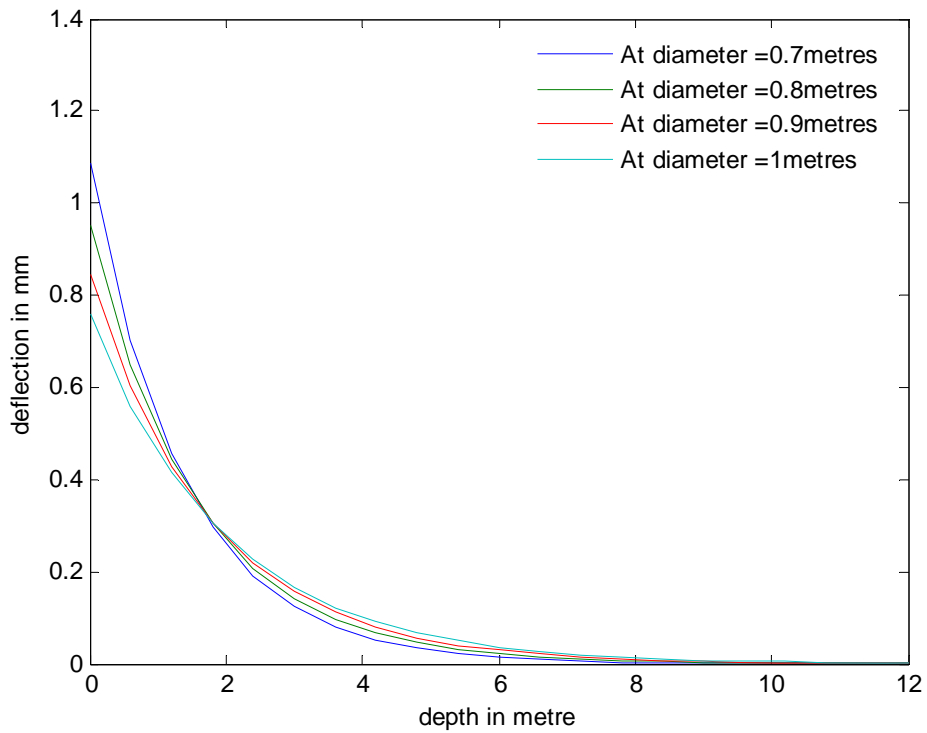


(b) Deflection variation with respected to depth

Fig 4.5: Effect of pile cross sectional shape on (a) moment (b) deflection

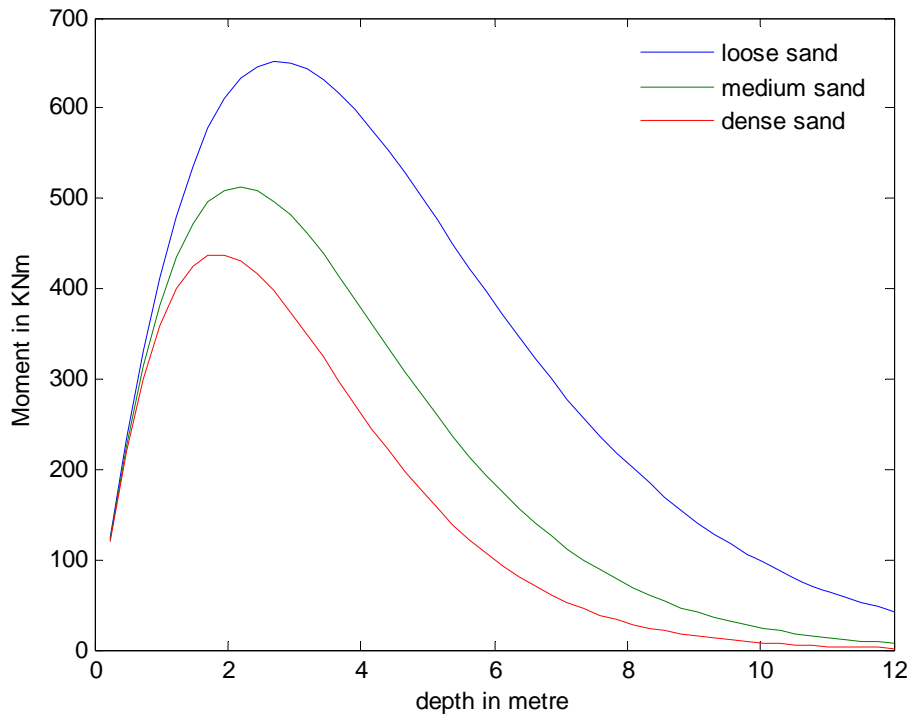


(a) Moment variation with respected to depth in clay

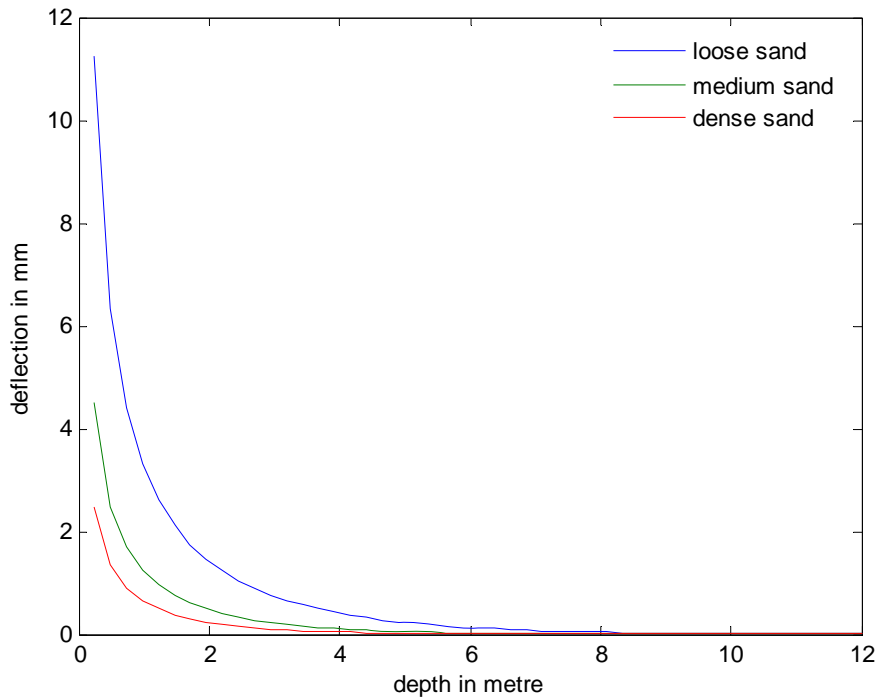


(b) Deflection variation with respected to depth in clay

Fig 4.6: Effect of pile cross sections size on (a) moment (b) deflection in clay



(a) Moment distribution with respected to depth



(b) Deflection variation with respected to depth

Fig 4.7: Effect of the modulus of sub-grade reaction on (a) moment (b) deflection (Using Terzaghi, 1955)

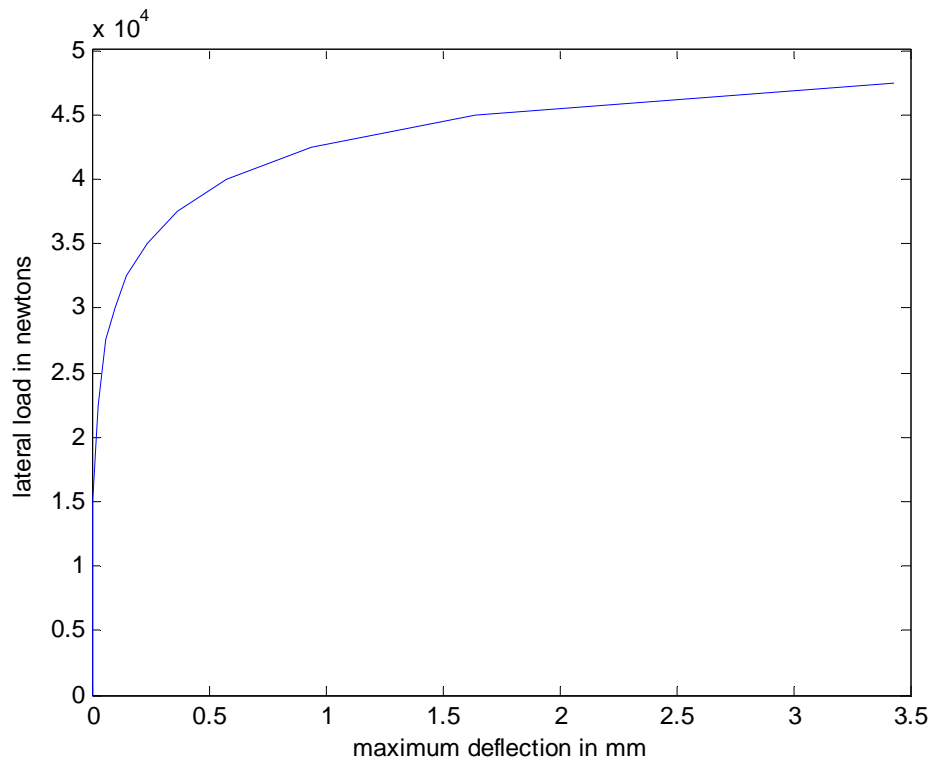


Fig 4.8: Load – deflection curve

4.3 SUMMARY

In this chapter, a simplified analysis of the laterally loaded single pile (mainly for free head piles) was done using Winkler’s beam on elastic foundation method. Behaviour of the piles under varying loads, soil types, pile materials, pile cross sections etc was made in detail. A relationship between the lateral load and pile head deflections has been obtained. Results obtained using this approach are briefly discussed. As this approach is based on the assumption that pile is taken as beam and the soil around it as elastic springs which is a limitation. In reality, soil – pile interaction behaviour will vary in the radial and circumferential direction also. It is with this motivation a new load transfer approach has been developed in the next chapter.

CHAPTER 5

NUMERICAL ANALYSIS OF LATERALLY LOADED PILES

5.1 INTRODUCTION

As a foundation problem, the analysis of a pile under lateral loading is complicated by the fact that the soil reaction is dependent on the pile movement, and the pile movement, on the other hand, is dependent on the soil response. Thus, the problem is one of soil-structure interaction. Many methods such as the subgrade reaction method, the elastic continuum approaches have been developed as an alternative to the time consuming finite element method for the analysis of laterally loaded soil-pile system (Broms 1965; Desai 1974; Poulos 1980; and Reese 1986). In most of these methods, the pile is modeled as a flexible beam. The main difference among the various methods is the approach of the soil behavior used in the model. The majority of the soil models can be grouped into two classes. In the first class, the soil behavior is represented by a series of independent nonlinear springs. This allows one to follow closely the soil profile by using p-y curves (Matlock and Reese 1960; Matlock 1970; Reese et al. 1974). In the second class of models, the soil is represented by an elastic continuum. The represented method of second class is developed by Poulos (1971a, 1971b, 1972). Poulos has presented an approximate numerical solution for laterally loaded pile and the pile is represented as an infinitely thin linearly elastic strip embedded in an elastic media. Some further developments of elastic continuum analysis (Randolph 1981) and finite-element methods (Desai 1974) are also done.

In the uncoupled (Winkler) model, the elastic springs are generally represented by the modulus of subgrade reaction. This modulus was obtained through fitting with relevant rigorous numerical solutions (e.g., Vesic, Terzaghi etc). The problem is that the fitting to different reactions (e.g. deflection or moment of a beam or a pile) generally leads to different values of modulus. This difference in modulus implies that (1) the uncoupled model is not sufficiently accurate for simulating the pile-soil interaction; and

(2) the use of the available modulus developed for beams to pile analysis is only an interim measure. The available experiments demonstrate that the displacement field around a laterally loaded pile is significantly different from that around a beam sitting on an elastic medium. Thus, different modulus for beams and lateral piles should be adopted.

As in the analysis of vertically loaded piles, the subgrade modulus is affected by the soil response in radial direction. To accommodate this effect, uncoupled expressions relating the pile displacement, $y(z)$, to a radial attenuation function for soil displacement, $\varphi(r)$ are generally assumed for displacements in the radial (u) and circumferential (v) directions, which are then implicitly linked (coupled) through a fitting factor, γ . The principal parameter (γ) is used in this model to present the elastic foundation, and an iterative technique is adopted to obtain a consistent energy solution based on the variational approach. The approach also leads to expressions as the sole variables of γ for the two parameters, namely the modulus of subgrade reaction, k (for the Winkler springs), and the fictitious tension, N (for a stretched membrane used to tie together the springs). Thus the model derived from the approach is normally referred to as a two-parameter (or Vlasov's foundation) model. The challenge of this modeling lies in the estimation of the fitting factor, γ which in turn depends on the uncoupled expressions for the (u , v) displacements. The modified Vlasov model for the static analysis of beams on elastic foundations has been proposed by Vallabhan and Das (1988, 1991). Both free and fixed head piles have been considered. Two kinds of boundary conditions of practical interest at the pile tip, floating tip and clamped tip, are also considered.

In using the variational approach, a potential energy for a pile-soil system is first determined in terms of the stress components in the pile and the soil, which, in turn, may be derived from the uncoupled expressions of the (u , v) displacements using elastic theory. Furthermore, the derived stress field may be simplified by ignoring higher order stress components, similar to those for vertical and torsional piles. To distinguish the cases using different derived stresses, in the present case the two-parameter model refers only to the former case; while the case using the simplified stress field is referred to as load transfer model. The fitting factor is termed accordingly as the load transfer factor (γ). The goal, of using assumed displacement (or displacement and stress) expressions, is

to estimate the fitting (load transfer) factor. The sacrifice of using an approximate stress field often leads to exact closed-form solutions for piles. In contrast, complicated expressions for piles may result from using assumed displacement expressions only (e.g. those adopted in the two parameter model). Particularly for a laterally loaded pile, the results from the two-parameter model are unstable and unreasonable at a high Poisson's ratio, e.g. $\nu_s \geq 0.3$.

In brief, the main features of this approach are:

(1) It shows that the effect of Poisson's ratio on pile response may be accounted for through the shear modulus.

(2) It shows that less important stress components may be ignored, in order to generate the load transfer factor.

(3) It illustrates that the modulus of subgrade reaction and the fictitious tension are the energy parameters due to the stress variations in radial direction, and vertical direction, respectively.

(4) It demonstrates that critical pile length depends on loading characteristics (lateral concentrated load, or moment) and pile-head, and/or base conditions.

5.2 DESCRIPTION OF MODEL

5.2.1 Displacement and stress field

As depicted in Figure 5.1(a), the problem addressed herein is the response of a circular pile subjected to horizontal loading of load P and moment M_0 at the pile-head level, which is represented (Figure 5.1(b)) by the displacement, y , the bending moment, M , and the shear force, Q . The pile is of length, L , and radius, r_0 and is embedded in an elastic medium. The medium is assumed to be linear, homogeneous and has isotropic properties. The displacement and stress fields in the soil around the pile are described by a cylindrical coordinate system r , θ and z as depicted in Figure 5.2(a). The displacement and stress fields in the soil around the pile are described by a cylindrical coordinate system r , θ and z as depicted in Figure 5.2(a).

The displacement field around the laterally loaded pile is nonaxisymmetric, and normally dominated by radial u , and circumferential displacement v ; while the vertical displacement, w is negligible. Thus, the field may be expressed in Fourier series

$$u = \sum_{n=0}^{\infty} y_n(z) \phi_n(r) \cos n\theta \quad v = -\sum_{n=0}^{\infty} y_n(z) \phi_n(r) \sin n\theta \quad w=0 \quad (5.1)$$

where $y_n(z)$ is the n^{th} component of the pile body displacement at depth, z and in the direction of the n^{th} loading component; $\phi_n(r)$ the n^{th} component of the attenuation function of soil displacement at a radial distance, r from the pile axis; and θ angle between the line joining the center of the pile cross-section to the point of interest and the direction of the n^{th} loading component. The elastic constitutive law in the cylindrical coordinates is given as

$$\begin{Bmatrix} \sigma_r \\ \sigma_\theta \\ \sigma_z \\ \tau_{r\theta} \\ \tau_{\theta z} \\ \tau_{zr} \end{Bmatrix} = \begin{bmatrix} \lambda_s + 2G_s & \lambda_s & \lambda_s & 0 & 0 & 0 \\ \lambda_s & \lambda_s + 2G_s & \lambda_s & 0 & 0 & 0 \\ \lambda_s & \lambda_s & \lambda_s + 2G_s & 0 & 0 & 0 \\ 0 & 0 & 0 & G_s & 0 & 0 \\ 0 & 0 & 0 & 0 & G_s & 0 \\ 0 & 0 & 0 & 0 & 0 & G_s \end{bmatrix} \begin{Bmatrix} \varepsilon_r \\ \varepsilon_\theta \\ \varepsilon_z \\ \gamma_{r\theta} \\ \gamma_{\theta z} \\ \gamma_{zr} \end{Bmatrix} \quad (5.2)$$

in which

$$G_s = \frac{E_s}{2(1+\nu_s)} \quad (5.3)$$

$$\lambda_s = \frac{\nu_s E_s}{(1+\nu_s)(1-2\nu_s)} \quad (5.4)$$

where

λ_s = Lami's constant

E_s = Modulus of Elasticity of soil

ν_s = poison's ratio

G_s = Shear modulus of the soil

In addition stress strain relationship for an elastic body can be expressed as

$$\begin{Bmatrix} \varepsilon_r \\ \varepsilon_\theta \\ \varepsilon_z \\ \gamma_{r\theta} \\ \gamma_{\theta z} \\ \gamma_{zr} \end{Bmatrix} = \begin{Bmatrix} \frac{\partial u}{\partial r} \\ \frac{\partial v}{r\partial\theta} + \frac{u}{r} \\ \frac{\partial w}{\partial z} \\ \frac{\partial u}{r\partial\theta} + \frac{\partial v}{\partial r} - \frac{v}{r} \\ \frac{\partial v}{\partial z} + \frac{\partial w}{r\partial\theta} \\ \frac{\partial w}{\partial r} + \frac{\partial u}{\partial z} \end{Bmatrix} = \begin{Bmatrix} \frac{\partial u}{\partial r} \\ \frac{\partial v}{r\partial\theta} + \frac{u}{r} \\ 0 \\ \frac{\partial u}{r\partial\theta} + \frac{\partial v}{\partial r} - \frac{v}{r} \\ \frac{\partial v}{\partial z} \\ \frac{\partial u}{\partial z} \end{Bmatrix} = \begin{Bmatrix} y(z) \frac{d\phi(r)}{dr} \cos(\theta) \\ 0 \\ 0 \\ -y(z) \frac{d\phi(r)}{dr} \sin(\theta) \\ -\frac{dy(z)}{dz} \phi(r) \sin(\theta) \\ \frac{dy(z)}{dz} \phi(r) \cos(\theta) \end{Bmatrix} \quad (5.5)$$

in which zero circumferential strain is due to assumed displacements as given in the equation 5.1.

Using elastic theory (equations 5.2 & 5.5) and Equation 5.1, the stresses in the soil surrounding the pile, may be expressed as

$$\begin{aligned}\sigma_r &= (\lambda_s + 2G_s) \sum_{n=0}^{\infty} y_n \frac{d\phi_n}{dr} \cos n\theta, \sigma_\theta = \sigma_z = \lambda_s \sum_{n=0}^{\infty} y_n \frac{d\phi_n}{dr} \cos n\theta \\ \tau_{r\theta} &= -G_s \sum_{n=0}^{\infty} y_n \frac{d\phi_n}{dr} \sin n\theta, \tau_{\theta z} = -G_s \sum_{n=0}^{\infty} \phi_n \frac{dy_n}{dz} \sin n\theta, \tau_{zr} = G_s \sum_{n=0}^{\infty} \phi_n \frac{dy_n}{dz} \cos n\theta\end{aligned}\quad (5.6)$$

In the present case as we are considering only concentrated load, P and moment, M_0 at the pile head will be considered, there exists only one term in the series of Equations (5.1) and (5.6) for $n = 1$, while the other terms vanish. In the case where the applied load and/or moment components are in different directions then other terms also may exist (e.g. $n = 2, 3$). The relevant solution for each term (n) may be obtained in the similar lines of the procedure adopted for the condition of $n = 1$. The solution for each n may be superimposed to yield the final results. The displacement and the derived stress field may be used directly to establish solutions (e.g. for laterally loaded piles by Sun, and beams by Vallabhan and Das). Particularly, under lateral loading, the effect of Poisson's ratio on pile response is generally minor, and may be represented well by using the modulus, G^* , where $G^* = (1+3/4\nu_s) G_s$. Thus, the stress field may be simplified by taking Poisson's ratio as zero, which is equivalent to a zero value of the Lamé's constant. By taking the above assumptions, the displacement and new stress fields can be expressed as:

$$u = y(z)\phi(r) \cos n\theta, v = -y(z)\phi(r) \sin \theta, w=0 \quad (5.7)$$

$$\begin{aligned}\sigma_r &= 2G_s y \frac{d\phi}{dr} \cos \theta, \sigma_\theta = \sigma_z = 0 \\ \tau_{r\theta} &= -G_s y \frac{d\phi}{dr} \sin \theta, \tau_{\theta z} = -G_s \frac{dy}{dz} \phi(r) \sin \theta, \tau_{zr} = G_s \frac{dy}{dz} \phi(r) \cos \theta\end{aligned}\quad (5.8)$$

The new, simplified stress field is exact at $\nu_s = 0$, and should gradually diverge from the exact by equation (5.6), with a maximum difference probably occurring at $\nu_s = 0.5$. Therefore, the numerical results that will be found will be focused for the case of $\nu_s = 0.5$. The stresses of $\tau_{\theta z}$ & $\tau_{\theta r}$ are proposed to cater for the possible shear in the vertical

direction (Figure 5.2(b)) and in the circumferential direction (Figure 5.2(c)) around the pile. As mentioned earlier, analysis done using this simplified stresses as shown in Figure 5.2(d) is referred to as the load transfer approach.

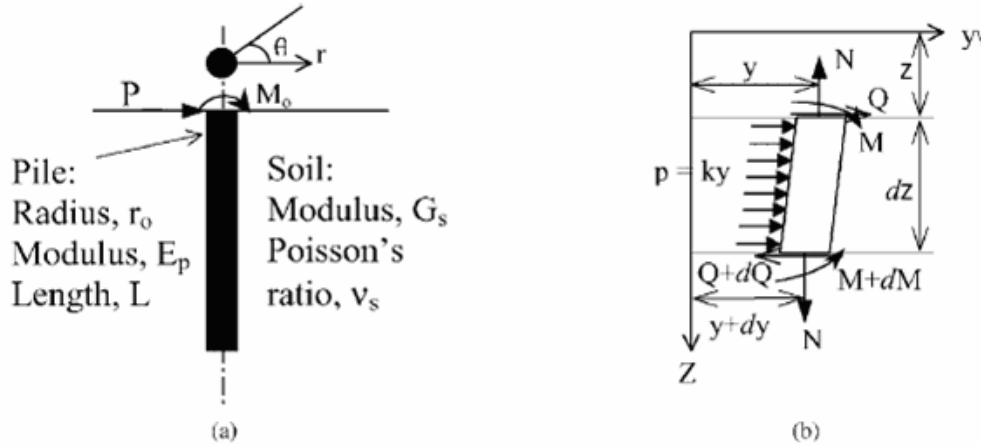


Fig 5.1: Schematic view of pile-soil system: (a) single pile; (b) pile element analysis.

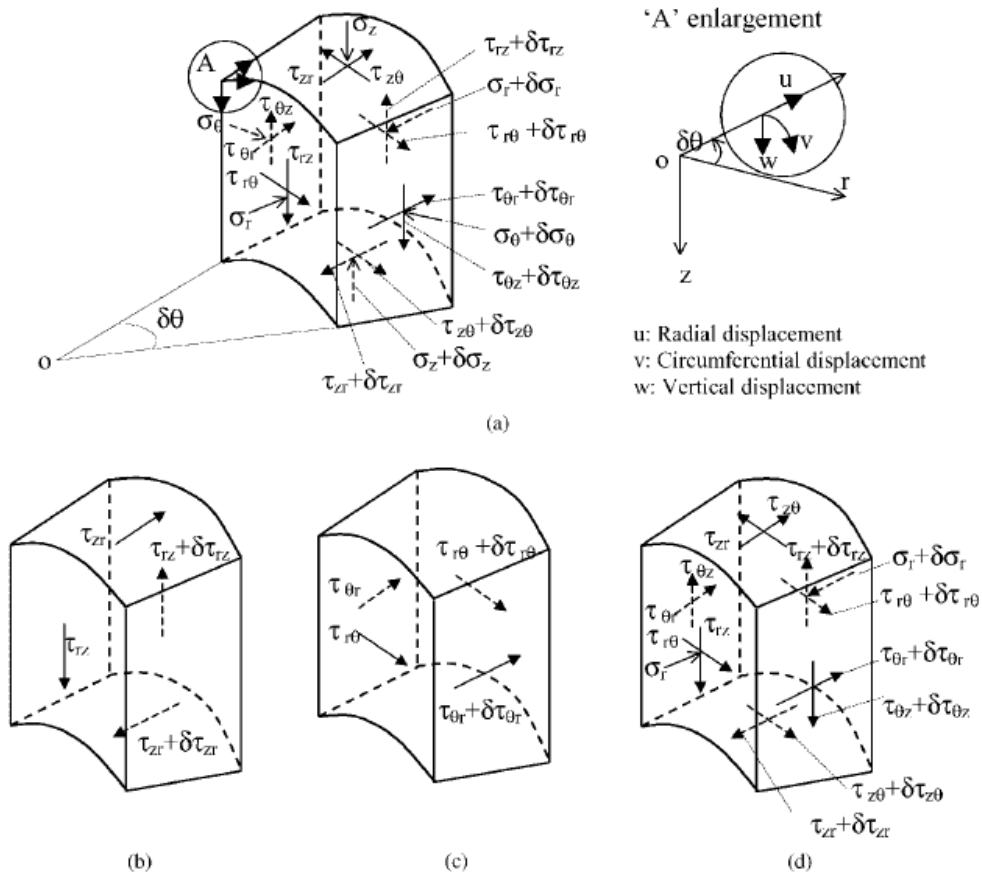


Fig 5.2: Stress and displacement field adopted in the load transfer analysis: (a) cylindrical coordinate system with displacements and stresses; (b) vertical loading; (c) torsional loading; (d) lateral loading.

5.2.2 Solutions for laterally loaded piles

To obtain coupled solutions, between the pile and the soil, for the problem shown in Figure 5.1(a), the variational approach is adopted, using the displacement field from Equation (5.7) and the stress field from Equation (5.8). The variation of potential energy, δU ; of the pile-soil system may be expressed as

$$\delta U = E_p I_p \int_0^L \frac{d^2 y}{dz^2} \delta \left(\frac{d^2 y}{dz^2} \right) dz + \pi r_0^2 \int_0^L G_s \frac{dy}{dz} \delta \left(\frac{dy}{dz} \right) dz + \iiint \sigma_{ij} \delta \varepsilon_{ij} r dr d\theta dz \quad (5.9)$$

where

E_p , I_p are the Young's modulus and moment of inertia of an equivalent solid cylinder pile,

r_0 the radius of an equivalent solid cylinder pile;

σ_{ij} & ε_{ij} the stress (from Equation (5.8)) and strain (from Equation 5.5) components in the surrounding soil of the pile, respectively.

The virtual work, δW , done by the load, P and the moment, M_0 due to a small displacement, δy , and rotation, $\delta (dy/dz)$, may be expressed as

$$\delta W = P \delta y|_{z=0} + M_0 \delta (dy/dz)|_{z=0} \quad (5.10)$$

For equilibrium of the soil-pile system

$$\delta U + \delta W = 0 \quad (5.11)$$

For the expansion of the above expression the following energy parameters can be introduced

$$U_k = \frac{1}{2E_s} \int_0^{2\pi} \int_0^\infty (\sigma_r^2 + 2(1+\nu_s)\tau_{r\theta}^2) r dr d\theta \quad (5.12)$$

$$U_N = \frac{1}{2E_s} \int_0^{2\pi} \int_0^\infty (2(1+\nu_s)(\tau_{r\theta}^2 + \tau_{z\theta}^2)) r d\theta dr \quad (5.13)$$

$$U_m = \frac{1}{2E_s} \int_0^{2\pi} \int_0^\infty (\sigma_r^2 + 2(1+\nu_s)\tau_{r\theta}^2) r dz d\theta \quad (5.14)$$

$$U_n = \frac{1}{2E_s} \int_0^{2\pi} \int_0^\infty (2(1+\nu_s)(\tau_{rz}^2 + \tau_{z\theta}^2)) r d\theta dz \quad (5.15)$$

where

U_k = the energy for unit pile movement ($y = 1$) per unit pile length;

U_N = the energy for unit pile rotation ($dy/dz = 1$) per unit pile length;

U_m = the energy for unit radial rotation ($d\phi/dr = 1$) per unit radial length, and

U_n = the energy for unit radial variation ($\phi = 1$) per unit radial length.

U_k and U_m reflect the potential energy due to the stress variations in radial direction.

U_N and U_n reflect the potential energy due to the stress variations in vertical direction.

Using Equation (5.8), the expressions for the energy parameters may be rewritten as

$$U_k = \frac{3}{2} \pi G_s \int_{r_0}^{\infty} r \left(\frac{d\phi}{dr} \right)^2 dr \quad U_N = \pi G_s \int_{r_0}^{\infty} r \phi^2(r) dr \quad (5.16)$$

$$U_m = \frac{3}{2} \pi G_s r \int_{r_0}^{\infty} y^2 dz \quad U_n = \pi G_s r \int_{r_0}^{\infty} r \left(\frac{dy}{dz} \right)^2 dz \quad (5.17)$$

Using these energy parameters, Equation 5.10 is expanded in order to obtain the boundary conditions and relevant solutions. In this expansion the parameters k and N are adopted such that

$$k = 2 U_k \quad \text{and} \quad N = 2 U_N \quad (5.18)$$

Expanding the Equation 5.10 ,

(1) Taking the coefficients of $\delta\phi$ for $r_0 \leq r < \alpha$. The governing equation for the radial attenuation function, $\phi(r)$ is obtained as

$$r^2 \frac{d^2\phi}{dr^2} + r \frac{d\phi}{dr} - \left(\frac{\gamma}{r_0} \right)^2 r^2 \phi = 0 \quad (5.19)$$

where γ is load transfer factor, which is given by

$$\gamma = r_0 \sqrt{\frac{U_n}{U_m}} \quad (5.20)$$

As $r \rightarrow \infty$, $\phi(\infty) \rightarrow 0$ and at $r = r_0$, $\phi(r_0) \rightarrow 1$, the equation 5.19 can be resolved and expressed as modified Bessel functions of the second kind of order zero, $K_0(\gamma)$ and can be given as below

$$\phi(r) = K_0 \left(\frac{\gamma r}{r_0} \right) / K_0(\gamma) \quad (5.21)$$

(2) Collecting the coefficients of δy for $0 \leq z < L$, the governing equation for the pile displacement, $y(z)$ is obtained as

$$(E_p I_p) \frac{d^4 y}{dz^4} - N \frac{d^2 y}{dz^2} + ky = 0 \quad (5.22)$$

where $y(z)$ is measured in the direction of lateral load P or moment M_0 .

k is the modulus of subgrade reaction for the Winkler's springs

N is the fictitious tension of a stretched membrane used to tie together the springs.

This is the differential equation which is same as basic differential equation for beam on elastic foundation acted upon by axial load and transverse loading.

(3) Using equations 5.21 and 5.16, and simplifying the equation 5.18 we will get

$$k = \frac{3\pi G_s}{2} \left(2\gamma \left(\frac{K_1(\gamma)}{K_0(\gamma)} \right) - \gamma^2 \left(\left(\frac{K_1(\gamma)}{K_0(\gamma)} \right)^2 - 1 \right) \right) \quad (5.23)$$

$$N = \pi \gamma_0^2 G_s \left(\left(\frac{K_1(\gamma)}{K_0(\gamma)} \right)^2 - 1 \right) \quad (5.24)$$

5.2.3 Boundary conditions

From the equation 5.10

(i) Collecting the coefficients for δy at $z = 0$, free head

$$(E_p I_p) \frac{d^3 y}{dz^3} - N \frac{dy}{dz} - P = 0 \quad (5.25)$$

(ii) Collecting the coefficients for $\delta (dy/dz)$ at $z = 0$, free head

$$(E_p I_p) \frac{d^2 y}{dz^2} + M_0 = 0 \quad (5.26)$$

(iii) Collecting the coefficients for δy at $z = L$, floating base

$$(E_p I_p) \frac{d^2 y}{dz^2} - N \frac{dy}{dz} - \sqrt{kN} y = 0 \quad (5.27)$$

(iv) Collecting the coefficients for $\delta (dy/dz)$ at $z = L$, floating base

$$\frac{d^2 y}{dz^2} = 0 \quad (5.28)$$

For a fixed-head and/or clamped-base pile, the rotation at the pile head and/or base is set to zero. Also the clamped base required a zero value of the displacement.

At $z = 0$, for fixed head pile

$$\frac{dy}{dz} = 0 \quad (5.29)$$

At $z = L$, for clamped base pile

$$\frac{dy}{dz} = 0, y=0 \quad (5.30)$$

The solution of the equation 5.22 has been calculated using Mathematica 5.1 and is given

$$y(z) = (C_1 \cos(bz) + C_2 \sin(bz))e^{az} + (C_3 \cos(bz) + C_4 \sin(bz))e^{-az} \quad (5.31)$$

The constants in the above equation have been found from the boundary conditions given by the equations 5.25 – 5.30 and the above solution may be rewritten as follows

$$y(z) = \frac{P}{E_p I_p \delta} \left(H(z) + \frac{\sqrt{kN}}{E_p I_p} B(z) \right) + \frac{M_0}{E_p I_p \delta} \left(I(z) + \frac{\sqrt{kN}}{E_p I_p} C(z) \right) \quad (5.32)$$

where

$H(z)$, and $I(z)$ are functions used to reflect pile-head boundary conditions,

$B(z)$, and $C(z)$ reflect pile-base conditions. For the head (with subscript 'o') and base (with 'B') boundary conditions described in the Figure 5.3, these functions and the factor δ are calculated using Mathematica 5.1 as functions of the parameter a and b , which are given as below

$$a = \sqrt{\frac{k}{4E_p I_p} + \frac{N}{4E_p I_p}} \quad b = \sqrt{\frac{k}{4E_p I_p} - \frac{N}{4E_p I_p}} \quad (5.33)$$

Equation (5.32) is a generalized expression for the deformation of the single pile. The derivatives of the equation give expressions for predicting the pile rotation, bending moment, deformation and shear force can be obtained using Mathematica 5.1 and MATLAB 7.0.

5.3 CRITICAL PILE LENGTH

Equation (5.32) and its derivatives may generally be used to predict the response of single piles. The prediction may be simplified in some cases, because there exist a critical length, L_c , beyond which pile-head response and maximum bending moment remain essentially at constant values. Various formulas were proposed for estimating the critical pile length, in terms of either modulus of subgrade reaction, k or the modified soil modulus, G^* . As shown later, the modulus, k may be as high as $10G_s$, thus the critical length; L_c may be as low as

$$L_c \approx 2.1r_0 \left((1 + 0.75v_s) (E_p / G^*) \right)^{0.25} \quad (5.34)$$

From the above expression, the critical pile-soil stiffness $(E_p/G^*)_c$ can be obtained as

$$\left(\frac{E_p}{G^*}\right)_c \approx \frac{.005}{(1+0.75\nu_s)} \left(\frac{L}{r_0}\right)^4 \quad (5.35)$$

When $L < L_c$ or $(E_p/G^*) > (E_p/G^*)_c$, the piles are referred to as ‘short piles’, otherwise as ‘long piles’. It can be seen from this that the critical pile length for lateral loading is generally shortest and short piles defined herein are not necessarily equivalent to rigid piles.

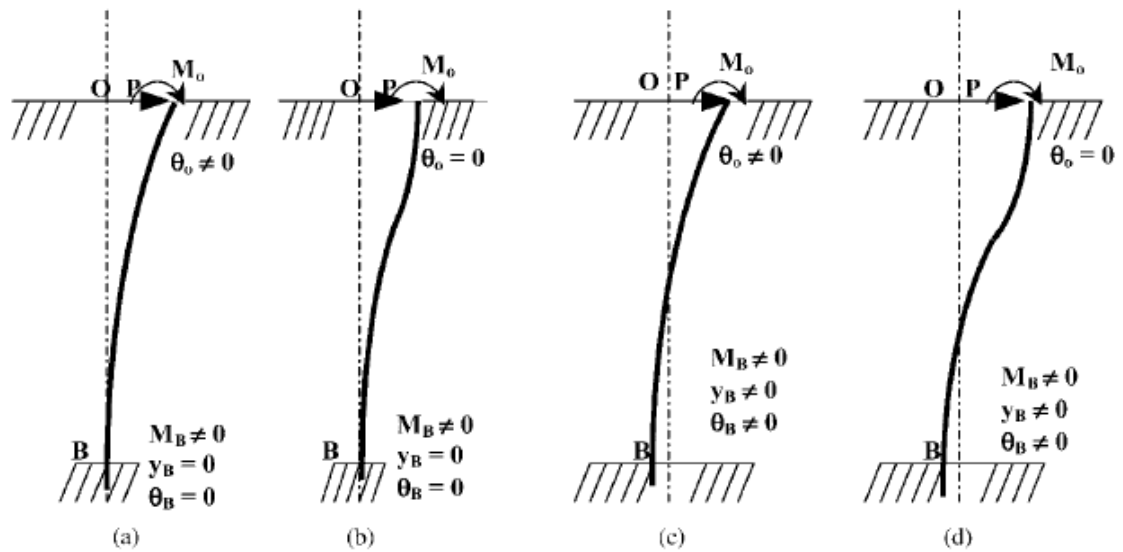


Fig 5.3 Pile- head and -base conditions.(a) FeHCP (free-head, clamped pile); (b) FxHCP (fixed-head, clamped pile); (c) FeHFP (free-head, floating pile); (d) FxHFP (fixed-head, floating pile).

5.4 LOAD TRANSFER FACTOR

As discussed earlier, in order to obtain the coupled response of the pile (displacement, $y(z)$) and the soil around it the radial attenuation function, $\phi(r)$ a fitting factor known as load transfer factor(γ) was introduced. From the equation 5.20 it can be known that this factor is proportional to the square root of the ratio of the energy parameters due to the stress variations in vertical direction, U_n over that in radial direction, U_m . Using the equation 5.17 equation 5.20 can be expressed as

$$\frac{r_o^2}{3} \frac{2 \int_0^L (dy/dz)^2 dz + \sqrt{k/N} y^2(L)}{\int_0^L y^2 dz + \sqrt{N/4k} y^2(L)} - \gamma^2 = 0 \quad (5.36)$$

Since $y(z)$, k , and the N are all dependent of γ , Equation (5.36) is non-linear, and has to be solved numerically. Generally for long piles, the terms including $y(L)$ may be ignored. In this situation, γ is a simple function of the rotation, dy/dz and the lateral displacement, $y(z)$ of the pile over the whole length.

5.4.1 Computational procedure for γ determination

1. Calculate the values of k and N for the assumed value of γ using the equations (5.23) and (5.24).
2. Obtain the values of $y(z)$ and dy/dz using the relation 5.32.
3. Calculate γ by solving the equation 5.36 from the values obtained from the steps 1 and 2.
4. Check out for required convergence for the obtained and assumed values of γ .
5. If convergence is not obtained repeat the procedure until the required convergence is obtained.
6. Likewise the values of γ can be obtained for different pile head and base conditions under lateral load and moments.

Following the above procedure an empirical expression that has been suggested by Guo (2001) was utilized in the present analysis for calculating load transfer factor which is

$$\gamma = k_1 \left(\frac{E_p}{G^*} \right)^{k_2} \left(\frac{L}{r_o} \right)^{k_3} \quad (5.37)$$

where k_1, k_2 and k_3 the coefficients given in Table 5.1.

Table 5.1: Parameters for estimating the load transfer factor (Guo, 2001)

Items	Long Piles			Short Piles		
	K_1	K_2	K_3	K_1	K_2	K_3
FeHCP(P)	1.0	-0.25	0	1.9	0	-1.0
FeHFP(P)	1.0	-0.25	0	2.14	0	-1.0
FeHCP(Mo)	2.0	-0.25	0	2.38	-0.04	-0.84
FeHFP(Mo)	2.0	-0.25	0	3.8	0	-1.0
FxHCP(P)	0.65	-0.25	-0.04	1.5	-0.01	-0.96
FxHFP(P)	0.65	-0.25	-0.04	0.76	0.06	-1.24

The validity of the above expression has been verified for a particular case of free head clamped base pile acted upon by a lateral load P using Mathematica 5.1 and MATLAB 7.0 programming language.

From figure (5.4) and (5.5) it may be noted that for the long piles, the value of γ depends on the pile – soil relative stiffness, E_p/G^* , loading characteristics (P or M_o) and the pile head and base conditions, but is nearly independent of the slenderness ratio. On the other hand, for short piles, the value of γ is nearly independent of the pile-soil relative stiffness and is approximately inversely proportional to the slenderness ratio. The effect of the Poisson's ratio is taken care of in the above equation by incorporating a parameter called modified shear modulus, G^* . From the figure (5.4) it is clear that there is not much difference in the calculated load transfer factors for a particular case with varying Poisson's ratios.

The values of parameters that are used for calculating the load transfer factor were determined from equation (5.32) for cases where in the pile is subjected to either lateral load P or moment M_o . In cases where the pile is subjected to a load and moment simultaneously, γ may be estimated by using the equation (5.36) directly together with the displacement $y(z)$ estimated by using equation (5.32) under combined loading. This differs from the conventional approach, wherein, the displacement fields due to the load P and moment M_o are estimated individually using different values of γ , and then superimposed to yield the displacement under combined loading. The value of γ for combined loading should lie in between the value of γ for the load P and that for the moment M_o .

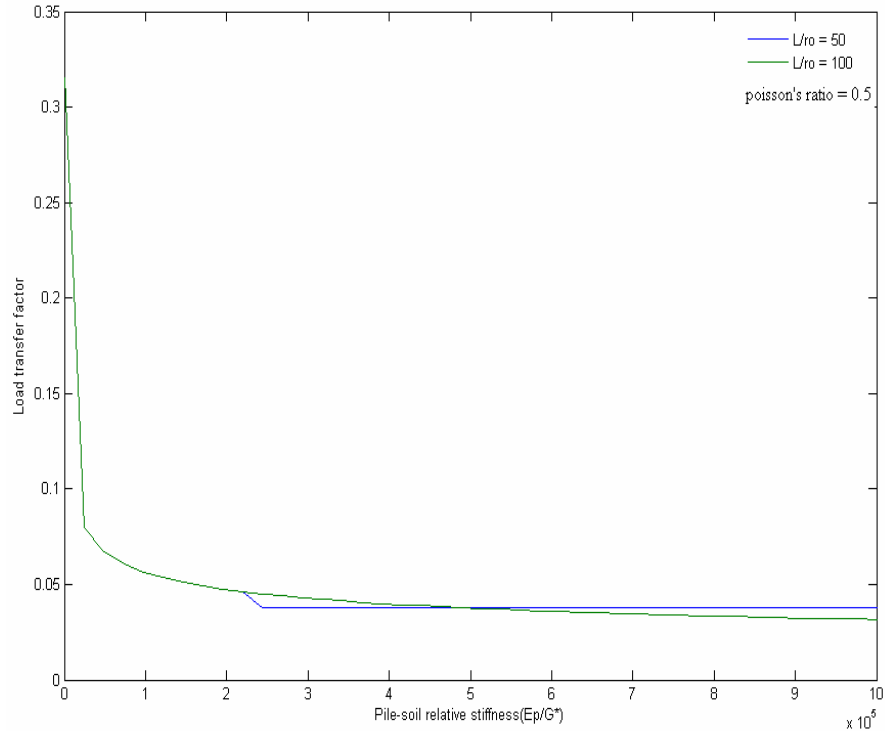


Fig 5.4(a) Effect of slenderness ratio L/r_o

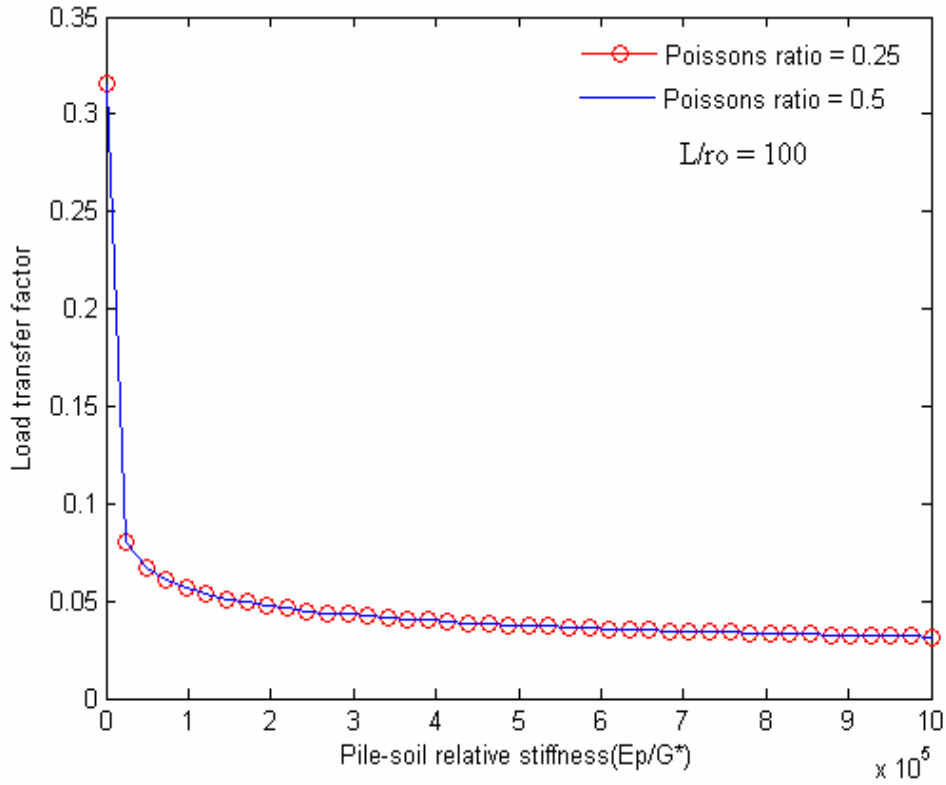


Fig 5.4(b) Effect of Poisson's ratio

Fig 5.4: Determination of load transfer factor (clamped base and free head).

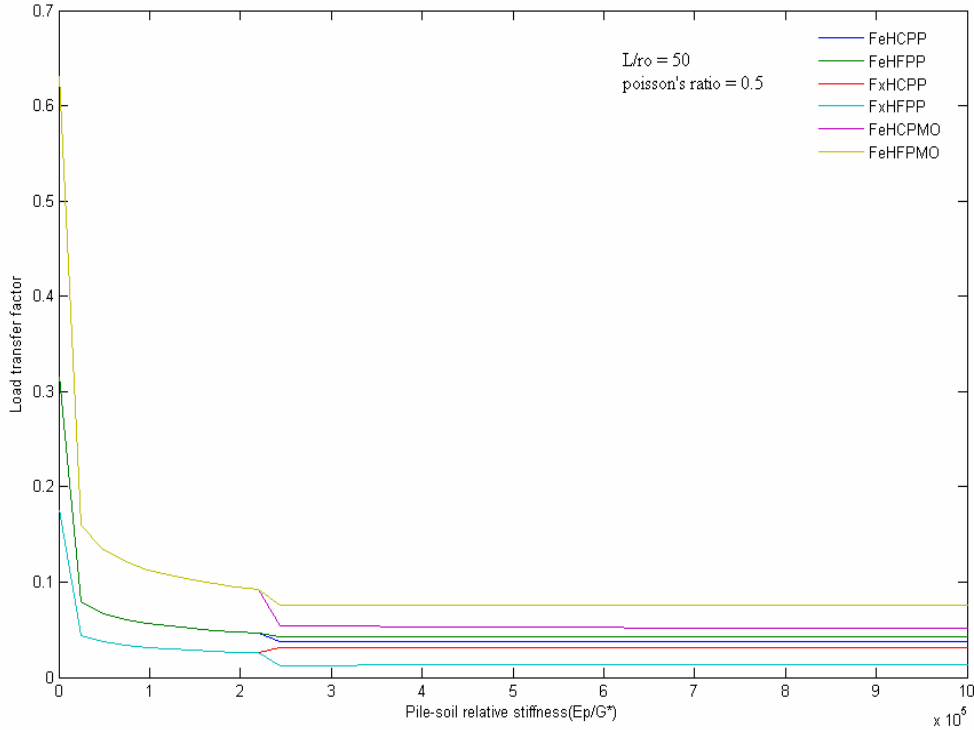


Fig 5.5: Determination of load transfer factor for various pile head and base conditions.

5.5 MODULUS OF SUBGRADE REACTION AND FICTITIOUS TENSION

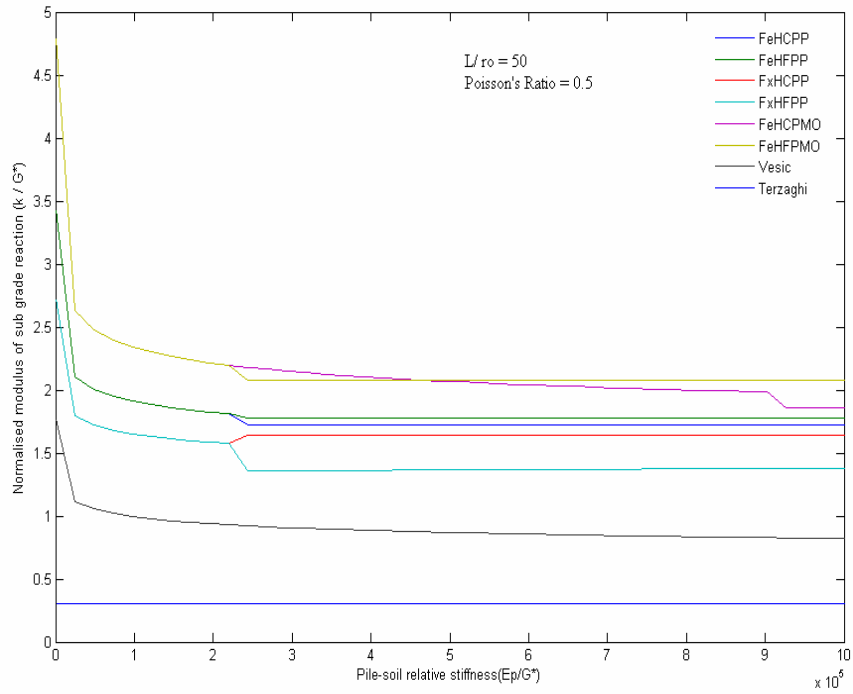
The current solutions (e.g. Equation (5.32)) are essentially represented through the two parameters k and N . The parameter k generally represents the energy parameter, U_k , due to the stress variations in radial direction, and reflecting the coupling effect of the independent springs around the pile shaft through the parameter γ . When y in Equation (5.8) is a constant $\tau_{\theta z}$ & $\tau_{\theta r}$ reduce to zero. The factor γ becomes zero from Equation (5.20). Using Equation (5.19), ϕ (hence k) becomes independent of variations in vertical directions. The parameter k becomes a ratio of an induced intensity of the local, uncoupled distributed reaction per unit area of the pile, p , over the pile deflection, y (Figure 5.1(b)) (i.e. the modulus of subgrade reaction.)

The fictitious tension, N is the energy parameter due to the stress variations in vertical direction (Equation (5.18)). The parameter N can be a pair of equilibrating external forces acting in the centre of gravity of the end cross-sections of the pile or be the ratio of the modulus of subgrade reaction, k , over a ‘shear stiffness’ of the pile. As a

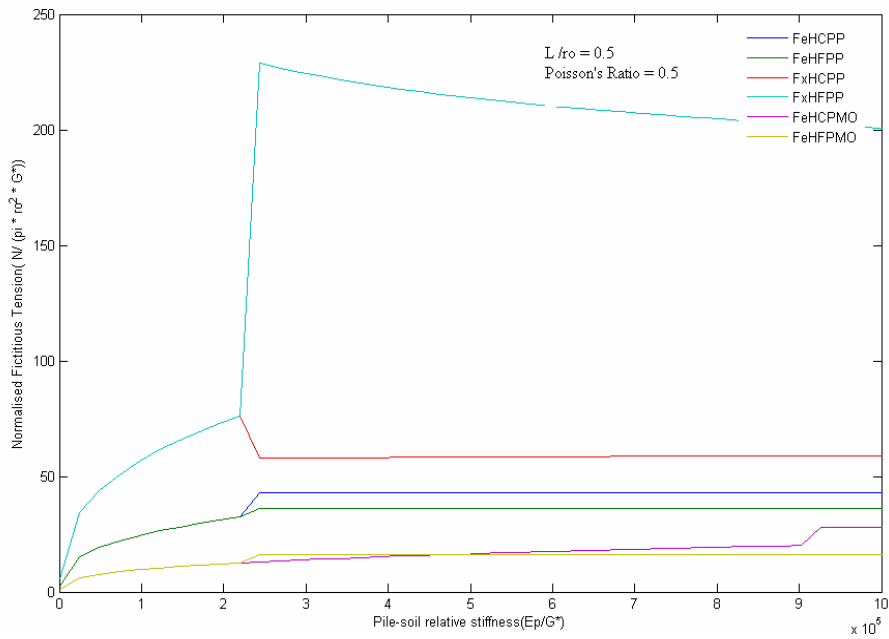
constant along a pile length, the parameter N is not the real tensile force in the pile. In the case of laterally loading, tensile force can be induced as noted previously for soil nails.

The parameter k and N are all functions of the stresses, thus depend on the loading properties, the pile slenderness ratio, and the pile-soil relative stiffness. Using Equation (5.23 & 5.24), the parameter N and k have been estimated and illustrated in Figure 5.6(a), and 5.6(b), due to either the moment (M_o) or the lateral load (P). For a typical slenderness ratio, the figure shows that, as the pile-soil relative stiffness increases, the fictitious tension increases (Figure 5.6(b)); while the modulus of subgrade reaction reduces (Figure 5.6(a)). Also the critical stiffness for the moment loading is higher than that for the other cases. For short piles, the parameter k and N are approximately independent of the pile-soil relative stiffness, since the total energy of U , the displacement, y , and the rotation, dy/dz , are all independent of the stiffness, but dependent on the slenderness ratio. As it can be observed from Figure 5.6 (a) that the maximum difference between the moduli of subgrade reaction for the two cases of P and M_o is generally less than 35% particularly for rigid piles. Therefore, superposition using two different y (*thus* k) may be roughly adopted for the analysis of piles under combined loading. This is in contrast with the current practice of using a single k for the combined loading.

A comparison has been made with the expressions as given by Vesic and Terzaghi with current k and it has been found that the values suggested are very much low compared with current k once again stressing the importance of loading conditions, slenderness ratio effect etc,. From the figure 5.7 and 5.8 it can be inferred that k and N values are inversely proportional to the poisson's ratio. But figure 5.7 depicts that for the long piles there is not much variation in k and N . But with increasing slenderness ratio, k values are inversely proportional to the pile-soil relative stiffnesses and reverse is the case with respect to N .

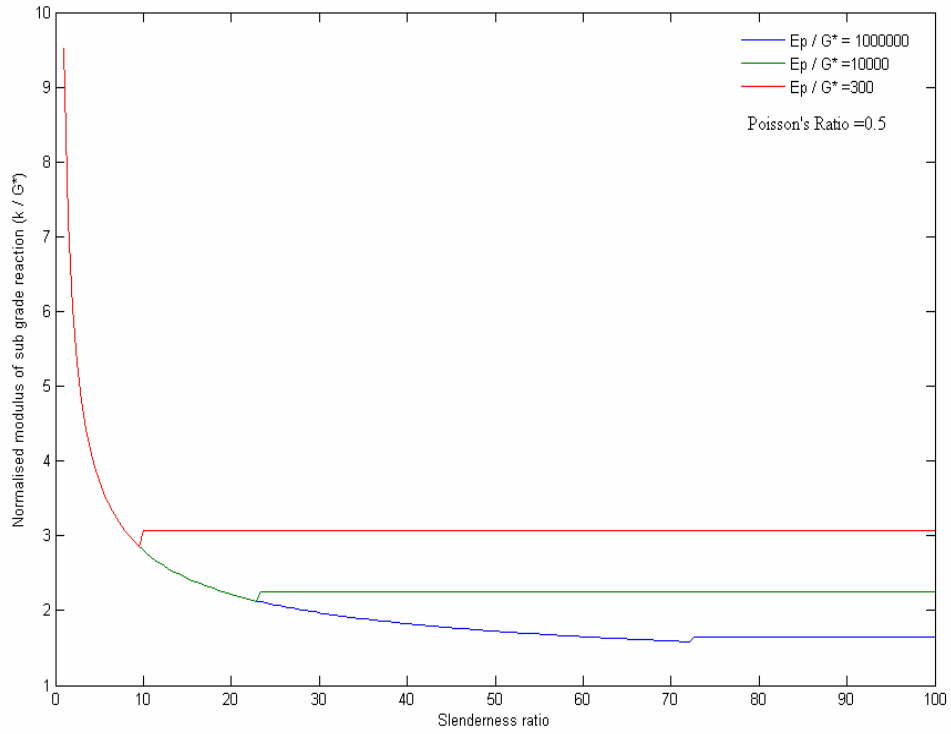


(a) Modulus of sub-grade reaction

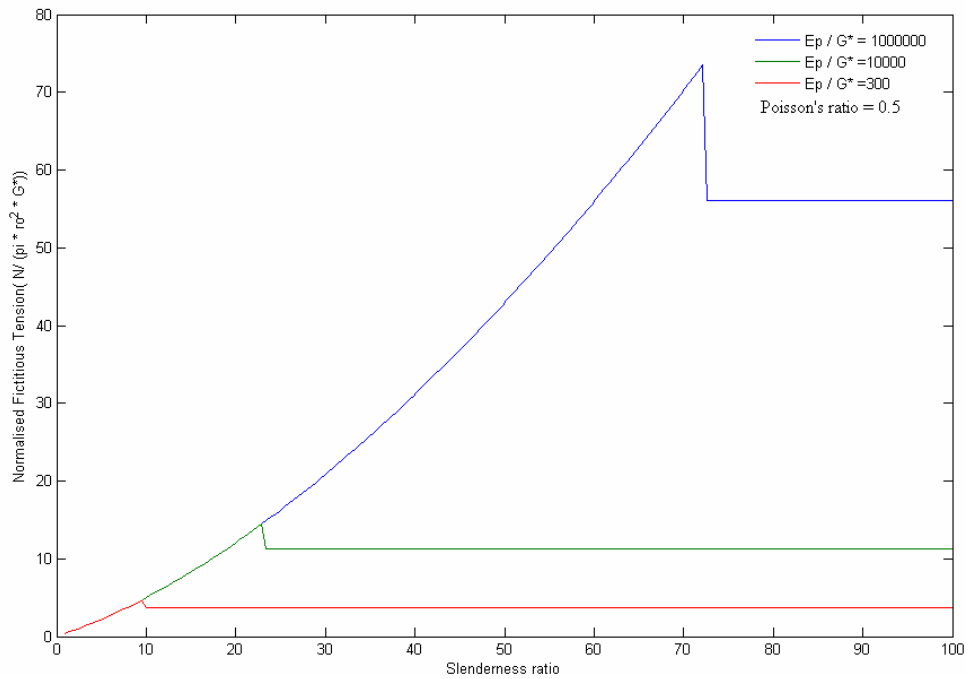


(b) Normalized Fictitious Tension

Fig 5.6: Variation of (a) Modulus of sub-grade reaction and (b) Normalized Fictitious Tension for various head and base conditions

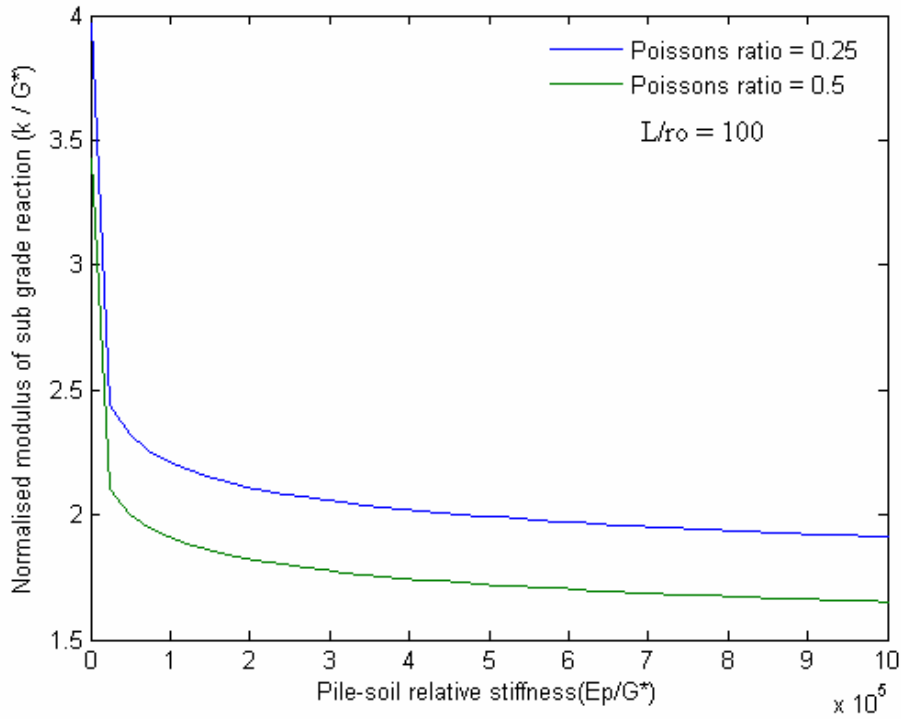


(a) Normalized modulus of sub-grade reaction

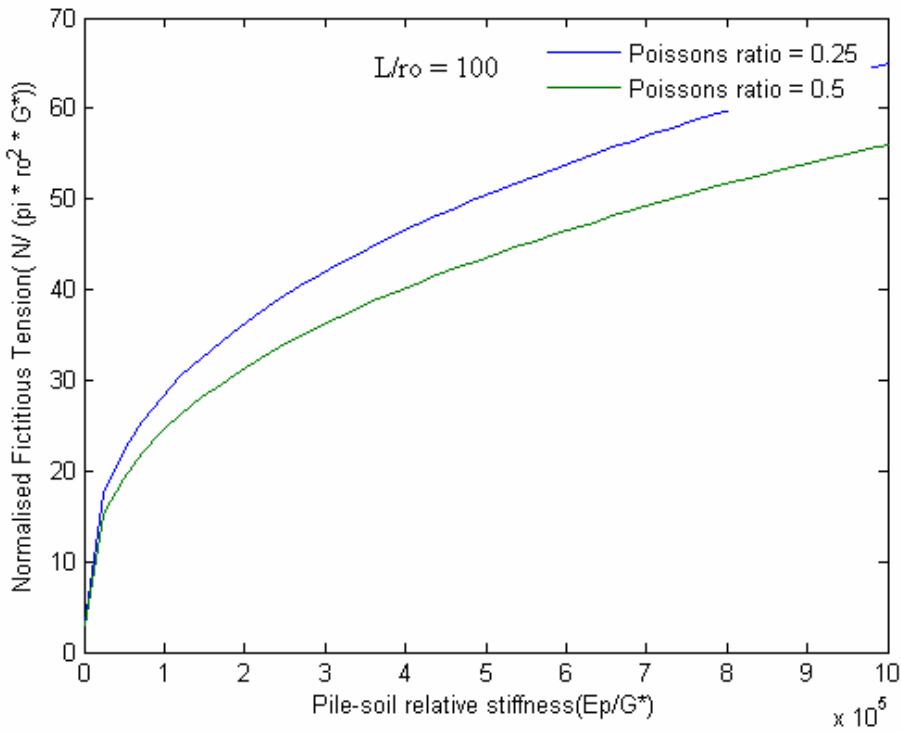


(b) Normalized Fictitious Tension

Fig 5.7: Variation of (a) the modulus of sub-grade reaction and (b) Normalized Fictitious Tension w.r.t. Slenderness ratio (FeHCP(P))



(a) modulus of sub-grade reaction



(b) Normalized Fictitious Tension

Fig 5.8: Variation of (a) the modulus of sub-grade reaction and (b) Normalized Fictitious Tension w.r.t. Poisson's ratio (FeHCP(P))

5.6 ANALYSIS OF PILE RESPONSE

The pile head deformation, the pile head rotation and the maximum bending moment are estimated for various pile head base conditions under different loading conditions, using the current approach i.e. equation (5.32) and its 1st & 2nd derivatives. The variations of which are represented graphically with discussions in the following sections.

5.6.1 Effect of various head and base conditions

The response of short piles may be affected by the pile-head and base conditions, which are illustrated below by focusing on the maximum bending moment, the pile-head rotation and the pile-head displacement.

For free-head, clamped piles (FeHCP(P)), the response of the piles has been illustrated as functions of the pile slenderness ratio in Figure 5.9(a) to 5.9(c), the pile-soil relative stiffness in Figures 5.10(a) to 5.10(c) and the Poisson's ratio from Figures 5.11(a) to 5.11(c). From the figures, the following main points are observed:

(1) At a low pile slenderness ratio, L/r_o , (and/or a high stiffness, E_p/G^*), the normalized pile head deformation and rotation are negligible; while the moment M_{max} is approximately equal to PL . The different gradients, shown in Figure 5.9(c), of the initial linear part are due to the fact that the L_c is different for each stiffness.

(2) At an intermediate pile slenderness ratio or stiffness, with the increases in the pile length (or decrease in the logarithmic value of the stiffness), the normalized pile head deformation and rotation increases almost linearly; while the normalized maximum bending moment, $M_{max}/(PL_c)$ increases slowly, until a peak is reached.

(3) After the peak, the normalized deformation and rotation still increases; while the slow increase in the M_{max} is offset by the faster increase in the critical length, L_c , thus, the ratio of $M_{max}/(PL_c)$ tends to decrease with the increase in pile length (or decrease in the logarithmic value of the stiffness).

(4) From figure 5.11(a) to (c) it can be inferred that the pile head deformation and normalized bending moment are increasing with increasing poisson's ratio and this variation is significant for long piles as compared to short piles. But pile head rotation is almost independent of the poisson's ratio.

For free head, floating piles as can be seen from the figure 5.10 it is found that pile head deformation and rotation are 2 to 3 times more than that of free head clamped

base pile condition. But this trend was reversed in the case of normalized bending moment.

For fixed-head piles, comparison between Figure 5.10(a) and 5.12(a) shows:

(1) The normalized pile head deformation for fixed head (Figure 5.12(a)) is about $\frac{1}{2}$ to $\frac{2}{3}$ that for free head (Figure 5.10(a)), given long, clamped piles; (b) is about $\frac{1}{3}$ that for free head (FeHFP(P)), given short, floating piles.

(2) Irrespective of the base conditions, the maximum bending moment for fixed head doesn't have much significance with the stiffness, (E_p/G^*).

The figures 5.10 and 5.12 indicate that

(a) For free- or fixed- head Figure 5-10 and 5-12 piles due to lateral load, the solutions using Vesic's k for beams offer invariably biggest difference from the current results. Therefore, the proposed ' k ' may be not suitable for lateral pile analysis.

(b) They also indicate that the effect of the fictitious tension (N) cannot be ignored, since the predictions using $N = 0$ compares poorly with results taking N and k .

(c) However, for moment loading, the effect of the fictitious tension may fortunately be ignored in the case of clamped piles, since it has a rather limited effect on the prediction of pile-head deformation and rotation, as compared floating piles where it is of much significant (Figure 5.13).

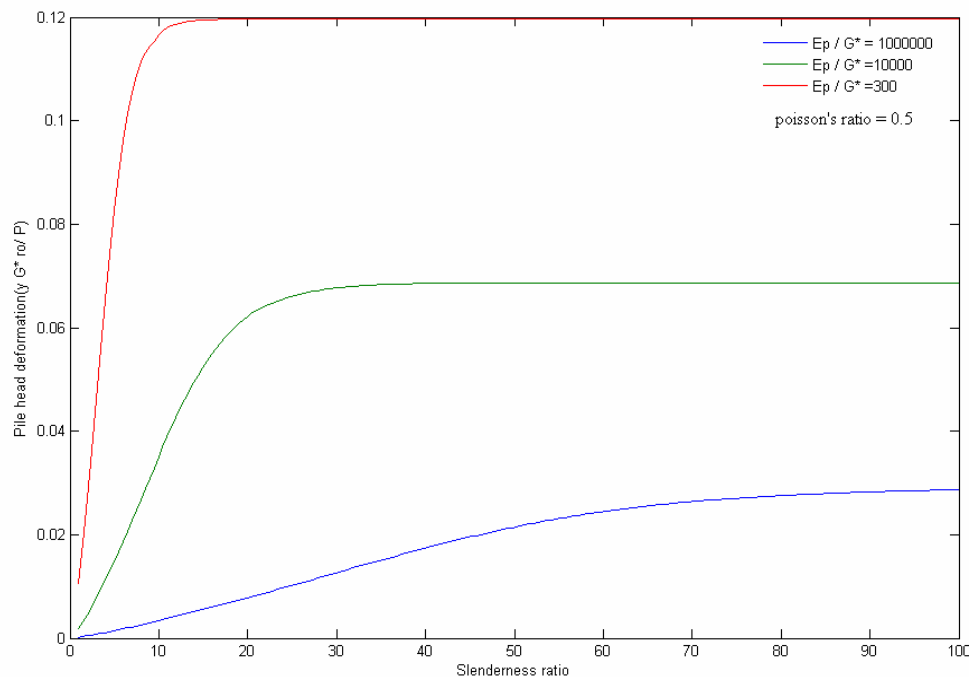


Fig 5.9 (a) Pile head deformation FeHCP(P)

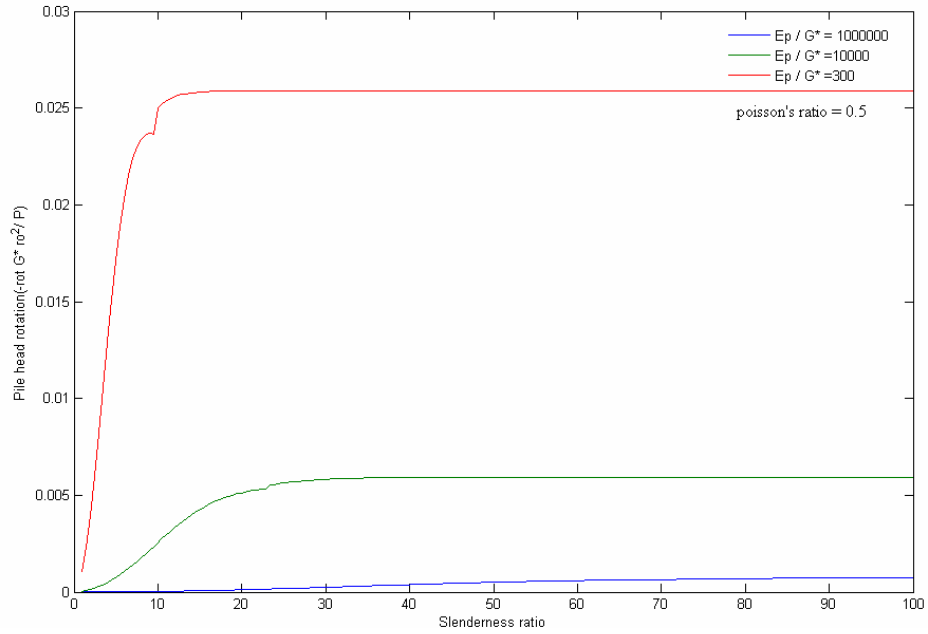


Fig 5.9 (b) Pile head rotation FeHCP(P)

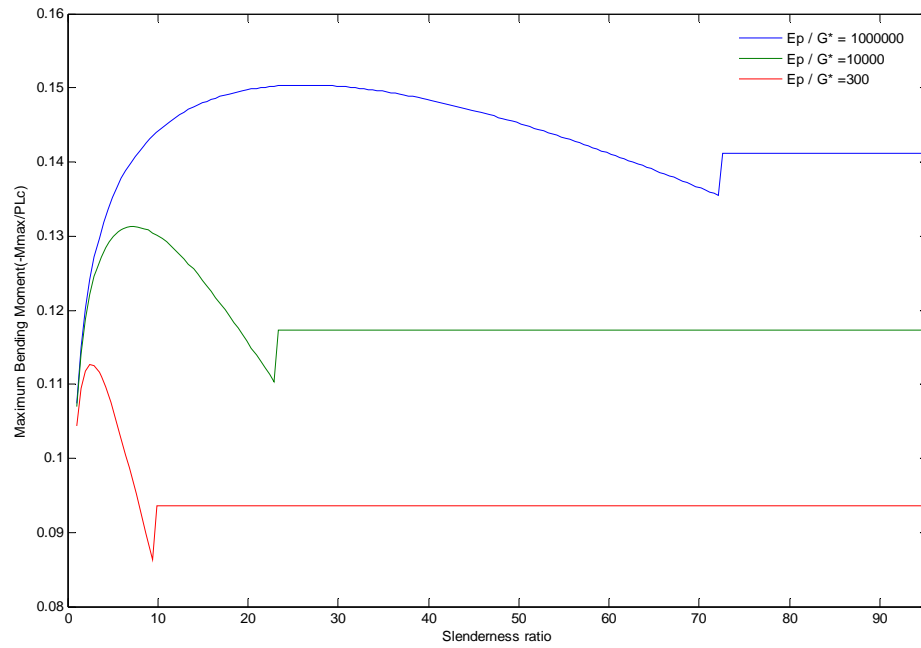


Fig 5.9 (c) Maximum bending moment FeHCP(P)

Fig 5.9 Single pile (free head clamped pile) response due to variation in slenderness ratio

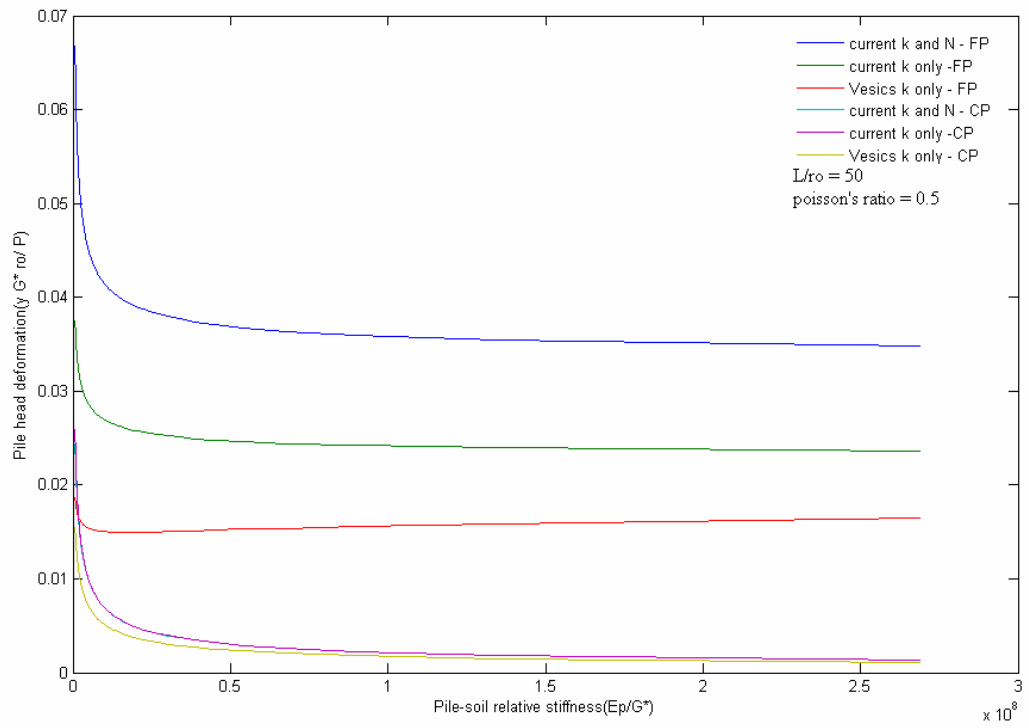


Fig 5.10(a) Pile head deformation (Free Head - P)

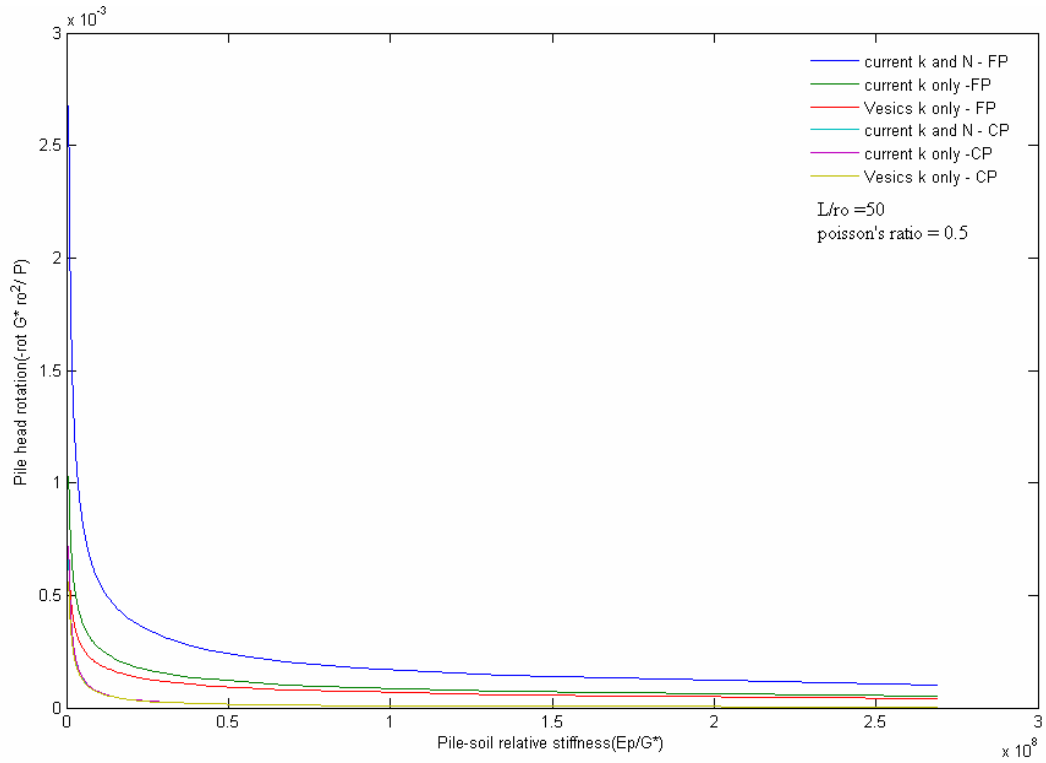


Fig 5.10 (b) Pile head rotation (Free head - P)

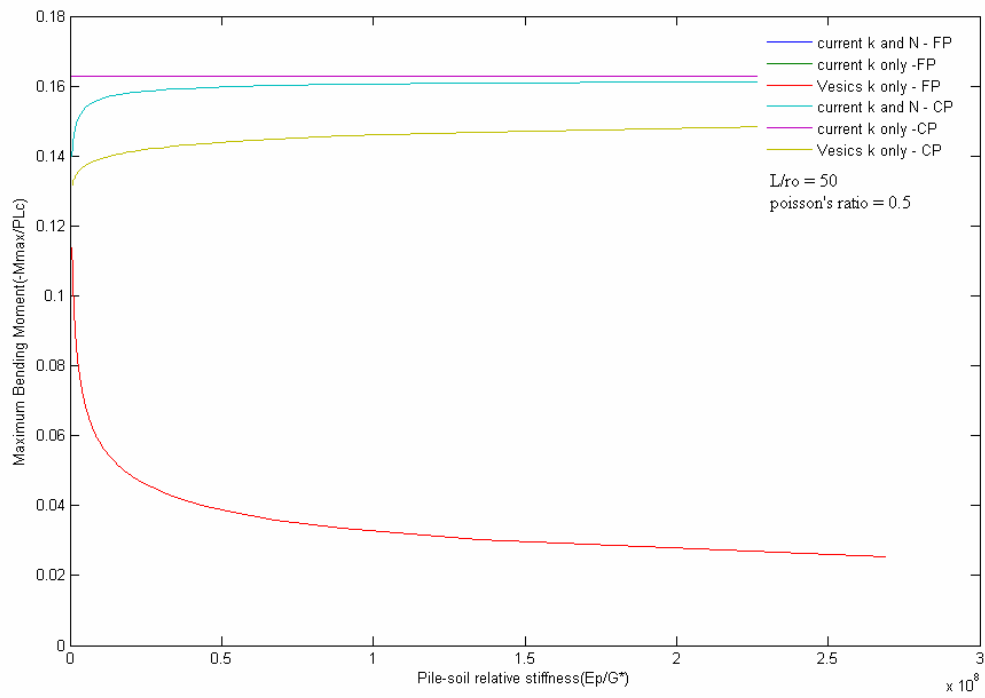


Fig 5.10(c) Maximum bending moment (Free head - P)
 Fig 5.10 Single pile (free head) response due to variation pile – soil relative stiffness

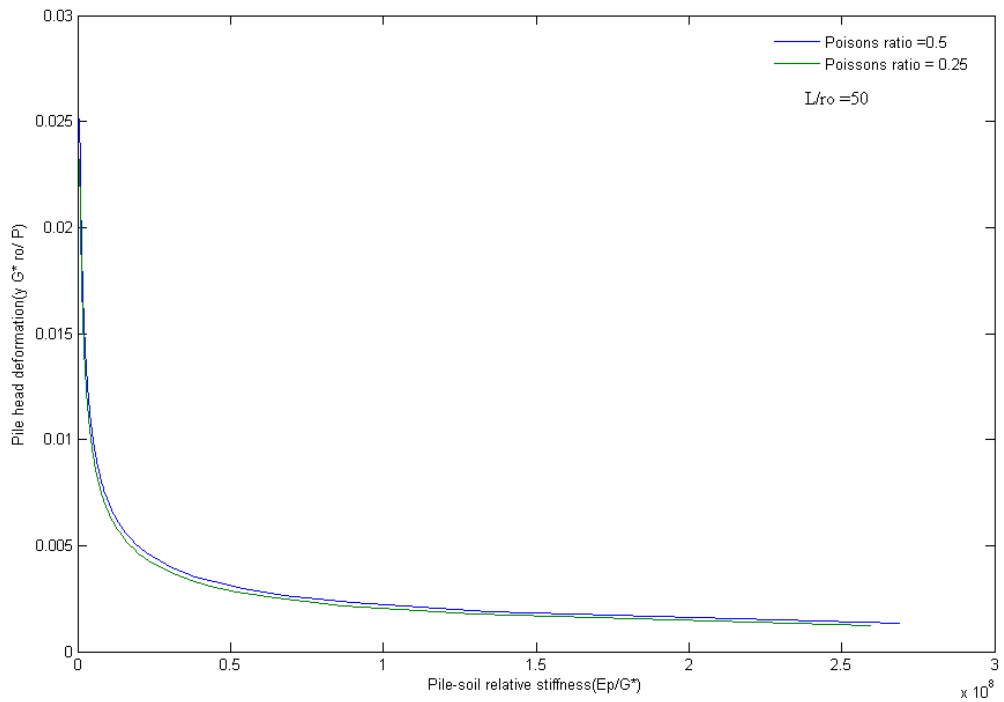


Fig 5.11 (a) Pile head deformation $F_e HCP(P)$

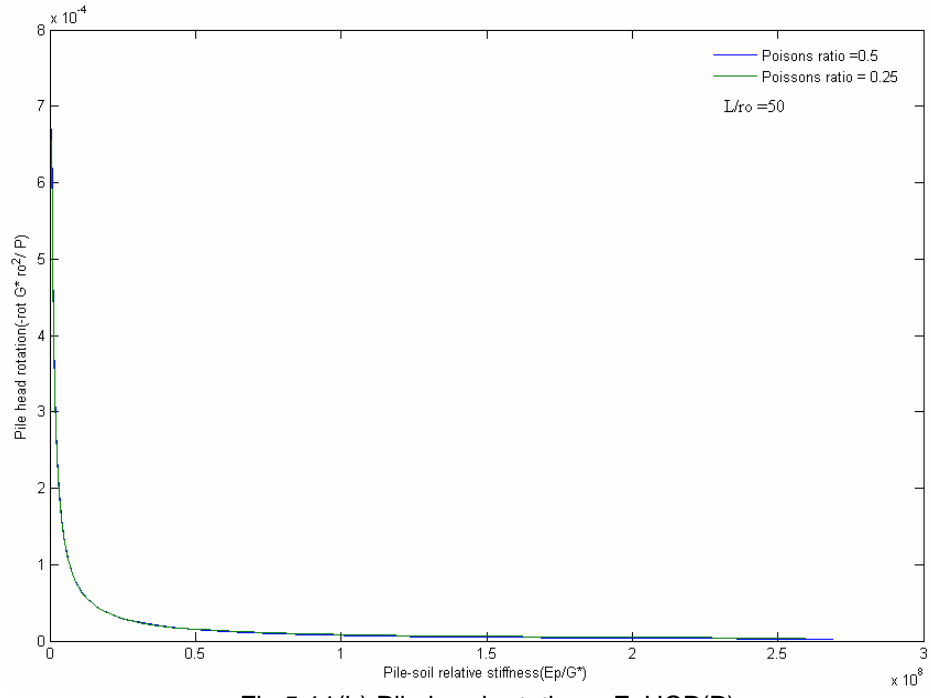


Fig 5.11(b) Pile head rotation – FeHCP(P)

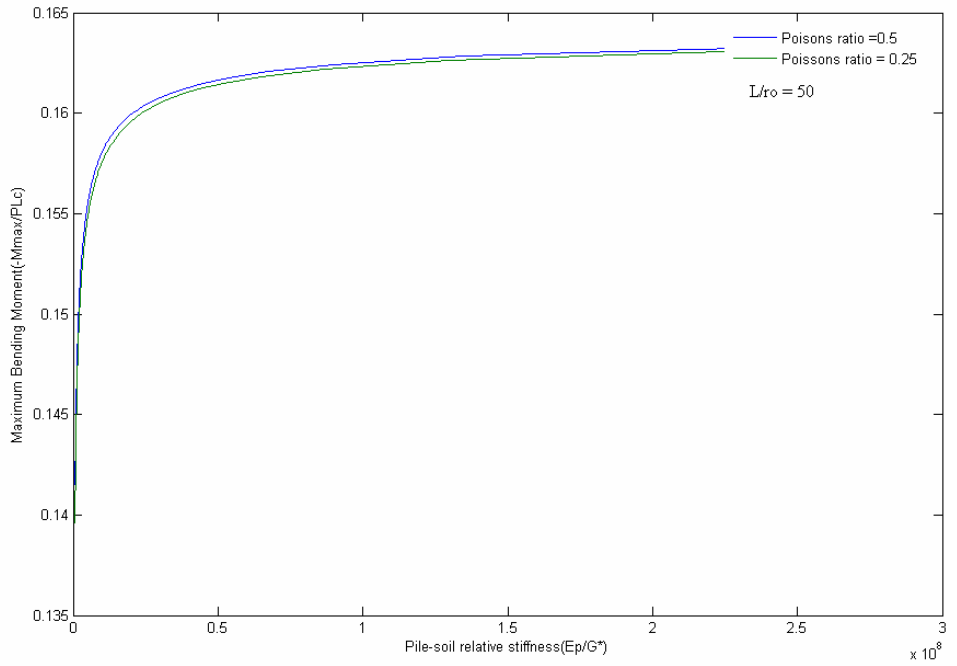
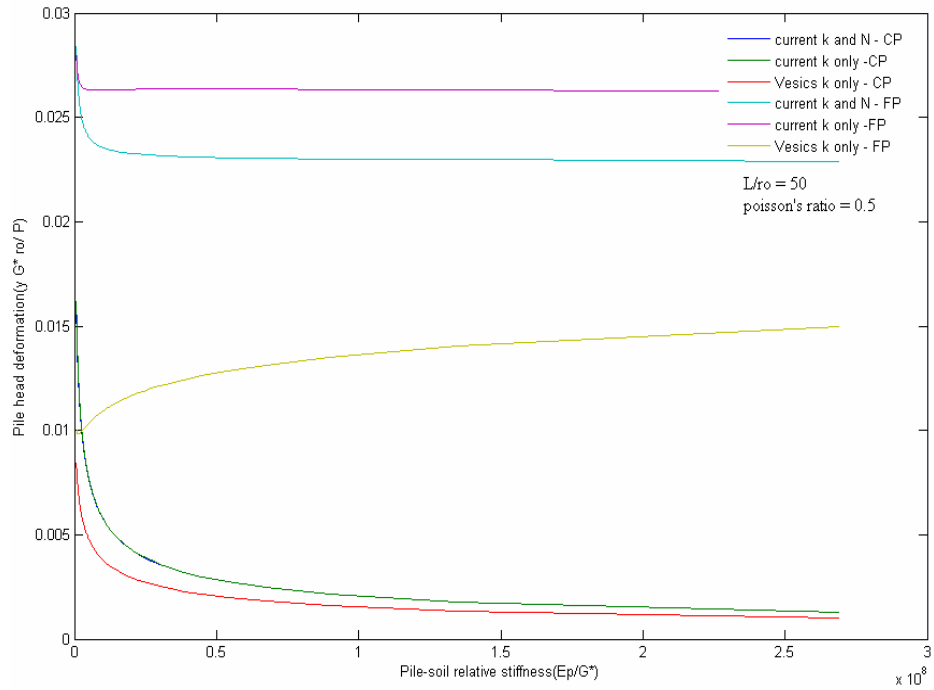
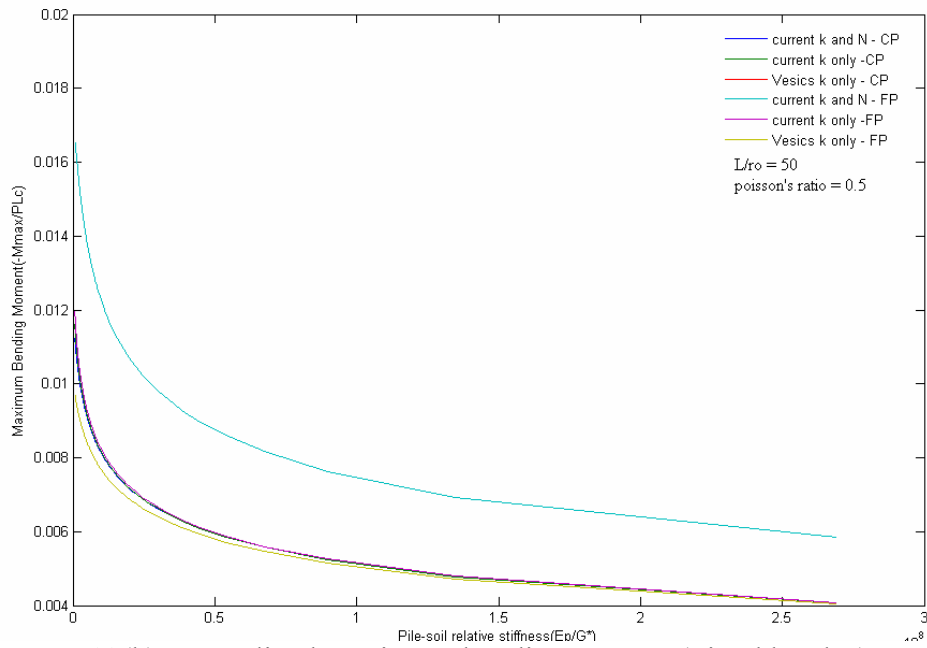


Fig 5.11 (c) Normalized Bending Moment FeHCP –P

Fig 5.11 Single pile (free head clamped base) response due to variation in soil pile relative stiffness with respect to poisson's ratio



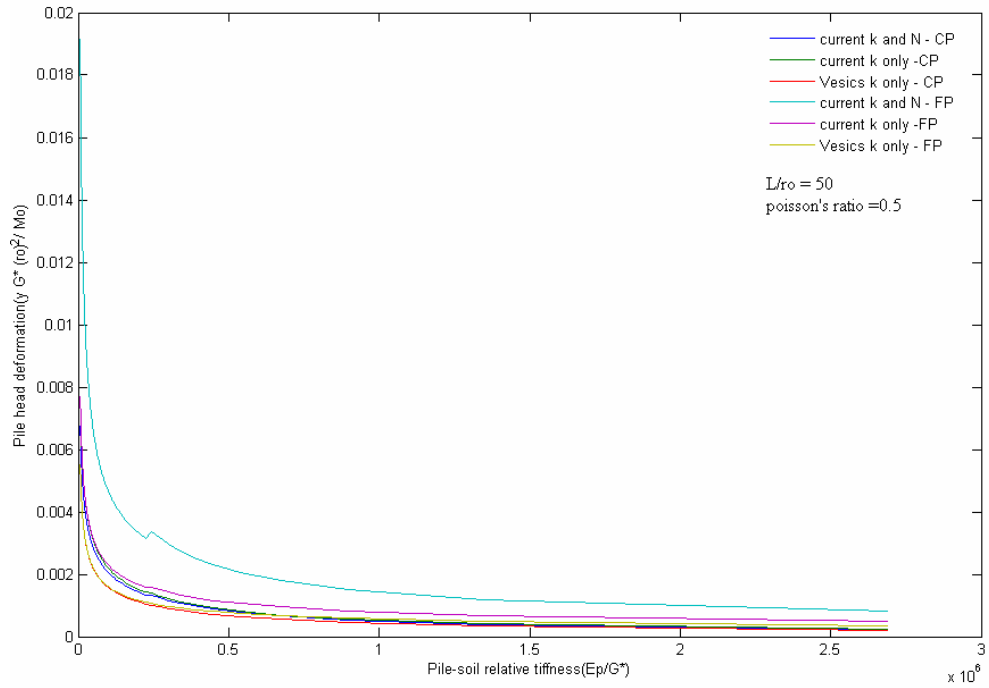
5.12(a) Pile head deformation (Fixed head-P)



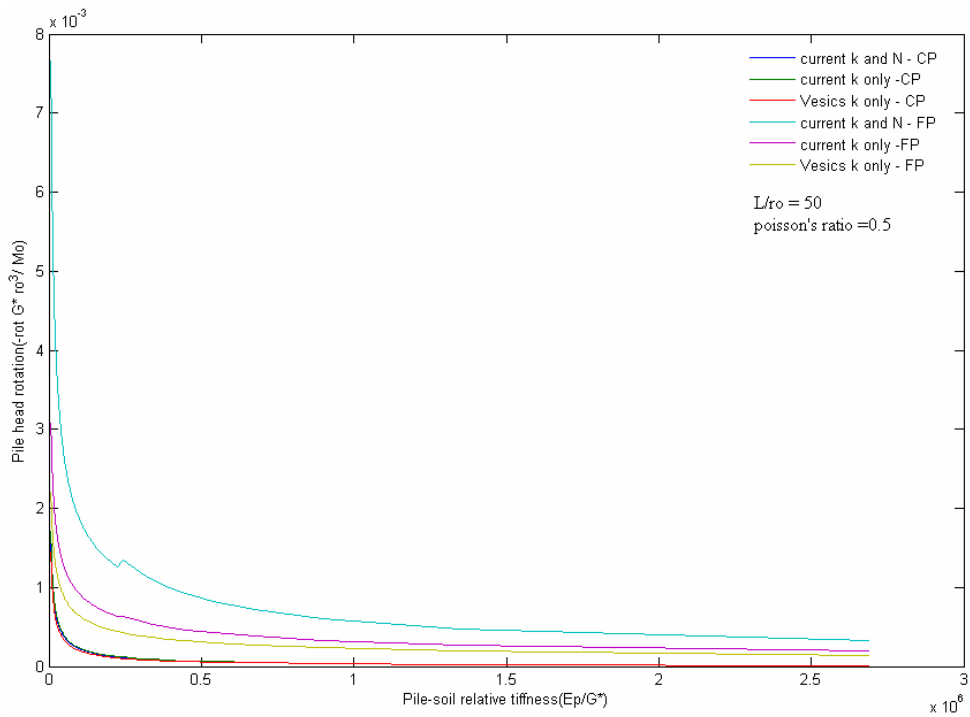
5.12(b) Normalized maximum bending moment(Fixed head-P)

Fig 5.12 Single pile (fixed head) response due to variation in pile – soil relative stiffness
(a) pile head deformation (b) normalized maximum bending moment

Moment induced pile response



5.13 (a) Pile head deformation (Free head-Mo)



5.13 (b) Normalized pile head rotation (Free head-Mo)

Fig 5.13 Single pile (free head) response due to variation in pile – soil relative stiffness acted upon by a moment M_o (a) pile head deformation (b) pile head rotation

5.6.2 Effect of fines content

For a free head clamped pile acted upon by lateral load P , the behavior of pile has been observed and presented graphically for varying fine contents in sand. It has been observed that the pile head deformation and rotation decreased steadily with increasing fine content later its behavior reversed. But in the case of normalized bending moment the behavior is entirely reversed.

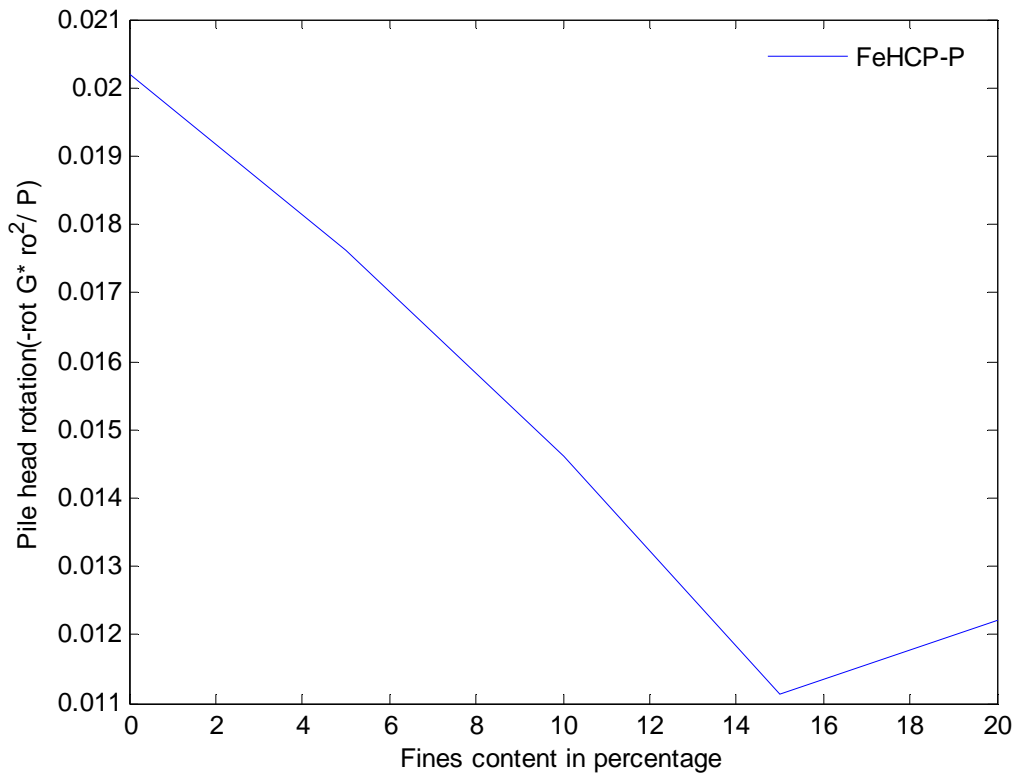


Fig 5.14 Effect of variation in percentage fine content on pile head rotation

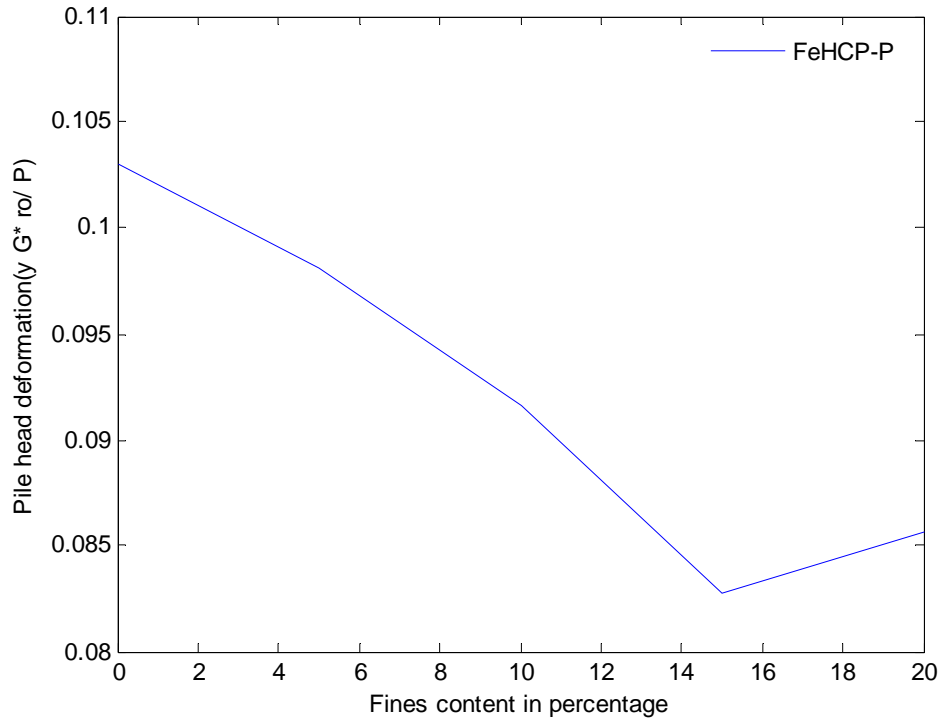


Fig 5.15 Effect of variation in percentage fine content on pile head deformation

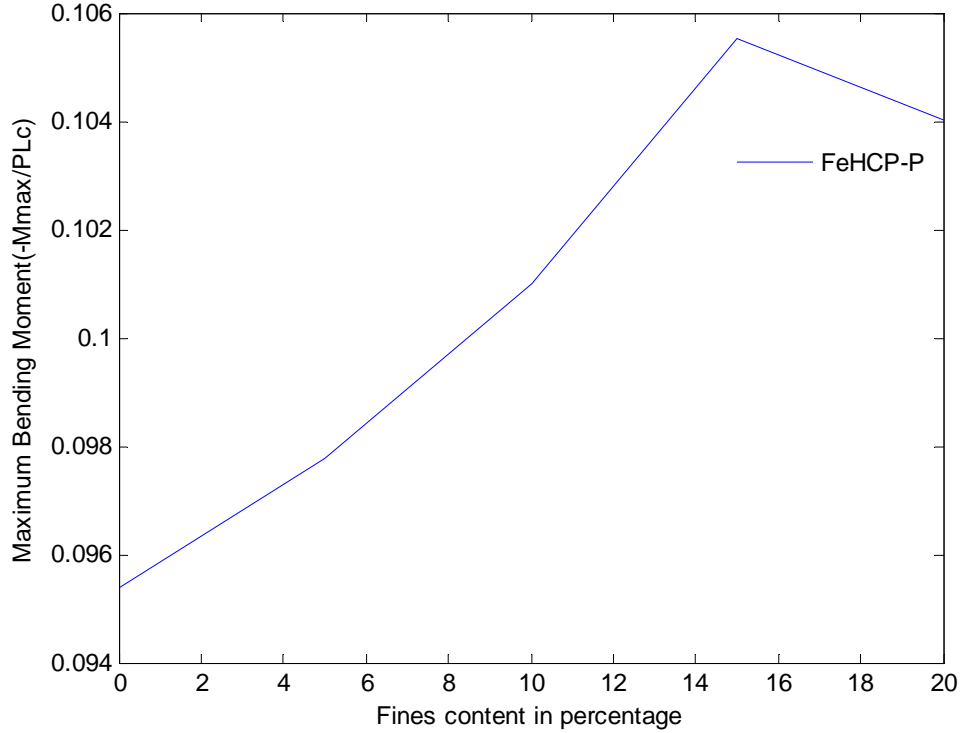


Fig 5.16 Effect of variation in percentage fine content on normalized bending moment

CHAPTER 6 CONCLUSIONS

In the present work, for laterally loaded piles a simplified analysis using Winkler's beam on elastic foundation method (mainly for free head piles) was done. Behavior of the piles under varying loads, soil types, pile materials, pile cross sections etc was made in detail. The relationship between the lateral load and pile head deflections has been observed using assumptions of Terzaghi and Bowles.

To account for the various limitations of the above method a new load transfer approach has been adopted to predict response of lateral piles in a homogenous, elastic medium. Closed-form expressions for the piles and the surrounding soil have been developed as functions of the load transfer factor. In particular, the generalized expression for the piles (1) well reflect the effect of the pile head and base conditions; (2) avoid the unreasonable predictions at high Poisson's ratio and (3) are applicable to any pile - soil relative stiffness.

The current approach is a coupled approach, represented by the two parameters: the modulus of subgrade reaction, k , and the fictitious tension, N , and linking the response of the pile and the soil around it by the load transfer factor. The approach can be reduced physically to the available uncoupled approach for beam using the Winkler model ($N=0$). A simplified expression provided for the factor under various pile head and base conditions has been used. The provided factor was intended for applying either the lateral load or the moment, individually. Using the load transfer factor for combined loading means that different factor k (and also N) for the P and M_0 will be adopted, which is different from the current practice of using a single factor k for the loading (Winkler model). This new adoption is equivalent to use superposition for displacements derived from the load and moment, individually.

Short piles of sufficiently high stiffness, or of free head, floating base, may be treated as 'rigid piles'. For rigid piles, the maximum bending moment for the free-head case can be 10 times that for the fixed-head case. The model parameters such as load transfer factor, Poisson's ratio, the slenderness ratio and the soil-pile relative stiffness are investigated in order to have a better understanding of the relationship between these parameters.

If the values of the modulus of subgrade reaction be adopted as per Terzaghi and Vesic, the effect of soil characteristics is not well visible in the evaluation of the parameters like pile head deflections, rotations and maximum bending moments. Therefore, the modern approach for the prediction of G_s based upon the soil material characteristics is coupled with the current load transfer approach to obtain the effect of fines contents present in the sand upon pile head deflections, rotations and maximum bending moment.

Future Scope of the Study

The current approach was developed for a concentrated lateral load and moment. For complicated loading, the loading may be decomposed into a number of components, thus allowing the approach to be used directly. The present study has been developed for homogeneous elastic soil, so this can be extended to include for non-homogeneous soils. Pile group analysis, dynamic analysis of piles can also be made. Work can also be extended to include further analysis of piles under lateral soil movements.

REFERENCES

1. K. Sun (1994), “Laterally Loaded Piles in Elastic Media” *Journal of Geotechnical Engineering Division*, ASCE 120(8):1324 – 1344.
2. F. Abedzadeh and Ronald Y.S. Pak (2004), “Continuum Mechanics of Lateral Soil–Pile Interaction” *Journal of Engineering Mechanics*, ASCE 130(11): 1309–1318.
3. W.D. Guo and F. H. Lee (2001), “Load Transfer Approach for Laterally Loaded Piles” *International Journal for Numerical and Analytical Methods in Geomechanics* 25: 1101-1129.
4. J.B. Anderson, F.C. Townsend and B. Grajales (2003), “Case History Evaluation of Laterally Loaded Piles”, *Journal of Geotechnical and Geo-environmental Engineering*, ASCE 129(3), 187 – 196.
5. B.T. Kim, N.K. Kim, W.J. Lee and Y.S. Kim (2004), “Experimental Load-transfer Curves of Laterally Loaded Piles in Nak-Dong river Sand” *Journal Of Geotechnical and Geo-environmental Engineering*, ASCE 130(4), 416 – 425.
6. M. Ashour and G. Norris (2003), “Lateral Loaded Pile Response in Liquefiable Soil” *Journal of Geotechnical and Geoenvironmental Engineering*, ASCE 129(6):404–414.
7. M.F. Randolph and W.D. Guo (1998), “Rationality of Load Transfer Approach for Pile Analysis”, *Computers and Geotechnics*, Elsevier Science Limited 23:85-112.
8. J. Liu, H.B. Xiao, J. Tang and Q.S. Li (2004), “Analysis of Load-Transfer of Single Pile in Layered Soil”, *Computers and Geotechnics*, Elsevier Science Ltd. 31:127–135.
9. R. Salgado, P. Bandini and A. Karim (2000), “Shear Strength and Stiffness of Silty Sand” *Journal of Geotechnical and Geoenvironmental Engineering*, ASCE 126(5):451–0462.

10. W.D. Guo, M.F. Randolph (1996), "Torsional Piles in Non-homogeneous Media" *Computers and Geotechnics, Elsevier Science Ltd.* 19(4):265-287.
11. S.A. Ashford and T. Juirnarongrit (2003), "Evaluation of Pile Diameter Effect on Initial Modulus of Subgrade Reaction" *Journal of Geotechnical and Geoenvironmental Engineering ASCE* 129(3):234-242.
12. H.G. Poulos (2005), "Pile Behavior-Consequences of Geological and Construction Imperfections" *Journal of Geotechnical and Geoenvironmental Engineering ASCE* 131(5):538-563.
13. V.G. Vallabhan and Y. C. Das (1991), "Modified Vlasov Model for Beams on Elastic Foundations" *Journal of Geotechnical Engineering ASCE* 117(6):956-966.
14. V.G. Vallabhan and Y. C. Das (1988), "Parametric Study of Beams on Elastic Foundations" *Journal of Engineering Mechanics ASCE* 114(12):2072-2082.
15. Y. Yang, S. Kuo and M. Liang (1996), "A Simplified Procedure for Formulation of Soil-Structure Interaction Problems" *Computers and Structures, Elsevier Science Ltd* 60(4):513 – 520.
16. A. T. C. Goh, C. I. Teh, and K.S. Wong (1997), "Analysis of Piles Subjected to Embankment Induced Lateral Soil Movements" *Journal of Geotechnical and Geoenvironmental Engineering ASCE* 123(9), 792-801.
17. "Structural Criteria for Piers and Wharves"
http://www.nfesc.navy.mil/pub_news/tr2103shr/criteria.pdf.
18. "Background: Design Methods for Laterally Loaded Piles",
http://nees.ucla.edu/caltrans/publications/6ftShaft/Part1/CaltransI_Ch02.pdf.
19. J.P. Carter, C.S. Desai, D.M. Potts, H.F. Schweiger and S.W. Sloan "Computing And Computer Modeling in Geotechnical Engineering", 1-96 *web search*.
20. J.E. Bowles (1997), "Foundation Analysis and Design" McGraw-Hill International Fifth Edition.
21. Rudra Pratap (2005), "Getting Started with MATLAB: A Quick Introduction for Scientists and Engineers" Oxford University Press.

APPENDIX A

Computational Procedure for the Determination of Shear Modulus of Elasticity - G_s

1. Assume a value for G_s .
2. Calculate modulus of subgrade reaction and fictitious tension.
3. Evaluate shear force from the equation 5.32 (third derivative) as a function of z .
4. Integrate the above result from zero to critical pile length to obtain horizontal effective stress (σ_h) due to a lateral load.
5. Vertical effective stress (σ_v) due to soil present around pile is found by integrating between the limits zero to pile length.
6. Calculate the mean effective stress (σ'_m) from the following expression
$$\sigma'_m = (\sigma_v + 2 \sigma_h) / 3$$
7. Now calculate G_s from the equation 2.19
8. Check out for the required convergence between assumed and obtained G_s values.
9. If the required convergence is not obtained repeat the steps from 2 to 8 until the required convergence is obtained.
10. With the obtained G_s , we can calculate response of piles.